M-Pos456 - M-Pos505

Reserved for High School Student Posters.

STUDIES OF PROTEIN COMPLEXES BY NMR: THE NEXT FRONTIER

Tu-AM-SymI-1

COMPLEXES OF HUMAN THIOREDOXIN AND ITS TARGET PEPTIDES
((A.M. Gronenborn)) NIDDK, NIH, Bethesda, MD 20892

It has recently been shown that human thioredoxin, a 12 kDa cellular redox protein, is involved in the activation of several transcription factors, in particular NFkB and Fos/Jun. Using multidimensional heteronuclear-edited and -filtered NMR spectroscopy, we have solved the solution structure of a complexes of human thioredoxin with target peptides from NFkB and Ref-1, representing kinetically stable mixed disulfide intermediates along the reaction pathway. The NFkB peptide is located in a long boot-shaped cleft on the surface of human thioredoxin delineated by the active site loop, helices α2, α3 and α4, and strands β3 and β4. The peptide adopts a crescent-like conformation with a smooth 110° bend centered around residue 60 which permits it to follow the path of the cleft. The Ref-1 peptide, in contrast, binds in the opposite orientation but uses predominantly the same binding cleft. In addtion to the disulfide bridge between Cys32 of human thioredoxin and the cysteines of the peptides, the complexes are stabilized by numerous hydrogen bonding, electrostatic and hydrophobic interactions with the latter being the most important one for defining the orientation of the peptide.

Tu-AM-SymI-2

STRUCTURES OF PROTEIN-LIGAND COMPLEXES INVOLVED IN SIGNAL TRANSDUCTION.
((S.W. Fesik[1], M.-M. Zhou[1], E.T. Olejniczak[1], A.M. Petros[1], R.P. Meadows[1], M.Sattler[1], J.E. Harlan[1], W.S. Wade[1], S. Crosby[1], K.S. Ravichandran[2], and S.J. Burakoff[2]))
[1]PPD, Abbott Laboratories, Abbott Park, IL 60064 [2]Division of Pediatric Oncology, Dana-Farber Cancer Institute and Department of Pediatrics, Harvard Medical School, Boston, MA 02115.

Signal transduction is a complicated process that may involve several steps mediated by specific intermolecular interactions. Recently, three-dimensional structures of protein/ligand complexes involved in signal transduction have been obtained which have greatly aided in our understanding of these processes at the molecular level. In this presentation, the NMR structure of the phosphotyrosine binding (PTB) domain of the adaptor protein Shc complexed to a phosphopeptide (TrkA) derived from the nerve growth factor receptor will be presented. The structure of the complex reveals an alternative means of recognizing tyrosine-phosphorylated proteins compared to SH2 domains. The PTB domain is structurally similar to pleckstrin homology domains (β-sandwich capped by an α-helix) and binds to acidic phospholipids, suggesting a possible role of this domain in membrane localization.

Tu-AM-SymI-3

NMR STRUCTURAL AND DYNAMIC STUDIES OF SH2 DOMAIN-PHOSPHOPEPTIDE COMPLEXES.
(J.D. Forman-Kay, N.A. Farrow, S.M. Pascal, A.U. Singer, T. Yamazaki, L.E. Kay) Hospital for Sick Children and University of Toronto, Toronto, Ontario, CANADA M5G 1X8.

The C-terminal Src Homology 2 (SH2) domain of phospholipase C-γ1 (PLCγ) binds specifically to the phosphorylated Tyr-1021 of the β-platelet-derived growth factor receptor (PDGFR) as well as to certain phosphorylated tyrosines on other growth factor receptors and to PLCγ itself. The NMR structure of a complex of the C-terminal SH2 domain of PLCγ (PLCC SH2) with a 12-residue peptide encompassing the Tyr-1021 site of the PDGFR (pY1021) has been determined and refined, demonstrating (1) SH2 interactions with residues from the -1 to +6 positions relative to the pTyr of the peptide, (2) bound water molecules, one of which bridges interactions between the SH2 domain and peptide, and (3) the presence of a small cavity. Insights into the interaction have also been derived from pH titrations which demonstrate significanty shifted pKa values for the phosphotyrosine (pTyr) of pY1021 and a conserved histidine near the pTyr-binding site. Backbone and sidechain ^{15}N and novel methyl ^{2}H relaxation experiments have been performed on free and pY1021-complexed PLCC SH2 domain. Dynamics have also been inferred from broadening of resonances and chemical shifts of arginine sidechain resonances. Results show significant μs-ms motion but restriction of ns-ps motion in the pTyr-binding site with the reverse in the hydrophobic binding region responsible for binding specificity through interactions with peptide residues C-terminal to the pTyr. Comparison with binding studies suggests a correlation between ns-ps time scale dynamic behavior and contribution to binding energy.

Tu-AM-SymI-4

Homeodomain-DNA Recognition: the NMR Solution Structure of the *Antennapedia* Homeodomain-DNA Complex.
Y.Q. Qian,[1] M. Billeter,[2] G. Otting,[3] Peter Güntert,[2] Peter Luginbühl,[2] M. Müller,[4] W. Gehring[4] and K. Wüthrich,[2]
[1]*Department of Physical & Structural Chemistry, SmithKline Beecham Pharmaceuticals, Mail Code UW-2940, PO Box 1539, King of Prussia, PA 19406-0939, USA*
[2]*Institut für Molekularbiologie und Biophysik, ETH-Hönggerberg, 8093 Zürich, Switzerland*
[3]*Department of Medical Biochemistry and Biophysics Karolinska Institutet S-171 77 Stockholm Sweden*
[4]*Biozentrum der Universität Basel, Abt. Zellbiologie, Klingelbergstr.70, 4056 Basel, Switzerland.*

Recent results on the determination of the NMR solution structure of the *Antennapedia* homeodomain-DNA complex will be presented. The *Antennapedia* homeodomain was uniformly labeled with ^{13}C or ^{15}N, and two-dimensional [^{1}H,^{1}H]-NOESY spectra, recorded with a $^{15}N(\omega_2)$-half-filter or a $^{13}C(\omega_1, \omega_2)$-double-half-filter, as well as three-dimensional heteronuclear-correlated [^{1}H ^{1}H]-NOESY spectra were used. The two macromolecules were docked using a simulated annealing approach and further refined by short runs of molecular dynamics in a water bath, followed by final energy refinements. The salient structure features are that the recognition helix is located in the major groove of the DNA with the turn of the helix-turn-helix motif outside the protein-DNA contact area, and that the N-terminal arm of the homeodomain penetrates the minor groove of the DNA. Although no constraints were imposed on water molecules during the structure calculations, hydration water molecules are found in the protein-DNA interface of the resulting structure, a feature that coincides with direct NMR observations of hydration waters. A subsequently recorded molecular dynamics trajectory covering 2 ns of the *Antennapedia* homeodomain-DNA-water system, using the program OPAL, further explored the implicated fluctuations of the network of specific protein-DNA interactions. Thus, the interfacial hydration water is short-lived and mediates numerous protein-DNA interactions. Several of the amino acid side chains responsible for specific DNA contacts undergo rapid motions between multiple contact sites on the DNA, indicating that fluctuations of the intermolecular interaction network play an important role.

Tu-AM-A1

STRUCTURE-FUNCTION STUDIES IN THE S4 REGION OF *SLOWPOKE*. ((A. Lagrutta, M. Köhler, and J.P. Adelman)) Vollum Institute, Oregon Health Sciences University, Portland, OR 97201.

All Kv potassium channels exhibit the seven-times repeated motif R/K/H-X-X in their S4 region. In contrast, *dslo* channels and its mammalian homologs possess S4 regions where most of this fixed positive charge component is neutralized or reversed. We substituted specific residues in the S4 region of *dslo* (P_{233}-D_{234}) for residues present in *Shaker*. The calcium-voltage dependence of wildtype and mutant channels was tested in macropatches of *Xenopus* oocyte membranes, using ionic conditions of symmetrical potassium (120 mM K^+). We plotted macroscopic conductance as a function of voltage, and derived parameters for half-activation ($V_{0.5}$) from Boltzmann fits. For WT, $V_{0.5}$ is -24.7 ± 4.34 mV of at 100 μM Ca (n=8), and +68.36 ± 2.87 mV at 10 μM Ca (n=8). For $D_{234}K$, $V_{0.5}$ is +79.78 mV ± 2.58 mV at 100 μM Ca (n=5), and >> +100 mV at 10 μM Ca . D234N and D234E are similar to WT. For $P_{233}F$, $V_{0.5}$ is -16.74 ± 13.27 mV at 10 μM Ca (n=9), and << -100mV at 100 μM Ca. At the single channel level, kinetic differences, but no current amplitude differences (γ_0 ~ 200 pS), were detected between WT and mutants. We propose that residues in the S4 of *dslo* channels are part of a calcium-voltage transduction machinery which permits charge neutralization but no charge reversal (e.g. $D_{234}N$ vs $D_{234}K$). We also propose that substitution of P_{233} in *dslo* "unhinges" this machinery.

Tu-AM-A2

HIGH CALCIUM INDUCES A LOW ACTIVITY MODE AND REVEALS CALCIUM-INDEPENDENT LONG SHUT INTERVALS IN BK CHANNELS. ((Brad S. Rothberg, Ricardo A. Bello, Lu Song and Karl L. Magleby)) Dept. Of Physiology and Biophysics, Univ. of Miami School of Med., Miami, FL 33101

Large conductance Ca^{2+}-activated K^+ (BK) channels often display long closed intervals at higher levels of Ca^{2+}. To gain insight into possible mechanisms for these intervals, currents were recorded from single BK channels with the patch clamp technique from patches of membrane excised from cultured rat myotubes. Data were filtered at 6-10 kHz. High Ca^{2+} induced a low activity mode (LAM) and revealed isolated long shut (ILS) intervals. Neither of these phenomena were due to the Ba^{2+} that typically contaminates reagent grade salts. The LAM was characterized by single brief open intervals with mean durations of 0.1 ms separated by long shut intervals with mean durations of 100 ms, and a very low P_{open} of about 0.001. The durations of sojourns in the LAM were exponentially distributed and ranged from 300 ms in 10 μM Ca^{2+} to 10 s in 1000 μM Ca^{2+}. With increased filtering, the brief open intervals would escape detection so that a sojourn to the LAM would appear as a single shut interval. A typical channel spent less than 5% of its time in the LAM for Ca^{2+}<10 μM, increasing to 30% for Ca^{2+}>100 μM. A kinetic model containing 3 closed states and 2 open states could approximate the gating during the LAM. The ILS intervals were not drawn from the LAM, suggesting a different underlying mechanism. Their frequency of occurrence (0.3/s) did not increase with Ca^{2+}, suggesting that they do not arise from a slow Ca^{2+} block. Their mean duration (127 ms) was independent of Ca^{2+}, suggesting that the closed state(s) underlying the ILS intervals were not on the direct Ca^{2+} activation pathway. These observations suggest that activation of BK channels by high Ca^{2+} can be limited by the LAM and ILS intervals, two phenomena that will need to be accounted for in the gating of BK channels. Supported by Grants from the NIH and Muscular Dystrophy Association to K.L.M.

Tu-AM-A3

CALCIUM-INDEPENDENT ACTIVATION OF THE MSLO CA-ACTIVATED K^+ CHANNEL AT VERY DEPOLARIZED VOLTAGES ((D. H. Cox, J. Cui, G. Talukder and R. W. Aldrich)). Dept. of Mol. and Cell Physiol., HHMI, Stanford University School of Medicine, Stanford CA 94305

The activity of large-conductance Ca-activated K^+ channels is sensitive to both internal Ca^{2+} concentration ([Ca]i) and membrane voltage such that a change in the level of one stimuli shifts the effective range of the other. As a step towards gaining a mechanistic understanding of this relationship, we have examined the question of whether a strong voltage stimulus alone is sufficient to activate a cloned Ca-activated K^+ channel expressed in *Xenopus* oocytes (mSlo ; mbr5, α subunit alone) . At voltages between -50 and +50 mV micromolar levels of [Ca]i are required to activate this channel significantly. With stronger depolarizations (>+140 mV), however, large macroscopic currents are observed with [Ca]i only in the low nanomolar range. These currents are blocked by 3 mM external TEA, have the large unitary conductance typical of mSlo channels, and correlate well with the amplitude of currents recorded at 124 μM [Ca]i, indicating that they are a product of mSlo expression. These currents might indicate activation via a Ca-independent mechanism, or they may be the result of a large increase in the channel's affinity for [Ca]i at high voltages. Two lines of evidence suggest that the former is the case. 1) When currents were recorded with [Ca]i buffered with EGTA to ~ 0.5 , 2 , or 10 nM, no significant differences in current level or time course were observed, suggesting that the channel is not displaying an affinity for [Ca]i in the low nanomolar range. 2) The time constant of activation for these currents at +180 mV is ~ 2 ms. In order for the activation of these currents to require Ca^{2+} binding then, Ca^{2+} must on average diffuse to its binding site at least this fast, corresponding to an on rate constant of 10^{12} $M^{-1}s^{-1}$ at 0.5 nM [Ca]i, which is orders of magnitude larger than the expected diffusion limited on rate constant, 10^9 $M^{-1}s^{-1}$. These results support the conclusion that the mSlo channel has an intrinsic voltage sensor which is separate from Ca^{2+} binding, and that the action of this sensor alone is sufficient to activate the channel.

Tu-AM-A4

EQUIVALENT GATING CHARGE OF THE MSLO CA-ACTIVATED K^+ CHANNEL MEASURED FROM THE LIMITING SLOPE OF THE VOLTAGE DEPENDENCE OF UNITARY CURRENT ACTIVATION ((J. Cui, D. H. Cox, and R. W. Aldrich)) Dept. of Mol. and Cell. Physiol., HHMI, Stanford University School of Medicine, Stanford, CA 94305

Our previous study shows that the voltage dependence of the mSlo Ca^{2+}-activated K^+ channel is predominately due to an intrinsic voltage sensor in the channel protein, and the apparent gating charge associated with activation varies little with $[Ca^{2+}]_i$. We have used the patch-clamp technique to measure the gating charge of the mSlo channel expressed in excised macropatches from *Xenopus* oocytes. The limiting slope of the voltage dependence of channel activation was measured at hyperpolarized voltages where the steady state open probability (P_o) is between 10^{-5} and 10^{-2}. Under such conditions, although the macropatch contained hundreds of mSlo channels discrete single channel openings were observed. The equivalent gating charge is calculated from the maximum slope of the $\ln(NP_o)$-Voltage relation (N is the total number of channels in the patch). This measured gating charge is relatively model independent. It is also relatively accurate since the contamination of noise and the activity of endogenous channels is carefully removed. The measured gating charge for the mSlo channel is 1.12 ± 0.24 elementary charges, which is similar to the charge measured from fitting the macroscopic G-V curve with a single Boltzmann distribution. One surprising observation from our measurements is that the slope of $\ln(NP_o)$-Voltage relation started decreasing as the voltage became more negative than -80 mV. Many possible mechanisms could explain this phenomena, one of which is that the polarizability of the channel protein changed at extreme voltages so the free energy of the channel is no longer linearly dependent on voltage. The equivalent charge would be 2.04 ± 0.80 if the change of polarizability is considered.

Tu-AM-A5

GATING CHARGE MOVEMENT FROM MSLO CA^{++}-ACTIVATED K^+ CHANNELS MEASURED VIA ADMITTANCE ANALYSIS. ((F.T. Horrigan, J. Cui, D.H. Cox, and R.W. Aldrich)) Dept. of Mol. and Cell. Physiol., HHMI, Stanford University School of Medicine, Stanford, CA 9430

Previous analysis of mSlo K^+ currents suggests that the weak voltage-dependence of channel activation largely reflects the movement of an intrinsic voltage-sensor rather than the binding of Ca^{++} to its receptor. Here we examine the properties of this voltage sensor directly by using the patch clamp technique to measure mSlo gating charge movement from channels that were expressed in excised macropatches from *Xenopus* oocytes. The membrane potential was clamped with a sinusoidal voltage command (3000 hz) in the absence of permeant ions and Ca^{++}. The resulting current was analyzed via admittance analysis in order to determine membrane capacitance (Cm). Cm was found to have a bell-shaped dependence on voltage with a peak at +100 mV. The integral of Cm vs V, representing the mSlo Q-V relationship, was well fit by a Boltzmann function with an equivalent charge of 0.6 e^- ($V_{1/2}$=100 mV) consistent with a weakly voltage-dependent channel gating process. An mSlo mutant (mSloS4) was constructed by altering a single residue in the S4 region. In the absence of Ca^{++}, mSloS4 K^+ currents were found to activate at more hyperpolarized potentials than mSlo. Consistent with this observation, the C_m-V relationship for mSloS4 had the same shape that for mSlo but was as shifted along the voltage axis by -250 mV.

Tu-AM-A6

TOWARDS AN UNDERSTANDING OF HOW VOLTAGE AND Ca^{2+} OPERATE IN A MAXI K CHANNEL, *hSlo*. ((L. Toro, F. Noceti, M. Ottolia, P. Meera, M. Wallner, R. Latorre, and E. Stefani)) Dept. of Anesthesiology, UCLA, Los Angeles , CA 90095, and CECS, Chile.

We have measured *hslo* macroscopic ionic and gating currents. The salient features of the activation and deactivation processes are: **1.** Depolarizing voltages and increasing $[Ca^{2+}]$ (100 nM to 5 mM) increase the open channel probability. **2.** Currents activate and deactivate in a quasi single exponential manner. However, when depolarizing pulses were delivered from very negative potentials, currents had a clear and distinct delay (0.2 ms at -180 mV) (Cole-Moore shift). Increasing $[Ca^{2+}]$ shift to more negative potentials the pre-pulse voltage that eliminates current delay. **3.** The half activation potentials obtained from G-V curves is shifted to more positive potentials when lowering internal Ca^{2+}. This voltage shift is linear in a semilog plot between 100 nM to 5 mM Ca^{2+}. **4.** Channel activation is independent of $[Ca^{2+}]i$ from 4 pM (isotonic EDTA) to 100 nM. **5.** The limiting gating valence from the G-V curve has approximately the same value (≈3 e^-) at all $[Ca^{2+}]i$ tested (4 pM-300 nM). **6.** At 4 pM Ca^{2+}, 0.11 e^- are moved during the ON, whereas at the OFF 0.20 e^- are involved. Given that the limiting gating valence is about 3 e^-, 90% of the charge should be moved in an initial C-C transition before channel opening. **7.** The voltage dependencies of the ON and OFF rates increase with $[Ca^{2+}]_i$; e.g, the ON rate z_{on} increased from 0.11 e^- to 0.27 e^- at 4 pM and 5 μM $[Ca^{2+}]$, respectively. For the same $[Ca^{2+}]$'s, the z_{OFF} are 0.2 e^- and 0.42 e^-, respectively. **8.** Gating currents activate in a similar voltage range as the ionic current and precede in time the activation of the ionic current (Ottolia, et al., this meeting). $[Ca^{2+}]_i$ shifts along the voltage axis both ionic and gating currents. These features do not support the voltage dependent version of the MWC model of allosteric proteins with the same voltage dependency between C to O transitions. The data agrees with Magleby's 1983 model with an additional C-C transition strongly voltage dependent and Ca^{2+} independent. This model should have C to O transitions with different voltage dependencies. Supported by NIH.

Tu-AM-A7

GATING OF MIN K CHANNELS IN *XENOPUS* OOCYTES. ((T. Tzounopoulos*, J.P. Adelman* & J. Maylie#)). *Vollum Institute, #Dept. of Obstetrics and Gynecology, OHSU, Portland, Oregon, 97201.

The gating mechanism for the structurally and functionally distinct min K channel was investigated using various voltage protocols. Current records obtained from a test pulse to 40 mV from a holding potential of -60 or -120 mV showed an unusual "cross over". Double exponential fits to current traces evoked by commands to 40 mV from various holding potentials revealed that as the holding potential was made less negative, the relative contribution of the fast time-dependent component decreased; the time constants were not significantly changed. Rate constants for this transition between the fast and slow component were determined, based on the time and voltage dependence of this process. Further, the currents obtained from various holding potentials could not be overlayed by a simple shift in the time base. This deviation from the Cole and Moore prediction suggests an activation mechanism that can not be explained by a scheme involving identical and independent steps. We propose a gating scheme in which min K channels, at more hyperpolarized holding potentials, reside in one closed state, and on depolarization enters alternate closed states as they approach a common open state. Rate constants for transitions near the open state were determined by examining channel reactivation, and for other forward transitions during activation by examining the voltage-dependence of the fast and slow components of activation. Using these derived rate constants, min K currents were accurately reproduced in computer modeling studies.

Tu-AM-A8

SUBUNIT BASIS FOR ION PERMEATION AND GATING SUGGESTED BY SUBCONDUCTANCE LEVELS IN K CHANNELS. ((M.L. Chapman, H.M.A. VanDongen, A.M.J. VanDongen)) Dept. of Pharmacology, Duke University Medical Center, PO Box 3813, Durham, NC 27710.

Two essential, but poorly understood, properties of ion channels are channel opening and ion permeation. Single channel analysis of a voltage dependent K channel suggested that subconductance levels may be associated with opening and closing transitions. Since K channels are formed by four identical subunits, it was hypothesized that individual subunits can support permeation, thereby producing subconductance levels. This subunit-subconductance hypothesis predicted that subconductance behavior would be more abundant when activation is incomplete. Experimental evidence supported this prediction as subconductance levels were increased tenfold in recordings near the activation threshold. To further test the hypothesis a mutation was introduced in the amino-terminal region of the voltage sensor of the channel. The resulting channel (drk1-LS) was found to have a slight reduction in the voltage-dependence of open probability but the voltage-dependence of the activation time constant was reduced nearly twenty-fold. Additionally, drk1-LS exhibited subconductance activity over a broadened voltage range. The subunit-subconductance hypothesis predicts just such behavior if the rate of activation is slow, relative to the rate of channel opening. Based on these results a subunit basis is proposed for channel opening and ion permeation.

Tu-AM-A9 *(See W-Pos402)*

SR Ca2+ RELEASE IN SKELETAL MUSCLE

Tu-AM-B1

TETANIC STIMULATION: A PHYSIOLOGICAL TOOL TO CRITICALLY INVESTIGATE EXCITATION-CONTRACTION COUPLING IN SKELETAL MUSCLE (A. Kim, M. DiFranco*, and J. L. Vergara) Department of Physiology, UCLA School of Medicine, Los Angeles, CA 90024, and *UCV, Venezuela.

The dynamic components of the excitation-contraction coupling process in skeletal muscle were investigated using electrophysiological and epifluorescence optical techniques while stimulating at tetanic frequencies. Single frog skeletal muscle fibers were stretched to sarcomere spacings between 3.6 - 4 μm, mounted in a triple vaseline gap chamber, and stimulated to elicit action potential trains of variable frequencies (10 - 100 Hz) and durations (0.1 - 5 sec). T-tubule depolarizations were monitored in fibers stained with 0.5 - 5 μM concentrations of the potentiometric dye di-8-ANEPPS. Ca^{2+} transients were recorded in fibers intracellularly stained with 100 - 500 μM CaOrange-5N. Epifluorescence signals were recorded with a PIN photodiode, using 1) a 610 nm barrier filter, a 440-490 nm band-pass excitation filter, and a 510 nm dichroic mirror for di-8-ANEPPS, and 2) a 590 nm barrier filter, a 510-560 nm band-pass excitation filter, and a 580 nm dichroic mirror for CaOrange-5N. Single action potential stimulation yielded changes in the potentiometric dye fluorescence of approximately -6% $\Delta F/F$, corresponding to T-tubule depolarizations of 150 mV. Tetanic stimulation (5 sec) affected T-tubule action potentials in a frequency dependent manner, reducing their peak values (to approximately 62% at 20 Hz and to 50% at 100 Hz) and increasing the negative after potential. At the corresponding frequencies, surface action potentials reflected these changes only partially. CaOrange-5N signals revealed that at lower tetanic frequencies (≤20Hz), fibers could, for a period of seconds, sustain phasic $[Ca^{2+}]$ release in response to individual T-tubule action potentials. At higher frequencies (≥50 Hz), the phasic responses disappeared within 1 sec. Concurrent with the phasic response inactivation there is a tonic elevation of the myoplasmic $[Ca^{2+}]$ to levels significantly higher than the phasic transients. Our results suggest that regulatory processes maintain an increased myoplasmic $[Ca^{2+}]$ in response to frequency demands. Supported by NIH AR25201.

Tu-AM-B2

HOW CAFFEINE-INDUCED AND VOLTAGE-INDUCED Ca^{2+} RELEASE INTERACT IN SKELETAL MUSCLE ((N. Shirokova and E. Ríos)) Rush University, Chicago, IL 60612.

A computer operated, 2-Vaseline-gap flow chamber was built for electrophysiological recording while rapidly changing extracellular solutions. The chamber was used with cut skeletal muscle fibers of *Rana pipiens*, to study the effect of high concentrations of caffeine, a potentiator of Ca^{2+}-induced Ca^{2+} release (Endo, 1975), on the two kinetic phases of Ca^{2+} release induced by pulse depolarization . Ca^{2+} release flux elicited by caffeine pulses was derived from recorded changes in intracellular $[Ca^{2+}]$ with the method used before to derive flux induced by voltage pulses (Melzer et al., 1984,1987). Ca^{2+} release induced by 10 mM caffeine increased rapidly upon drug exposure, reaching a maximum of 2.5 mM/s or less at about 3 s, then decaying to essentially zero. When depolarizing pulses were applied after increasing times of exposure to 10 mM caffeine, the Ca^{2+} release flux induced by voltage first increased, peaked after 1 s exposure to caffeine, and decreased at longer exposures, reaching zero by about 5 s. In contrast, the voltage-induced release permeability, calculated dividing release flux by sarcoplasmic reticulum Ca^{2+} content, increased monotonically with time of exposure to caffeine. Both in reference solution and in 10 mM caffeine, the time course of the release permeability increase during a depolarizing pulse had the usual kinetics of release: an early peak, followed by decay to a maintained level. Both the peak and the steady permeability depended sigmoidally on pulse voltage. 10 mM caffeine changed the voltage dependence equally for both components: it shifted the mid-activation voltage by -15 mV, increased the steepness by 15 % and the maximum permeability, attainable at high voltages, by 30% for the peak and 25% for the steady component. Caffeine at 10 mM did not interfere with decay of release flux or permeability upon repolarization - release activated by voltage remained always under voltage control. Given the similarity of caffeine effects on both components of Ca^{2+} release, the present results do not support two current ideas: that the peak of release flux, but not its steady component, involve Ca^{2+}-induced Ca^{2+} release, and that the two components of release course trough different subsets of Ca^{2+} release channels (Ríos and Pizarro, 1989). (Supported by NIH and MDA).

Tu-AM-B3

CAFFEINE ENHANCES CHARGE MOVEMENT IN SKELETAL MUSCLE BY INCREASING CYTOPLASMIC Ca^{2+} CONCENTRATION. ((N.Shirokova and E.Ríos)) Rush University, Chicago, IL 60612. (Spon. by J.Tang)

Intramembranous charge movement and intracellular Ca^{2+} transients were recorded simultaneously in single frog skeletal muscle fibers subjected to combined action of voltage clamp depolarization and "pulses" of extracellular solution with a high concentration of caffeine. When external solution with 10 mM caffeine was applied prior to and maintained during pulse depolarization, the charge transferred by pulses from holding potential to between -60 and -40 mV increased by about 40% of the charge transferred in reference condition (no caffeine). Whenever the prior exposure to caffeine resulted in a large increase in $[Ca^{2+}]_i$ at the start of the depolarizing pulse, there was an increase in I_β, the monotonically decaying component of charge movement. When caffeine enhanced Ca^{2+} release induced by the pulse, there was an increase in I_γ, the "hump" component. In fibers depleted of Ca^{2+} in the sarcoplasmic reticulum (SR), caffeine had no effect on charge transferred or charge movement kinetics. When the SR was partially depleted, the effect on charge movement was present but reduced. The increase in charge transfer grew monotonically with time of exposure to 10 mM caffeine. Ca^{2+} release induced by the voltage pulse increased during the first second of caffeine application and then decreased with longer exposure times. The effect of caffeine was therefore not associated with the increase in Ca^{2+} release that it caused. The increase in charge transfer was instead a uniform function of $[Ca^{2+}]_i$ attained in the fiber at the end of the voltage pulse. The function was monotonically increasing up to the highest $[Ca^{2+}]_i$ reached (1.2 μM). Charge transferred, as a function of voltage and $[Ca^{2+}]_i$, could be simulated with a model of Pizarro et al. (1991), in which Ca^{2+} binds to intracellular sites and increases the electrical potential near the voltage sensor. Two sites were needed to fit the observations, with dissociation constants of 60 nM and 2 to 10 μM. The existence of a high affinity Ca^{2+} binding site may explain seemingly contradictory results from researchers studying I_γ. (Supported by NIH and MDA).

Tu-AM-B4

QUANTAL RELEASE OF CALCIUM IN SKELETAL MUSCLE. ((G. Pizarro[1], N. Shirokova, A. Tsugorka, L.A. Blatter[1] and E. Ríos)) Rush University, Chicago, IL 60612, [1]Universidad de la República, Montevideo, Uruguay, [1] Loyola University Chicago, Maywood, IL 60153.

In skeletal muscle, ryanodine receptor/channels are the pathway for Ca^{2+} release upon action potential depolarization. In other cells, Ca^{2+} release (through $InsP_3$-sensitive channels) is ***quantal***. Increasing doses of the agonist appear to recruit specific pools with different sensitivities. Activation by voltage is instead believed to recruit randomly among identical channels. We found that activation by voltage of the release channels of skeletal muscle has quantal properties. Ca^{2+} release flux was determined by optical techniques in frog muscle cells under voltage clamp. We found that fast inactivation of release channels (to a state lasting 150 ms) is an obligatory, strictly coupled consequence of activation: all the inactivatable release channels that open inactivate, and only the channels that open inactivate. This fatality of inactivation predicts that any submaximal pulse would inactivate all channels in the ensemble if maintained for sufficient time. This does not happen, and there are two possible explanations. **1)** All channels may not be equal. This ***heterogeneous population model***, tested in the communication that follows, has been used to explain $InsP_3$-induced quantal release (Ferris et al., PNAS, 1991). **2)** ***Memory models***, in which individual channels have the quantal property (Swilléns, Molec. Pharmacol. 1992), could also explain the phenomena. (Supported by NIH, AHA, MDA).

Tu-AM-B5

EAGER TRIADS IN SKELETAL MUSCLE: HETEROGENEOUS DISTRIBUTION OF VOLTAGE-ELICITED Ca^{2+} RELEASE REVEALED BY CONFOCAL MICROSCOPY. ((L. A. Blatter[1], A. Tsugorka[2], N. Shirokova[2] and E. Rios[2])) [1]Department of Physiology, Loyola University Chicago, Maywood, IL 60153, and [2]Department of Molecular Biophysics and Physiology, Rush University, Chicago, IL 60612.

In skeletal muscle cells, Ca^{2+} release to trigger contraction occurs at triads, specialized junctions where sarcoplasmic reticulum channels are opened by voltage sensors in the transverse (T) tubule. In single skeletal muscle fibers under voltage clamp Ca^{2+} release at individual triads was revealed by laser scanning confocal microscopy. Fluo-3 was used to visualize changes of intracellular calcium ($[Ca^{2+}]_i$) as a function of space and time during voltage-step pulses. $[Ca^{2+}]_i$ gradients at individual triads were found to be proportional to Ca^{2+} release flux. In cells stimulated with small depolarization pulses the $[Ca^{2+}]_i$ gradients broke down into elementary events (Tsugorka et al., Science 269, 1995). At very low voltages elementary events favored specific triads with a much higher level of activity. These 'eager triads' kept gating for the duration of the pulse, suggesting that activation was not random. Two sets of experiments were done to rule out a trivial explanation that the appearance of eager triads results from unequal representation of triads (and release channels) within the optical plane imaged by the confocal microscope. With increasingly higher voltages applied to the same fiber, additional triads became active until Ca^{2+} release of about the same magnitude was observed at every triad. Additionally, a regular pattern of T tubule staining was obtained with the extracellular membrane-specific probe di-8-ANEPPS (indicating a homogeneous representation of triads in the confocal slice) while simultaneous fluo-3 measurements revealed triads with different levels of activity.

If indeed eager triads correspond to subpopulation of channels with greater sensitivity to voltage, this would contradict the fundamental assumption that individual channels are representative members of a statistical ensemble with a single set of properties. A heterogeneous population of channels, with a spectrum of voltage sensitivities, would explain the 'quantal' properties of Ca^{2+} release discussed in the preceding communication.

Tu-AM-B6

LOCAL CALCIUM RELEASE EVENTS ACTIVATED BY DUAL MECHANISMS IN FROG SKELETAL MUSCLE ((M.G. Klein, H. Cheng, L.F. Santana, Y.-H. Jiang, W.J. Lederer and M.F. Schneider)) Departments of Biological Chemistry and Physiology, University of Maryland School of Medicine, Baltimore, MD, 21201

We have investigated Ca^{2+}-release at high spatial and temporal resolution using confocal line scan imaging of voltage-clamped frog cut skeletal muscle fibers loaded with the Ca^{2+} indicator fluo-3. During small depolarizations, we detected discrete regions of locally elevated Ca^{2+} of about 100 nM. These Ca^{2+}-release events were found to originate at the location of the t-tubule (TT) and were stochastically activated by depolarization. The frequency of Ca^{2+}-release events was steeply voltage dependent (e-fold in 3 to 4 mV over -80 to -68 mV). Spontaneous events observed at holding potentials of -90 or 0 mV could not be accounted for by voltage sensor activation, but are consistent with Ca^{2+}-induced Ca^{2+} release (CICR). Histograms of the amplitude of the events observed during depolarization showed 3 populations of events: the smallest events had the same amplitude as the spontaneous events; the larger events were 2 and 3 times the amplitude of the unitary events. Unitary events may correspond to the opening of a single SR Ca^{2+}-release channel, activated either by the TT voltage sensor during depolarization or by CICR at rest. The larger amplitude events during depolarization could consist of the activation of one channel by the voltage sensor and secondary activation of 1 or 2 additional channels by local CICR.

Tu-AM-B7

AMIODARONE ATTENUATES EXCITATION-CONTRACTION COUPLING IN SKELETAL MUSCLE. ((B.E. Flucher, S.B. Andrews and A. Shainberg)) Inst. of Biochemical Pharmacology, Univ. Innsbruck, Austria; Lab. of Neurobiology, NIH, Bethesda MD, USA; Dept. Life Sciences, Bar-Ilan Univ., Ramat-Gan, Israel.

The effect of the anti-arrhythmic drug amiodarone on excitation-contraction coupling was compared in cardiac and skeletal muscle in culture. Differentiated cardiac myocytes or myotubes of the skeletal muscle cell line C_2C_{12} were stimulated by electric field stimulation and the Ca^{2+} release response was measured with the fluorescent Ca^{2+} indicator fluo-3. Treatment of myocytes with 15μM amiodarone for 1 h reduced the spontaneous contractile activity and increased the minimal interval between consecutive twitches to ≥1.5 s. During stimulation trains of 1 Hz, only every other pulse triggered a Ca^{2+} release response. This "skipping" of contractions was also observed in skeletal myotubes incubated in 15μM amiodarone for 1 h. Whereas untreated C_2C_{12} myotubes responded to tetanic stimulation at frequencies of 20 Hz and higher, amiodarone-treated myotubes only responded at frequencies of 0.5 Hz or less. Depolarization-induced Ca^{2+} release in untreated and in treated myotubes stimulated at low frequencies behaved in an all-or-none manner to increasing pulse potentials indicative of action potential-induced Ca^{2+} release events. Elevation of pulse potentials overcame the skipping of contractions in amiodarone-treated myotubes. However, in this case the depolarization-induced Ca^{2+} release was voltage-dependent, indicating that excitation-contraction coupling was stimulated directly by the voltage sensor in the absence of action potentials. Thus amiodarone effects excitation-contraction coupling primarily by attenuating excitability but not depolarization-induced Ca^{2+} release. The physiological effects of amiodarone in myocytes and myotubes were accompanied by an accelerated compartmentalization of the Ca^{2+} indicator. In electron micrographs this corresponded to an increased density of multi-lamellar bodies and dilated smooth-membrane vacuoles. This suggests that amiodarone increases membrane turnover, which may be functionally related to the reduction in excitability of skeletal and cardiac muscle.

Tu-AM-B8

SARCOPLASMIC RETICULUM (SR) CALCIUM RELEASE IN INTACT SUPERFAST TOADFISH SWIMBLADDER (TSB) AND FAST FROG TWITCH MUSCLE FIBERS. ((Hollingworth, S. and Baylor, S.M.)) Department of Physiology, University of Pennsylvania, Philadelphia PA 19104.

Tsb fibers are among the fastest vertebrate fibers. In comparison with frog, they have a greater concentration of SR Ca pumps (8x), parvalbumin (parv; 2x) and SR Ca release sites (2x); in response to an action potential, their Ca transients (Δ[Ca]) are larger (peak: 47±2 SEM vs 17±1 μM) and briefer (half-width: 3.4±0.1 vs 9.8±0.7 ms) (16°C). SR Ca release was estimated from Δ[Ca] by model calculations of Ca binding to troponin and parv. Tsb fibers revealed a greater amount (476±5 μM vs 324±3 μM), a larger peak rate (330±36 vs 142±5 $\mu M\ ms^{-1}$), and a briefer half-width (1.5±0.2 vs 2.2±0.1 ms) of release. With inclusion of the pump model of Fernandez-Belda et al. (J. Biol. Chem. 259:9687, 1994), the estimated amount and rate of release are increased in frog fibers by 10-15%, whereas, in tsb fibers, they are doubled (to 982±41 μM and 602±49 $\mu M\ ms^{-1}$). Thus, with this pump model, about 50% of the Ca release in tsb fibers is bound directly to the pump. This redundant release would be reduced if Ca binding to the pump were in fact delayed, e.g., by a mechanism analogous to that in which Mg bound to parv slows the rate at which Ca can bind.

If the fiber is stimulated by two action potentials separated by a delay, the second release is reduced, because of Ca inactivation of Ca release. The time constant for recovery from this inactivation is very similar in both tsb and frog fibers, ~25 ms.

Supported by NIH (NS 17260)

Tu-AM-B9

EFFECTS OF SUPRAMEMBRANE POTENTIAL ON CHARGE MOVEMENT CURRENTS ON FROG SKELETAL TWITCH MUSCLE FIBERS ((W. Chen, Y. Han, and R.C. Lee)) Department of Surgery, The University of Chicago, Chicago, IL 60637

To study the effects of supramembrane potential on DHP receptors in T-tubular membrane, charge movement currents were measured pre- and postshock by using an improved double Vaseline-gap voltage clamp on frog twitch muscle fibers.

Protocol and solutions were similar to those previously used. A sequence of stimulation pulses were ranged holding the membrane potential from -70 to +30 mV. With a P/N method, the nonlinear charge movement current was identified. A supraphysiological membrane potential pulses ranged from -250 to -500 mV with a duration of 4 ms were used to mimic an electrical shock. Immediately before and after the shock the stimulation pulse sequence were applied to detect any changes in magnitude, time course and shape of both components, Q_β and Q_γ, of the charge movement currents.

Comparisons of raw traces of charge movement currents obtained by traditional and our improved configurations showed an identity in magnitude, time course and shape for both components. Results also include: 1. for skeletal twitch muscle, *Semitendinosus* of frog, *Rana Pipes*, a -350 ±30 mV/4ms pulse was able to introduce a measurable reduction of the charge movement currents. 2. After being shocked, the shape of the hump became wider and the magnitude of the hump became smaller. The peak point of the hump had an increament of time-delay ranged from hundreds of μs to a few ms responding to the same stimulation pulse sequence. 3. Both "on" and "off" charge movement are reduced, and the half-amount point of the "on" charge movement also delayed after electric shock.

These results indicated that DHP receptors on T-tubular membrane is more sensitive to supramembrane potentials than K channels. Based on facts of 1-2 ms width of a action potential, even a few hundreds of μs delay of the charge movement may cause a significant reduction of the amount of Ca^{2+} released from SR. It is possible that after electrical shock, the normal action potential may not be able to trigger SR to release enough Ca^{2+}, resulting in a loss or a weaker muscle contraction.

This report is partially supported by grant from NIH GM-50785 (W.C.) and EPRI (R.C.L.)

Tu-AM-C1

EQUILIBRIUM MEASUREMENT OF CADHERIN-CADHERIN BINDING ENERGY. ((R. A. Foty, C. R. Cho, P. MacNutt, and M. S. Steinberg)) Department of Molecular Biology, Princeton University, Princeton, NJ 08540

During morphogenesis, embryonic cell systems self-assemble to form specific tissue and organ structures. This assembly process has been attributed to the selective adhesive properties of different motile cell types. According to this hypothesis, as cells move relative to each other, the exchange of weaker for stronger intercellular bonds guides the system toward an equilibrium configuration of minimal adhesive free energy. The specific interfacial free energy of such a system can be quantified by determining the surface tension of a multicellular aggregate. Such measurements have confirmed the role of adhesive energies in tissue assembly. We transfected and cloned normally non-cohesive L cells to express the homophilic cell adhesion molecule P-cadherin at various levels. We then determined, for each clone, (1) the number of surface cadherin molecules per cell, by quantitative fluorescence labeling and flow cytometry; and (2) the surface tension (σ) of cell aggregates, by compression between parallel plates. σ was independent of the force applied to measure it, characterising these aggregates as Newtonian liquids. In order to determine the cohesion energy of a single cadherin-cadherin pair, we determined (3) the volume and surface area per cell in an aggregate. Cell volume was measured using confocal microscopy and computer-aided 3-dimensional reconstruction. Cell surface area was estimated based on the ideal cell-packing geometry that minimizes the ratio of surface area to volume of close-packed cells in an aggregate. The binding energy per cadherin pair was calculated and is reported here as both an absolute value and per $Å^2$ of adhesion dimer interface. This is the first equilibrium determination of cohesive energy between adhesion molecules *in vivo* .

Tu-AM-C2

NMR STUDIES OF CD4 PEPTIDES BOUND TO HIV GP120. ((D.B. Moffett, S.C. Busse, D. Gizachew, E.A. Dratz, M. Teintze)) Department of Chemistry and Biochemistry, Montana State University-Bozeman, Bozeman, MT 59717.

HIV, the virus which causes AIDS, primarily infects CD4+ T-lymphocytes. The initial step of HIV infection is the binding of the viral envelope glycoprotein gp120 to the CD4 receptor. Mutagenesis studies have suggested that the CDR2 region in the amino-terminal domain (D1) of CD4 is involved in gp120 binding. Peptides corresponding to parts of the CDR2 region of CD4 were synthesized and subjected to ELISA competition studies in order to determine their candidacy for TR-NOESY ^{1}H NMR studies. A 24 residue peptide was selected for TR-NOESY experiments to study the gp120-bound conformations. TR-NOESY spectra at different mixing times were used to determine ^{1}H-^{1}H distance constraints based on ISPA. Approximate structures were refined using Mardigras and simulated annealing. Spin echo filtered TR-NOESY data proved to be invaluable in the determination of ligand protons which were in the closest contact with the receptor and in the correction for the effects of spin diffusion between the ligand and the receptor. The use of the above methods has allowed us to determine a family of bound structures which suggest some deviation from the two published crystal structures of the CD4 D1D2 fragment determined in the absence of gp120. (Supported by NSF OSR-9350546).

Tu-AM-C3

GLYCOPHORIN AS A RECEPTOR FOR SENDAI VIRUS. (([1]R.M. Epand, [1]L. Wybenga, [1]R.F. Epand, [2]F.J. Sharom, [2]J. Chu, [3]S. Nir and [4]T. Flanagan)) [1]Dept. of Biochem., McMaster Univ., Hamilton, ON, L8N 3Z5, Canada; [2]Dept. of Chem. and Biochem., Guelph Univ., Guelph, ON, N1G 2W1, Canada; [3]Faculty of Agriculture, The Hebrew Univ. of Jerusalem, Rehovot 76100, Israel; [4]Dept. of Microbiol., School of Medicine and Biomedical Sciences, State University of New York at Buffalo, Buffalo, NY, 14214

Glycophorin A, the major sialoglycoprotein of the erythrocyte, was reconstituted into membranes of egg phosphatidylcholine. The size of the resulting liposomes was determined by quasielastic light scattering. Sendai virus was labelled with octadecylrhodamine. The fusion of this labelled virus with liposomes containing various mol fractions of glycophorin was studied by fluorescence dequenching. It was found that the presence of glycophorin markedly increased the fusion of Sendai virus with these liposomes. The kinetics and final extents of fusion were determined by the mass action analysis. Glycophorin increases both the association of the virus to a liposome as well as the rate of fusion of the bound virus. At equal mol fractions, glycophorin is more effective in accelerating fusion than is the sialic acid containing ganglioside, G_{D1a}. These results demonstrate that despite the fact that sialic acid would be on average situated further from the membrane surface in the case of glycophorin, this sialoprotein is nevertheless an effective receptor for Sendai virus, even enhancing the fusion rate constant.

Tu-AM-C4

ANTHRAX TOXIN AS A VEHICLE FOR PROTEIN TRANSLOCATION INTO CELLS. ((E. L. Lyszak, J. C. Milne, S. R. Blanke and R. J. Collier)) Department of Microbiology and Molecular Genetics, Harvard Medical School, Boston MA 02115.

Anthrax toxin is a member of the *binary* class of intracellularly acting bacterial toxins, in which the A and B moieties are synthesized as discrete proteins that associate with each other only after contact with sensitive mammalian cells. The B moiety, termed PA (protective antigen; 83 kDa), binds to receptors and is proteolytically activated by removal of a 20 kDa N-terminal segment. The remaining 63 kDa fragment (PA_{63}) then binds either of the two alternative A moieties (EF, edema factor, an adenylate cyclase; or LF, lethal factor, biochemical action unknown) and translocates them to the cytosol. Receptor-mediated endocytosis brings the receptor-bound complex to a low-pH compartment, presumably the endosome, where acidic conditions trigger insertion of PA_{63} into the membrane and translocation of bound EF/LF. The homologous N-terminal domains of EF and LF (e.g., LF_N, residues 1-255) bind these proteins to PA_{63}. When genetically fused to certain heterologous proteins, LF_N mediates the PA-dependent entry of these proteins into cells. We have found that a poly-cationic N-terminal tag (e.g., His_6 or Lys_6) can substitute for LF_N in mediating the entry of the A chain of diphtheria toxin. In contrast to LF_N-mediated entry, Lys_6-mediated entry is not blocked by free LF_N. Models of PA_{63}-mediated translocation of proteins containing LF_N or a poly-cationic tail will be presented, making reference to the crystallographic structure of native PA recently determined by C. Petosa, R. Liddington and coworkers. Potential applications of the anthrax toxin system for introducing heterologous proteins into cells will be discussed.

Tu-AM-C5

THERMODYNAMIC ANALYSIS OF BINDING OF THE *ESCHERICHIA COLI* REPRESSOR OF BIOTIN BIOSYNTHESIS TO SMALL LIGANDS ((Yan Xu and Dorothy Beckett)) Department of Chemistry and Biochemistry, University of Maryland Baltimore County, Baltimore, MD 21228

BirA is the transcriptional repressor of biotin biosynthesis and a biotin holoenzyme synthetase. It catalyzes synthesis of biotinyl-5'-AMP from the substrates biotin and ATP. The adenylate is the activated intermediate in the biotin transfer reaction as well as the positive allosteric effector for site specific DNA binding.The affinity of BirA for the adenylate is considerably greater than its affinity for biotin and both binding reactions are coupled to changes in the conformation of the protein. The temperature dependencies of the two binding interactions have been determined using kinetic techniques.Van't Hoff analyses of the resulting equilibrium dissociation constants indicate that while the two binding processes are characterized by large negative enthalpies, the entropic contributions are small for both. Binding enthalpies have also been determined by isothermal titration calorimetry. Consistent with the results of the van't Hoff analyses, the calorimetric enthalpies are large and negative.The greater precision of the calorimetric measurements allowed more accurate estimation of the entropic contributions to the binding processes, which are of opposite sign for the two ligands. In addition, the apparent heat capacity changes associated with the two binding reactions are small. The large favorable enthalpic contributions to the binding reactions are consistent with processes driven by formation of hydrogen bonding and van der Waals interactions and the lower affinity of BirA for biotin reflects an unfavorable entropic contribution to the binding process. Analysis of the heat capacity changes in terms of coupled folding events indicates that while a disorder to order transition accompanies biotin binding, a net disordering of the polypeptide chain occurs upon binding of bio-5'-AMP.

Tu-AM-C6

BINDING OF FATTY ACIDS TO ALANINE MUTANTS OF INTESTINAL FABP MONITORED WITH ADIFAB. ((Alan M. Kleinfeld, Gary V. Richieri, and Ronald T. Ogata)) Medical Biology Institute, La Jolla CA.

Fatty acid binding protein from rat intestine binds fatty acids (FA) in a cavity buried within the protein. Eighteen of the protein s amino acid side chains in this binding cavity are located along the length of the FA hydrocarbon chain. In the present study we have engineered and expressed single alanine mutants of each of these 18 amino acids. Binding of FA to these 18 variants was measured using the fluorescent probe, ADIFAB. Affinities were found to vary for the same FA, up to 1000 fold for the different mutants. Relative to the native protein, these mutations resulted in proteins with both lower as well as higher affinities and with proteins having altered FA specificities. A number of mutants revealed binding patterns that were unexpected. For example, binding was significantly reduced (4 to 10 fold) for the Arg126Ala mutant, although Arg 126 does not directly interact with the FA. In contrast, binding was reduced by less than 50 % for the Tyr70Ala mutant, although Tyr70 is only 3.9 ∝ from the C2 carbon of the FA and appears to be involved in maintaining a sharp bend in the FA at C2. Even more surprising are results for the Arg106 mutant which is expected to form an electrostatic interaction with the carboxylate of the FA. Depending upon the FA type, the affinity of the Arg106Ala mutant is between 5 and 30 fold greater than the native. The thermodynamic parameters for this mutant reveal an approximately 2-6 kcal/mol reduction in the enthalpic contribution to the free energy, as would be expected for a loss of electrostatic interaction, but this reduction is more than compensated for by a large increase in entropy. Thus, in general this study reveals that the interactions governing binding of FA to FABP involve admixtures of large enthalpy and entropy changes that tend to compensate. Even relatively small imbalances, however, in this enthalpy-entropy mixture can result in large changes in affinities. This work was supported with a grant GM46931 from the NIH.

Tu-AM-C7

AN EFFECTIVE POTENTIAL EXPLAINS CO BINDING TO HORSE-MYOGLOBIN ((Noam Agmon)) Physical Chemistry, The Heberw University, Jerusalem 91904, Israel.

CO binding to horse-myoglobin can be fitted quantitatively to the two-dimensional Agmon-Hopfield model over the entire temperature range if the effective protein-mode potential is made proportional to temperature. This implies that the effective protein potential is entropic, as in the theory of rubber elasticity. From the fits to the data it is possible to determine, at each temperature, when the protein relaxation begins and ends. This is corroborated by multi-pulse kinetics. Before the onset of relaxation one expects inhomogeneous kinetic hole burning effects. After its termination, ligand escape commences and the model is no longer applicable.

Tu-AM-C8

Structural Energetics of Na^+ Binding to Thrombin.

Enrico Di Cera and Enriqueta R. Guinto. Dept Biochem & Mol Biophys, Washington Univ Med School, St. Louis, MO 63110.

Binding of Na^+ to the loop connecting the last two β-strands of the B chain of thrombin converts the enzyme from the anticoagulant slow form to the procoagulant fast form. The binding interaction is linked to a significant change in heat capacity (ΔC_P=−1.5±0.2 kcal/mol/K), suggesting a substantial structural reorganization of the water channel around the Na^+ site in the slow→fast transition. Changes in ionic strength, from 50 to 800 mM, have little effect on Na^+ binding. These findings suggest that the origin of Na^+ specificity in thrombin is largely due to hydrophobic, rather than electrostatic components, and have a bearing on the study of monovalent cation effects in proteins in general. Site-directed mutagenesis of residues in the allosteric core of thrombin reveals perturbations of the Na^+ binding energetics that carry over to the recognition of physiological substrates, effectors and inhibitors.

Tu-AM-C9

HYDROGEN BONDING IN CYCLODEXTRIN: EXPERIMENTAL REALITY AND COMPUTATIONAL MODELS. ((T. Kozar[1] and C.A. Venanzi[2])), [1]Inst. of Experimental Physics, Slovak Academy of Sciences, Kosice, Slovakia, and [2]Chemistry Div., New Jersey Inst. of Tech Newark, NJ

Cyclodextrins are macrocycles built from glucose units. In addition to their ability to form inclusion complexes with aromatic substrates and to serve as templates for artificial enzyme design, they are good molecules with which to study hydrogen bonding. The intramolecular O2...O3' hydrogen bonding between adjacent glucose units is a characteristic feature of these molecules. This hydrogen bonding stabilizes the structure of the macroring, as was shown by our recent molecular mechanics and dynamics modeling studies of ß-cyclodextrin. In contrast, the X-ray crystal structures of methylated cyclodextrins, where the O2...O3' hydrogen-bonding cannot exist, reveal not only deformation in the structure of the macroring but also a distortion of one of the chair conformations of glucoses to a non-chair form. Many other structures of cyclodextrins are available in the Cambridge Crystallographic Database. In addition, the structures of α- and ß-cyclodextrin bound to soybean ß-amylase and to the maltodextrin binding protein are available from the Brookhaven Protein Databank. Analysis of this multitude of structures offers the oportunity to probe the relationship between the composition of the cyclodextrin molecule (substituent pattern, ring size), environmental effects (crystal, solvent, or protein), and the structure and hydrogen bonding stabilization of the macroring. Such a comparison based on statistical analysis of the experimental structural data and theoretical modeling of the hydrogen bonding is the aim of the present study. This work was supported by a grant to T.K. and C.A.V. from the National Science Foundation.

CALCIUM CHANNEL GATING

Tu-AM-D1

INACTIVATION OF IONIC CURRENT AND INTERCONVERSION OF GATING CHARGE IN α_{1C}/β_{2a} Ca^{2+} CHANNELS EXPRESSED IN A MAMMALIAN CELL LINE. ((G.Ferreira, E.Rios and R.Shirokov)) Rush University, Chicago, IL 60612.

Intramembrane charge movement and ionic currents were recorded in tsA 201 cells transfected with α_{1C} and β_{2a} Ca^{2+} channel cDNA. To record charge movement, ionic currents were blocked by 10 μM Gd^{3+} added extracellularly.

The mobile charge (Q) available correlated with maximal current density (r^2=0.8). 0.23 ± 0.08 fC (n=10) of Q corresponded to 1 pA of current at +20 mV in 10 mM Ca^{2+} solution. The ratio of charge/current was about one tenth of that of native channels. This has two possible, not exclusive interpretations: the open probability of the expressed channels is much higher than that of the native channels, and/or Q in cardiomyocytes is generated by a heterogeneous population of voltage sensors some of which do not pass current.

Steady state availability of Q and Ba^{2+} currents (I_{Ba}), was studied. Minimal availability of Q (70±15%, n=4) was greater than that of I_{Ba} (16±5%, n=10). Long depolarization promoted charge mobile at negative voltages (Q2), associated with transitions in inactivated channels (Brum & Rios, 1987), in parallel with the reduction of charge related to channel opening (Q1). Reduction of Q1 after depolarization was close to the amount of Q2 that appeared.

As Q2 moves at very negative voltages, it was possible to measure it with and without the ionic current blocker. Gd^{3+} did not alter the amount of Q2. Verapamil (100 μM) blocked I_{Ba} and promoted appearance of a charge mobile at negative voltages, as it does in native channels (Pizarro et. al, 1988, Shirokov et. al, 1991). The amount of this charge was equal to Q2 induced by depolarization.

The results show that inactivation of expressed channels is accompanied by Q1-Q2 interconversion. However, the interconversion is less complete than inactivation of ionic current. To describe gating of native channels a four state model in which Q2 moves between two inactivated states was used. This model cannot account for the present data. (Supported by AHA-MC and NIH).

Tu-AM-D2

CARDIAC L-TYPE CALCIUM CHANNELS EXPRESSED IN HEK293 CELLS EXHIBIT TWO COMPONENTS OF VOLTAGE-DEPENDENT GATING AND CHARGE MOVEMENT. ((T.J. Kamp and E. Marban)) Johns Hopkins University, Baltimore, MD, 21218.

In isolated cardiac myocytes L-type Ca channels exhibit classical voltage-dependent gating and also display voltage-dependent potentiation of channel activity. The relationship between these forms of channel gating and the movement of gating charge is unknown. Plasmids encoding the α_{1C}+β_{1a} subunits of the Ca channel were transiently transfected into HEK293 cells by the Ca phosphate method. Using 10 mM Ba^{++} as the charge carrier, tail currents were recorded after families of 25 ms depolarizing pulses (-50 to 120 mV). Following threshold depolarizations up to -20 mV the tail current could be described by a single exponential decay, but following more positive pulses (≥-10 mV) the tail currents were best described by two exponentials. The relationship between test potential and instantaneous tail current amplitude is best described by two Boltzmann distributions ($V_{1/2}$=9±5 mV and $V_{1/2}$=74±12 mV). Charge movement (Q) was also examined in the presence of 2 mM Cd and 0.1 mM La to block ionic current. The Q vs. voltage relationship also consisted of two Boltzmann distributions ($V_{1/2}$=-8±7 mV and $V_{1/2}$=58±14 mV). The relative amplitudes of the two Q components varied greatly among cells as did the extent of potentiation of ionic current. These results suggest that an additional gating charge movement process recruited at positive potentials underlies voltage-dependent potentiation.

Tu-AM-D3

CALCIUM-DEPENDENT INACTIVATION OF HETEROLOGOUSLY EXPRESSED CARDIAC L-TYPE CALCIUM CHANNELS. ((Brett Adams and Tsutomu Tanabe)) Dept. of Physiology & Biophysics, University of Iowa, Iowa City, IA 52242 and Dept. of Cellular & Molecular Physiology, Yale University School of Medicine, New Haven, CT 06536-0812.

We investigated the structural basis for Ca-dependent inactivation (CDI) of the cardiac L-type Ca channel. Expression plasmids encoding the rabbit wild-type cardiac α1C subunit, or chimeras of α1C and the rabbit skeletal muscle α1S subunit, were transiently coexpressed in HEK293 cells along with rabbit skeletal muscle α2 and β1a subunits. Whole-cell currents were recorded using standard patch-clamp techniques. Currents mediated by the full-length (C1-2171) wild-type α1C displayed clear CDI, as did currents mediated by a 3' deletion mutant of α1C (C1-1812;C2167-2171). In contrast, CDI was not exhibited by CSk4, a chimera of the α1C and α1S subunits (C1-1622; Sk1498-1873). Interestingly, CDI was unambiguously displayed by CSk5, which is identical to CSk4 except that its C-terminus is truncated (C1-1622; Sk1498-1662). These results provide new insights into the molecular basis of CDI. Supported by the Iowa Heart Association (B.A.) and HHMI (T.T.).

Tu-AM-D4

EF-HAND REGION CONTAINING BOTH SUFFICIENT AND REGULATORY STRUCTURAL ELEMENTS FOR Ca^{2+} INACTIVATION OF L-TYPE Ca CHANNELS ((Y. Wang, M. de Leon and D.T. Yue)) Johns Hopkins Univ., Baltimore, MD 21205

Ca^{2+} inactivation of L-type (α_{1C}) Ca channels provides critical feedback regulation of Ca^{2+} entry into a wide variety of cells. Taking advantage of the lack of Ca^{2+} inactivation in neuronal α_{1E} Ca channels, we have recently used chimeric analysis of α_{1C} and α_{1E} channel subunits to demonstrate that an EF-hand motif in the C-terminus of α_{1C} is a *necessary* molecular determinant of inactivation (de Leon et al., *Science*, in press). Here, we argue that this EF-hand alone is *sufficient* to confer Ca^{2+} inactivation upon the main α_{1C} backbone, and that flanking regions of the channel modulate the degree of Ca^{2+} inactivation. CE-5Δ (below) demonstrates the sufficiency of the EF hand to support the inactivating phenotype: although only the α_{1C} EF hand is paired with the α_{1C} backbone, this construct still manifests detectable, albeit blunted Ca^{2+} inactivation. The regulatory influence of adjacent α_{1C} sequence becomes apparent with the progressive restoration of Ca^{2+} inactivation to intact α_{1C} levels by incremental inclusion of ≈150 amino acids located immediately C-terminal to the EF hand (Ca^{2+} inactivation of CE-5Δ < CE-4Δ < Δ1733 = α_{1C}). Alternatively, the identity of the channel backbone also influences the extent of Ca^{2+} inactivation. While Ca^{2+} inactivation can be donated to the α_{1E} backbone by the C-terminus of α_{1C}, more of the C-terminus is required to confer inactivation (below right). These results localize domains that may be functional in isolation, thereby opening the way for biochemical studies of the Ca^{2+} inactivation mechanism.

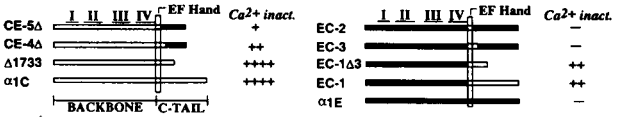

Tu-AM-D5

ALTERED VOLTAGE DEPENDENCE OF L-TYPE CALCIUM CURRENT BY S4 SEGMENT AND LEUCINE-HEPTAD REPEAT MUTATIONS. ((J. García, J. Nakai*, K. Imoto* & K.G. Beam)) Colorado State University and *Natl. Institute for Physiological Sciences.

Single charged residues (Arg) were exchanged for neutral (Gln) or negative (Glu) amino acids in the S4 segments of repeats I-IV of a chimeric L-type calcium channel (SkC15). Additionally, Leu and an Ile in the first and third repeats were exchanged for Val in the leucine-heptad repeat region between segments S4-S5 since this region is important for activation of *Shaker* potassium channels (McCormack et al., PNAS, 1991). Most of the mutations caused a decrease in the slope of the voltage dependence, indicating a reduced sensitivity of the channel to potential. S4 mutations in repeats I and III, but not in II or IV, significantly affected the half-activation potential. In both repeats I and III, substitution of Leu closer to the S4 segment caused a positive shift of the half-activation potential while substitution of Leu closer to S5 (or the corresponding Ile in repeat III) caused a negative shift. These shifts were similar in magnitude to those of the S4 mutants. The shifts caused by the heptad repeat mutations were in the same direction (negative or positive) as for the *Shaker* channel. All the mutants in the S4 segment of repeats I and III and the Leu close to IS4 caused a change in the time constant of activation of the current. These results suggest that repeats I and III are especially important for activation of the calcium current. Supported by NIH.

Tu-AM-D6

INTERACTION BETWEEN N-TYPE Ca^{2+} CHANNEL INACTIVATION GATING AND BINDING OF AN ω-CONOTOXIN. ((J.W. Stocker, L. Nadasdi#, D. Silva#, R.W. Aldrich* and R.W. Tsien)) Dept. Mol. Cell. Physiol., *HHMI, Stanford University, CA 94305 and #Neurex Corporation, Menlo Park, CA 94025.

SNX-331, a derivative of ω-conotoxin MVIIC, is one of several toxins found to reversibly block N-type Ca^{2+} channels. We expressed N-type channels in *Xenopus* oocytes (α_{1B}, α_2, β_1 cRNAs) and found that block by SNX-331 increases in severity as the holding potential (HP) is progressively depolarized (Figure). Changes in HP markedly alter the kinetics of the onset and wash-off of toxin. Simple exponential kinetics are seen at HP=-120 mV, where few of the channels are inactivated. In contrast, biphasic kinetics are seen at HP=-70 mV, where ~50% of the channels are inactivated. The complex kinetics can be accounted for by a four-state modulated receptor model in which toxin dissociation from the inactivated state (I) is ~100-fold slower than from the resting state (R), and bound toxin retards equilibration between R and I. Since ω-conotoxins are known to act from outside cells, these results suggest that an external region of the channel which interacts with the toxin undergoes a conformational change as part of the process of inactivation.

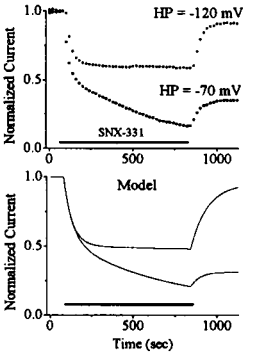

Tu-AM-D7

The β Subunit Increases Ca^{2+} Currents *and* Gating Charge Movements of Human Cardiac L-Type Ca^{2+} Channels ((I.R. Josephson and G. Varadi)) Mol. & Cell. Physiol. and Inst. of Mol. Pharm. & Biophys., University of Cincinnati, Cincinnati, OH.

The properties of the gating currents (nonlinear charge movements) of human cardiac L-type Ca^{2+} channels, and their relationship to the activation of the Ca^{2+} channel (ionic) currents were studied using a mammalian expression system. Cloned human cardiac $\alpha_1+\alpha_2$ subunits, or human cardiac $\alpha_1+\alpha_2+\beta$ subunits were transiently expressed in HEK293 cells. The maximum Ca^{2+} current density increased from - 3.9 +/- 0.9 pA/pF for the $\alpha_1+\alpha_2$ subunits to -11.6 +/- 2.2 pA/pF for $\alpha_1+\alpha_2+\beta$ subunits. Calcium channel gating currents were recorded following the addition of 5 mM Co^{2+}. The maximum nonlinear charge movement (Q_{max}) increased from 2.5 +/- 0.3 nC/uF for $\alpha_1+\alpha_2$, to 12.1 +/- 0.3 nC/uF for $\alpha_1+\alpha_2+\beta$ subunit expression. The Q_{ON} was equal to the Q_{OFF} for both subunit combinations. The Q_{ON}-V_m data were fit by a sum of two Boltzmann expressions and ranged over more negative potentials, as compared with the activation of the Ca^{2+} conductance. We conclude that: 1) the β subunit increases the number of functional α_1 subunits expressed in the plasma membrane of these cells, and 2) the activation of the human cardiac L-type calcium channel involves the movements of at least two, functionally distinct gating structures.

Tu-AM-D8

ALTERATION OF VOLTAGE-DEPENDENT GATING OF P-TYPE AND α_{1A} CALCIUM CHANNELS BY ω-GRAMMOTOXIN-SIA ((S.I. McDonough[1], F. Noceti[2], E. Stefani[2], R.A. Lampe[3], and B.P. Bean[1])) [1]Vollum Institute, OHSU, Portland OR 97201; [2]Dept. Anesthesiology, UCLA, Los Angeles CA 90095; [3]Zeneca Pharmaceuticals, Wilmington DE 19897 (Spon. by B.P. Bean)

ω-Grammotoxin SIA (GsTx), a 36 residue peptide from *Grammostola Spatulata* venom, completely inhibited Ba^{2+}-carried inward current through P-type calcium channels in rat cerebellar Purkinje neurons at concentrations ≥ 50 nM. However, Cs^+-carried outward currents elicited by depolarizations to >+110 mV were actually larger with GsTx and activated more slowly than in control. Tail current activation curves fit by Boltzmann functions showed that GsTx shifted the midpoint for channel activation by +111 ± 2 mV and made the curve more shallow (slope factor changed from 7 ± 1 mV in control to 26 ± 3 mV with GsTx). Reversibility of GsTx block was dramatically enhanced by trains of depolarizing pulses. Effects of GsTx were also studied on cloned Ca^{2+} channels expressed in *Xenopus* oocytes. At ~ 1 μM, GsTx inhibited peak inward current through α_{1A}-β_{2a} channels by ~ 90% but had little effect on α_{1E}-β_{1b} channels (~ 10% inhibition) and none on α_{1C} channels. As for native P-type channels, the α_{1A} activation curve was shifted to dramatically more positive potentials and the slope was made more shallow.

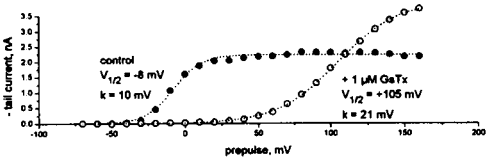

Tu-AM-E1

SUPRAMOLECULAR STRUCTURES OF Aβ AGGREGATES AND CELLULAR RESPONSES. ((W.B. Stine, A. Roher†, L.J. Van Eldik,* J. Hu,* F. Castets,* W.L. Klein,‡ C. Zhang,‡ M.M. Berg,‡ G.A. Krafft)) Depts. of Molecular Pharmacology and Biological Chemistry, *Cell and Molecular Biology, Northwestern University Medical School, Chicago, IL 60611-3008; †Dept. of Neurobiology and Physiology, Northwestern Univ., Evanston, IL 60208 'Sun Health Research Institute, Sun City, AZ 85351

The amyloid β (Aβ) peptide has been implicated as a major causative or contributory factor in Alzheimer's disease (AD). Aβ exists in several different forms in the brain, including neuritic core plaques and diffuse deposits. Many diffuse deposits, but also some dense Aβ plaques are not associated with any neuronal pathology. This *in vivo* circumstance has certain parallels with *in vitro* experiments involving Aβ and neurotoxicity, i.e. some forms of Aβ elicit cell death while others (monomer and "overaged" aggregates) do not. In this presentation, we describe the highest resolution images of Aβ aggregates obtained by atomic force microscopy (AFM), images that have allowed us to identify distinct supramolecular forms of Aβ. We also describe experiments demonstrating that particular forms of Aβ are capable of inducing certain responses in glial cells, including glial activation. Certain other Aβ preparations are capable of inducing specific neuronal responses, including an increase in focal adhesion kinase (FAK) phosphorylation on tyrosine, and specific localization of FAK and the *src* family kinase *fyn* to the triton insoluble, cytoskeletal fraction. On the basis of these results, we hypothesize that glial activation by Aβ induces an inflammatory glial-neuronal micro-environment that can modify the specific supramolecular structures of Aβ aggregates that form, and enhance the ability of these aggregates to induce neuronal pathology.

Tu-AM-E2

PURIFICATION OF RI, RII AND RIII SODIUM CHANNEL SUBTYPES FROM ADULT RAT BRAIN WITH IMMUNOAFFINITY COLUMNS ((A.M. Corbett)) Dept. of Biochemistry & Molecular Biology; Wright State University, Dayton, OH 45435.

Partially purified rabbit polyclonal antibodies, directed against unique sequences in the carboxyl tail of sodium channels RI, RII and RIII, were coupled to cyanogen-bromide activated Sepharose beads. Sodium channels were solubilized from rat brain P2 and P3 membranes and the solubilized material (approximately 72 mg total) was run over the antibody affinity columns overnight. Lightly bound material was eluted with 0.5 M KCl (approximately 1 mg/column), but although assays indicated that these were pure sodium channels, but exact subtype composition remains to be determined. Material which bound with high affinity to the columns was eluted with 3 M $MgCl_2$: these fractions displayed a single band of 200-260 kDa in the absence of β-mercaptoethanol on SDS-PAGE and were recognized by sodium channel antibodies on western blots. Approximately 300 μg of purified sodium channel subtypes were obtained from each column: these ran as a single peak on C4 reverse phase columns. Purified channel subtypes were subjected to V8 protease (Glu-C) hydrolysis overnight and run on C18 reverse phase columns: each purified subtype produced a unique chromatographic pattern of peptide digests, indicating that each is a unique gene product. Supported by NIH NS28377.

Tu-AM-E3

SUBUNIT INTERACTIONS OF THE VOLTAGE-GATED *SHAKER*- LIKE K^+ CHANNEL. ((J. Xu, W. Yu, M. Bezanilla, and M. Li)) Department of Physiology, School of Medicine, Johns Hopkins University, Baltimore, MD 21205

There are at least five subfamilies of the *Shaker* -like K^+ channels: Kv1 to Kv5. Four α-subunits within a given subfamily can form a channel, either as a homotetramer or heterotetramer. The diverse functions of K^+ channels are thought to be further modulated by hydrophilic β-subunits, such as Kvβ1. To understand the molecular mechanisms of assembly and regulatory interactions among the various subunits, we have investigated molecular determinants that are essential for the physical and functional interactions. Using a combination of biochemical binding, yeast two hybrid system, and electrophysiological analysis, we have shown that the conserved regions (called NAB) within the hydrophilic NH_2-terminal domains of Kv1 to Kv4 α-subunits mediate the subfamily-specific interactions between α-subunits. Additionally, the NAB_{Kv1} interacts with Kvβ1 in a subfamily manner; and this interaction is essential for the Kvβ1-mediated inactivation. Our data suggest that Kvβ1 selectively modulates a subset of K^+ channels through the specific assembly of α–β complexes, and reveal the dual function of the NAB domain in mediating the assembly of both α–α and α–β complexes.

Tu-AM-E4

FUNCTIONAL INTERACTIONS OF α AND β SUBUNITS OF THE K^+ CHANNEL. ((M. Bezanilla, J. Xu, W. Yu, and M. Li)) Department of Physiology, School of Medicine, Johns Hopkins University, Baltimore, MD 21205

Functional interactions between the pore-forming α and the cytoplasmic β subunits of the K^+ channel have been observed as kinetic alterations of channel properties when these subunits were coexpressed in either *Xenopus* oocytes or mammalian cells. We have recently demonstrated that Kvβ1 binds the N-terminal region of the α subunit from the Kv1 subfamily and that this physical interaction is required for Kvβ1 to accelerate the inactivation of the α subunit. However, little is known about other types of functional interactions between these subunits. We have coexpressed various α and β subunits in COS cells in order to study how expression of one subunit can be modulated by the presence of another subunit. Using a combination of biochemical and electrophysiological techniques, we have begun to identify a complex network of regulatory interactions, which may have important physiological implications.

Tu-AM-E5

INTRACELLULAR K^+ ALTERS FLICKER GATING OF BK CHANNELS FROM EMBRYONIC RAT TELENCEPHALON. ((J.-M. Mienville and J.R. Clay)) NIH, Bethesda, MD 20892 (Spon: D. Alkon)

We have observed significant effects of changes in K^+_i on flickering of the large conductance Ca-activated K channel (BK) during patch clamp recordings from E12-14 rat telencephalon. Specifically, flicker gating was voltage dependent, i.e., it was reduced by depolarization in the -60 to -10 mV range with equimolar concentrations of K^+ ions (150 K^+_o/150 K^+_i). Removal of K^+_i resulted in significant flickering at all potentials in this voltage range. In other words, the voltage dependence of flicker gating was effectively eliminated by the removal of K^+_i. This suggests that a K^+ ion entering the channel from the intracellular medium binds, in a voltage-dependent manner, at a site which locks the flicker gate in its open position. No effects of changes in K^+_i were observed on the primary, voltage-dependent gate of the channel. The change in flickering did not cause a change in the mean burst duration, which indicates that the primary gate is stochastically independent of the flicker gate. Intracellular Rb^+ can substitute for - and is even more effective than - K^+_i in suppressing flickering. Substitution of Rb^+_i for K^+_i also increased the mean burst duration for V > -30 mV. Both effects of Rb^+_i were removed by membrane hyperpolarization.

Tu-AM-E6

THE RAT BRAIN *ETHER-A-GO-GO* POTASSIUM CHANNEL: A HIGH AFFINITY CALCIUM SENSOR. ((C. Stansfeld, J. Röper, J. Ludwig, R. Weseloh, S. Marsh, D. Brown and O. Pongs)) *ZMNH, Haus 42, Martinistrasse 52, D-20246 Hamburg, Germany and Dept. Pharmacology, University College London, Gower St, London WC1E 6BT*

The rat *ether-a-go-go* (*eag*), voltage-gated K channel is widely expressed in brain (Ludwig et al., EMBO J. 13, 4451-4458 (1994)) and it is a mammalian homologue of the *Drosophila eag* channel (Warmke et al., Science 252, 1560-1562 (1991)). We have studied the currents generated by rat *eag* channels following their expression in human embryonic kidney cells, and we observed an essential dependency on low cytosolic Ca^{++}. In whole cell recordings, currents declined within seconds if pipette free calcium was above 200 nM. Recording via patches perforated with amphotericin B, whole cell currents were reversibly inhibited by either extracellular application of a calcium ionophore, 5 μM ionomycin, or 10 μM muscarine. Muscarine induced a series of transient, total suppressions of the rat *eag* current which mirrored the occurrence of cytosolic calcium spikes, as observed using the fluorescent Ca^{++} indicator indo-1. Current suppression was not voltage-dependent and did not involve obvious change in either activation kinetics or leak conductance. In inside-out patches, in a physiological K gradient, the unitary currents of 7 pS were reversibly blocked by Ca^{++} with an IC_{50} of 67 nM and a Hill slope of 1.5. No change in unitary conductance, or open times occurred, but long shut intervals increased. Together the observations propose an interesting role for the rat *eag* channel in combined calcium and voltage signal integration.
(*Supported by the Deutsche Forschungsgemeinschaft and Wellcome Trust.*)

Tu-AM-E7

A SLOW VOLTAGE-ACTIVATED OUTWARD CURRENT IN PITUITARY NERVE TERMINALS. ((G. Kilic, A. Stolpe and M. Lindau)) Max-Planck Institute for Medical Research, 69120 Heidelberg, Germany.

In isolated nerve terminals of the posterior pitutary Na-current, A-current, Ca-currents and K(Ca) currents have been described (Lemos et al.1986 Nature 319:410, Wang et al.1992 J Physiol 457:47). After blocking A-current (4-AP 20 mM) and Ca-current (Cd^{2+} 0.1 mM) in the patch-clamp whole-terminal configuration we observed a novel slow current which was activated by depolarization for several seconds. Activation was detectable at -60 mV with $V_{1/2}$ of about -40 mV (holding potential -84 mV). A positive shift of reversal potental after increasing external [K^+] indicated K^+ selectivity. Activation time constants ranged from 1 s at +30 mV to 5 s at -40 mV. Slow current was detectable (>20 pA/pF) in 88% of the terminals when a pipette solution with low free [Mg^{2+}] (< 100 µM) was used. At +6 mV after 5 s of depolarization the mean current was 75 ± 53 pA/pF (SD, n=66). At the end of recording terminals were sucked into the pipette and analyzed for vasopressin content. No correlation between vasopressin content and current amplitude was detectable. Using noise analysis single-channel current was estimated to be 0.4 pA at +6 mV. When the pipette solution contained 5 mM free Mg^{2+}, the slow current was never observed (n=12). The slow current in pituitary nerve terminals is very similar to the slowly activating delayed rectifier (slow I_K) present in heart cells (Simmons et al.1986 J Gen Physiol 88:739). Although the absolute size of the current is small, the current density (75 pA/pF) is much higher than in heart cells (14 pA/pF, Duchatelle-Gourdon et al.1991 J Physiol 435:333). This current may contribute to shape the slow variations in bursting patterns required to optimize hormone release (Cazalis et al. 1987 J Physiol 390:71).

TRANSMEMBRANE SIGNALING - MECHANISMS

Tu-AM-F1

STRUCTURE OF THE CYTOPLASMIC SURFACE OF BOVINE RHODOPSIN. ((P.L. Yeagle, J.L. Alderfer and A.D. Albert)) Department of Biochemistry, University at Buffalo School of Medicine and Biomedical Sciences, Buffalo, NY 14214 and Department of Biophysics, Roswell Park Cancer Institute, Buffalo, NY 14263

An alternative approach to determination of the three-dimensional high resolution structure of rhodopsin is described. We are pursuing the structure of the cytoplasmic domains of this G-protein receptor by ^1H nuclear magnetic resonance. Each of the domains that has been studied showed biological activity, inhibiting the light-stimulated activation of the rod cell phosphodiesterase by rhodopsin in rod outer segment disks. These domains therefore likely contain structural elements characteristic of native rhodopsin. Previously the structure of the 33 amino acid carboxyl terminal domain was reported. More recently, the structure of a larger peptide, the 43 amino acid carboxyl terminal domain which includes part of the seventh transmembrane helix of rhodopsin, was solved. The structure of the peptide, rhoIII, with the sequence of the third cytoplasmic loop of bovine rhodopsin, was also solved. Work is in progress on the second cytoplasmic loop. Together the structure of these biologically active domains provide a view of the structure of much of the cytoplasmic surface of rhodopsin. Examination of potential interactions between this surface and the G protein, tranducin, suggested a molecular switch for activation of the G protein by the receptor.

NEI EY03328

Tu-AM-F2

GLU^{134}-ARG^{135} IN RHODOPSIN IS A GDP-RELEASE-SWITCH FOR TRANSDUCIN. ((Shreeta Acharya and Sadashiva Karnik)) Department of Molecular Cardiology, Research Institute, The Cleveland Clinic Foundation, Cleveland, Ohio.

GDP-release from guanine nucleotide binding proteins (G-proteins) is the rate-limiting step in switching their conformation from the inactive GDP-bound state to the active GTP-bound state[1-4]. The cytoplasmic domain of activated G-protein coupled receptors (GPCRs) directly binds and activates heterotrimeric ($\alpha\beta\gamma$) G-proteins[3-12]. We show here that Glu^{134} Arg^{135} in the cytoplasmic domain of the photoreceptor rhodopsin regulates GDP-release in the activation of the retinal G-protein, transducin (G_t). Mutations at Arg^{135} abolish release of GDP from G_t and specific mutations at Glu^{134} stimulate GDP release without light activation. In the double mutants, constructed to combine both these effects, GDP release is abrogated. The spectroscopic characteristics and stabilisation of their metarhodopsin II state by G_t-derived peptides are not affected implying that the global structure is undisturbed. We propose that Glu^{134} and Arg^{135} constitute the site that directly provides the "signal" from rhodopsin to activate GDP-release from transducin. Conservation of a charged pair, Asp/Glu-Arg sequence at a topologically similar location in the putative cytoplasmic domain of most GPCRs implies that they too might deploy the same GDP-release-switch to initiate the signal transduction cascade.

Tu-AM-F3

NEW EVIDENCE THAT ALZHEIMER'S BETA-AMYLOID PEPTIDE ENTERS CELL MEMBRANES. ((Z. Galdzicki, G. Ehrenstein, A. Balbo, S.I. Rapoport, F.J. Castellino, and B.A.K. Chibber)) Laboratory of Neurosciences, NIA, NIH and Biophysics Section, NINDS, NIH, Bethesda, MD 20892, and Dept. of Chemistry and Biochemistry, Univ. of Notre Dame, Notre Dame, IN 46556

Beta-amyloid peptide is a product of processing of amyloid precursor protein (APP). A number of mutations involving APP have been shown to occur in early-onset Alzheimer's disease. We previously showed that beta-amyloid peptide (1-40) increases the permeability of PC12 cell membranes to choline and to calcium, implying entry of peptide into the membranes. We now have visualized that entry by use of fluorescent labelled beta-amyloid peptide. PC12 cells were grown in culture conditions and were exposed to dansylated beta-amyloid (1-40) and (1-42) at 46 µM for periods of up to 48 hours. Because fluorescence from the dansyl group is strongly quenched by a hydrophilic micro-environment, detection of a fluorescent signal after excitation at 340 nm indicates that this group is embedded in a hydrophobic micro-environment of membrane or of membrane protein. The fluorescent signal showed a steady increase for at least 24 hours, consistent with time-dependent changes in calcium and choline permeability. The spatial distribution of the signal indicated localization at the membrane. The fluorescent signal was not attenuated when the cells were permeabilized with 10 µM of digitonin for peptide (1-40), whereas the signal was diminished for peptide (1-42). Our observations are consistent with entry of beta-amyloid peptide (1-40) into membranes of PC12 cells.

Tu-AM-F4

ASYMMETRICAL DISPLACEMENT CURRENTS ASSOCIATED WITH THE INCORPORATION OF AMYLOID β-PROTEIN [AβP(1-40)] INTO PLANAR BILAYERS (J. Vargas, N. Arispe and E. Rojas). Dept. Physiol. Biophys., Fac. of Med., Univ. of Chile, Stgo. and LCBG, NIDDK, NIH, Bethesda, MD

Specific interactions between Alzheimer's Disease AβP(1-40) molecules in solution and the lipids in planar bilayer membranes allow the formation of cation-selective channels. To study the details of these interactions, we measured the charge movements across planar bilayer membranes associated with the incorporation of AβP(1-40) added to the solution (50 mM KCl) on the *cis* side (*ca.* 1-2 µM). As predicted from our model of the channel (Durel *et al*, Biophys. J. 67, 2137, 1994), the insertion of AβP(1-40) molecules across the bilayer should induce the appearance of a non-linear component of the membrane capacitance which could be detected as an asymmetrical charge movement. For a small circular bilayer (*ca.* 35 µm diameter), the AβP(1-40)-specific transfer of charge reached a maximum value of *ca.* 35 fC when the *cis* side potential was taken to *ca.* 160 mV. The time course of the displacement current both during and after a rectangular pulse could be fit using two time constants. Furthermore, the size of the AβP(1-40)-specific charge displaced in one direction during a pulse was always equal to the charge returning to the original configuration after the pulse. We also determined that the maximum increase in amyloid-dependent membrane capacitance (*ca.* 250 fF) occurred at 160 mV. These properties of the AβP(1-40)-specific charge displacement support our view that the hairpin domain of the AβP(1-40), containing charged aminoacids (D_1, E_3, R_5, H_6 and D_7), might be a voltage sensor and, probably, the pore of the multimeric AβP(1-40)-channels. Further support for this hypothesis was provided by our observation that Zn^{2+} (50-250 µM), only from the *cis* side, reduced the initial value of the AβP(1-40)-dependent displacement current and slowed down the kinetics. It is possible that these properties may be related to the mechanism by which AβP(1-40) promotes the formation of asymmetrical cation channels in natural and artificial membranes (Supported in part by FONDECYT 1950774 and Fundación ANDES).

Tu-AM-F5

DIRECT INCORPORATION OF AMYLOID β-PROTEIN CATION CHANNELS INTO EXCISED MEMBRANE PATCHES FROM GnRH NEURONS

(M. Kawahara, Y. Kuroda, N. Arispe and E. Rojas). Tokyo Metropolitan Inst. Neurosci., Dept. Physiol. Biophys., Fac. of Med., U. of Chile, Stgo. and LCBG, NIDDK, NIH, Bethesda, MD

Alzheimer's Disease 40-residue amyloid β-protein (AβP[1-40]) forms cation-selective channels across planar acidic phospholipid bilayer membranes (Arispe *et al.*, PNAS, 1993a,b). To determine whether direct incorporation of AβP(1-40) molecules from the solution also occurs in neuronal membranes, we exposed either inside-out (or outside-out) excised membrane patches from hypothalamic GnRH neurons to AβP[1-40] molecules dissolved in a saline mimicking the composition of the internal (or external) medium. We now report that although AβP[1-40] molecules can interact with the excised membrane patch from either side, peptide incorporation leading to channel formation occurred within 3-40 minutes and was more efficacious from the inner aspect of the excised patch. As expected, the reversal potential of the Aβ[1-40] specific channel currents in a CsCl solution system followed the Cs^+ gradient. As shown in the inset (left side), the channel at -40 mV) exhibits spontaneous conductance changes over a wide range (50-500 pS). Zn^{2+} (50-500 μM), reported to bind to AβP[1-40] with high affinity, effectively blocked the channel (right side). This blockade was reversed by the Zn^{2+} chelator *o*-phenanthroline in the millimolar range. These properties of the AβP[1-40] channel formed across a neuronal membrane patch are similar to those observed in the bilayer. These results support the idea that AβP(1-40)-channel formation might be the mechanism of amyloid β-protein neurotoxicity. (Supported in part by Japan Health Sciences Foundation; FONDECYT 1950774 and Fundación Andes, Chile).

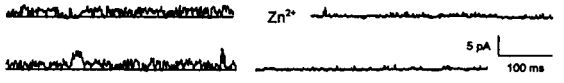

Tu-AM-F6

PTHE ROLE OF RESIDUE POLARITY AT POSITION 9' IN THE M2 DOMAIN OF THE ACETYLCHOLINE RECEPTOR IN CHANNEL GATING.

((G.N. Filatov and M.M. White)) Medical College of PA and Hahnemann Univ., Philadelphia, PA 19129

Ligand-gated ion channels contain a conserved leucine in the middle of the M2 domain (position 9') of each subunit. Replacement of this leucine by the more polar amino acids threonine or serine in the muscle-type AChR leads to a shift in the dose-response curve towards lower concentrations, and a prolongation of the channel mean open time. We have proposed that upon channel opening, the conserved leucines move into a more polar environment, and that the polarity of the residues at position 9' sets the residence time in the open state. We have further examined the effect of polarity at position 9' by making a series of substitutions in the γ subunit (γL9'X, where X= V, F, T, N, or H). The substitutions cover a wide range of polarity, spanning almost the entire Kyte-Doolittle hydropathy scale. The EC_{50} values for ACh-activated macroscopic currents range from 18 μM for wild-type receptors to 0.4 μM for γL9'H receptors. When the effective free-energy of channel opening ($\Delta G = -RT \ln(EC_{50})$) of the mutant receptors is compared to various properties of the amino acids, a linear relationship between ΔG and the Kyte-Doolittle hydropathy value of the amino acid at position 9' is observed. The ΔG values are not related to other properties of the amino acids, such as volume or accessible surface area. These data provide strong confirmation of the notion that the leucines at position 9' move into a more polar environment upon channel opening.

Supported by NIH NS23885 and an AHA Established Investigatorship.

Tu-AM-F7

A PROPOSED STRUCTURAL MECHANISM FOR REGULATING PROTEIN ASSOCIATION BY TYROSINE PHOSPHORYLATION

((M.L. Schneider and C.B. Post)), Department of Medicinal Chemistry, Purdue University, West Lafayette, IN 47907

A novel mechanism for tyrosyl-phosphorylation control of protein-protein association is proposed from structural studies on the complex of band 3 and aldolase. Band 3 inactivates glycolytic enzymes, including aldolase, by binding these enzymes at the cytoplasmic N-terminus of band 3, and can control glycolysis levels in the erythrocyte. Phosphorylation of band 3 Y8 disrupts inactivation. In order to elucidate the structural basis for control by phosphorylation, the conformation of a synthetic peptide corresponding to the N-terminal 15 residues of band 3 when bound to aldolase was determined by using the exchange-transferred nuclear Overhauser effect of nmr. Based on differential linebroadening effects, binding involves a heterogeneous conformation for band 3 peptide (B3P). The family of structures was determined by nmr and molecular dynamics. An important conformational feature of B3P is a folded loop structure involving residues 4-9 and 12 that surrounds Y8, and is stabilized by a hydrophobic cluster. From modeling the complex (using the nmr B3P structure and the xray aldolase structure), we propose a mechanism by which tyrosyl phosphorylation controls protein-protein association through intramolecular electrostatic interactions that may be applicable to other signaling complexes.

Tu-AM-F8

EQUIVALENT GATING CHARGE OF DIDS-INSENSITIVE CHLORIDE CONDUCTANCE IN HUMAN RED BLOOD CELLS TREATED WITH VALINOMYCIN OR GRAMICIDIN

((J.C. Freedman and T.S. Novak)) Dep't. of Physiology, SUNY Health Science Center, Syracuse, NY 13210

Current voltage curves for DIDS-insensitive Cl conductance in human red blood cells from 5 donors have been determined from the rate of cell shrinkage using differential laser light scattering, with membrane potentials estimated from the change in the pH of unbuffered suspensions using the proton ionophore FCCP. After pretreatment of the cells for 30 min with 10 μM DIDS, net effluxes of K and Cl were induced by 3 μM valinomycin and were measured in the continued presence of DIDS; inhibition was maximal at around 65% either at 25°C or 37°C. Electrodiffusion adequately describes the measured transmembrane voltage at varied $[K]_o$, with a constant field permeability ratio P_K/P_{Cl} of 74 ± 9, corresponding to 73% inhibition of P_{Cl} with 10 μM DIDS at pH 7.4 and 23°C. Fitting the constant field current equation to the measured outward Cl currents at varied $[K]_o$ yields a value of P_{Cl} of 0.13 hr^{-1} with DIDS, in comparison with 0.49 hr^{-1} without DIDS, in good agreement with some previous studies. The nonlinear outward-rectifying DIDS-insensitive chloride current (inward-rectifying for positive current), however, is inconsistent with electrodiffusion, but instead is well-described by a Hodgkin-Huxley type voltage-gated mechanism according to which the maximal conductance is 0.055 ± 0.005 S/g Hb, half the channels are open at -27 ± 2 mV, and the equivalent gating charge is -1.2 ± 0.3.

(Supported by National Kidney Foundation of Central NY, Inc.)

RETINAL PROTEINS

Tu-AM-G1

STRUCTURAL CHANGES IN THE CYTOPLASMIC DOMAIN OF BACTERIORHODOPSIN IN THE L INTERMEDIATE.

((Y. Yamazaki[1], S. Tuzi[2], H. Saito[2], H. Kandori[1], R. Needleman[3], J. K. Lanyi[4], & A. Maeda[1]) [1]Dept.of Biophysics, Faculty of Science, Kyoto University, Kyoto 606, Japan. [2]Dept. Life Science, Himeji Inst. Technology, Harima Science Garden City, Hyogo 678-12, Japan, [3]Dept. Biochem., Wayne State Univ. Medicine, Detroit, MI 48201, [4]Dept. Physiol. & Biophysics, Univ. California, Irvine, CA 92717.

FTIR spectra upon L formation of mutants of light-adapted bacteriorhodopsin were examined for water, peptide C=O and Asp96 C=O. Two water molecules located in the cytoplasmic region were detected by the use of mutants of Thr46 [1]. One of these is shown to be present close to the peptide C=O of Val49, and suggested to affect the water molecule coordinated with Asp85. The mutation of Val49 causes a downshift of the C=O stretch of Asp96, in contrast to the upshift in the wild type. A close interaction between Asp96 and Val49 could be achieved through the O-H of Thr46. These work for the long range interaction from Asp85 to Asp96.

[1] Yamazaki et al. (1995) Biochemistry 34, 7088-7093.

Tu-AM-G2

ULTRAFAST STUDIES OF ELECTRONIC STATES AND PROTEIN BOUND WATER MOLECULES IN BACTERIORHODOPSIN

((K. Wynne*, G. Haran*, A. Xie+, Q. He+, M.R. Chance*, R. M. Hochstrasser*)) * Department of Chemistry, University of Pennsylvania, Philadelphia, PA19104-6923, + Department of Physiology and Biophysics, Albert Einstein Hospital, The Bronx, NY10461.

The spectroscopic investigation of the dynamics of photosensory cofactors, proteins and protein bound water molecules is crucial for the understanding of protein function. In a series of experiments we have applied femtosecond IR pulses, ranging in frequency from 1,500 to 10,000 cm^{-1}, to study energy flow in hemeproteins (T. Lian et al. (1994) J. Phys. Chem. **98**, 11648), excited electronic states of the bacterial photosynthetic reaction center (K. Wynne et al, submitted to J. Phys. Chem.) and protein dynamics in bacteriorhodopsin (bR) (R. Diller et al. (1995) Chem. Phys. Lett. **241**, 109-115). In our presentation we will show new results on excited electronic states of bR and the dynamics of water molecules buried in the interior of the protein.

The dynamics of the BR_{570} to J (500 fs) and J to K (3.4 ps) transitions have been studied extensively by probing bR with visible light pulses. We will present new results of probing bR in the near-IR where low-lying excited electronic states can be observed at *circa* 7,000 cm^{-1} above BR_{570}. This provides a novel probe of the initial events in the isomerization of retinal that will give new insights in the reaction pathway and (coherent) dynamics. There is considerable evidence that protein bound water molecules play a role in proton transfer in bR although the exact location and role of water molecules in bR are unknown. A previous FTIR difference spectroscopy study in the OH-stretch region (W.B. Fischer et al. (1994) Biochemistry **33**, 12757) has shown that at least one water molecule undergoes an increase in H-bonding during the $BR_{570} \rightarrow K$ transition. We will present direct time-resolved data in the region 3,700-3,500 cm^{-1} on the changes that occur in this process. This work is supported by NIH.

Tu-AM-G3

KINETIC FOURIER TRANSFORM INFRARED SPECTROSCOPY OF THE PHOTOCYCLE OF HALORHODOPSIN WITH MICROSECOND TIME RESOLUTION. ((A.K. Dioumaev, S.E. Plunkett, M.S. Braiman)) Dept. of Biochemistry, University of Virginia, Charlottesville, VA 22908.

The photocycle of halorhodopsin, a light-induced chloride pump from *Halobacterium salinarium*, was studied by time-resolved step-scan spectroscopy with 5 μs time resolution. The data, obtained at room temperature and approximately 1 M Cl^- concentration, were analyzed by global kinetic fitting. The rise of the chromophore bands at 1523/1555 cm^{-1} (C=C stretch) and 1210/1189/1168 cm^{-1} (C-C stretch) was faster than the temporal resolution of our experiment. An additional slower increase in the intensity of these bands takes place throughout the sub-millisecond time domain. The chromophore vibrational difference bands decay with at least two-component kinetics. The main component has a time constant of approximately 7 ms. Few of the non-chromophore bands in the halorhodopsin vibrational spectra have yet been assigned to particular amino acids residues. The negative 1695 cm^{-1} band, which was previously the residue Arg-108 [Braiman et al. *Biochemistry* 1994, 33:1629; Rüdiger et al. *EMBO J.* 1995, 8:1599], is already present 5 μs after photolysis. Its decay appears multi-exponential, with the main component somewhat faster than the 7 ms time constant of the chromophore bands. Assignment of this and other vibrational bands to specific intermediates is dependent on assumption of a photocycle model. Possible assignments, corresponding to two previously-proposed models [Tittor et al. 1987, *Biophys. J. 52:999*; Váró et al. *Biophys. J.* 1995, 68:2062], will be discussed. (This work was supported by NIH Grant No. GM46854 to MSB and by Fogarty Fellowship 1-F05-TW05212-01 to AKD.)

Tu-AM-G4

THEORY OF RAPID PH CHANGE DUE TO BACTERIORHODOPSIN MEASURED WITH A TIN-OXIDE ELECTRODE.

((B. Robertson and H. H. Weetall)) NIST

The photocurrent transient generated by bacteriorhodopsin (bR) on a tin-oxide electrode is due to pH change and not to charge displacement as previously assumed. Films of purple membranes are deposited on transparent electrodes made of tin-oxide coated glass. When excited with yellow light through the glass, the bR pumps protons across the membrane. The result is a rapid local pH change as well as a charge displacement. Experiments show that it is the pH change rather than the displacement that produces the current transient. The theory of the transient current and the calibration of pH measurement are given. The sensitivity of a tin-oxide electrode to a transient pH change is very much larger than its sensitivity to a steady-state pH change.

Tu-AM-G5

FUNCTIONAL EXPRESSION OF BACTERIORHODOPSIN IN *XENOPUS LAEVIS* OOCYTES REVEALS VOLTAGE DEPENDENCE OF PUMP CURRENT. ((G. Nagel, B. Möckel*, G. Büldt*, & E. Bamberg)) Max-Planck-Institut für Biophysik, D-60596 Frankfurt & *IBI-2, Forschungszentrum D-52425 Jülich, F.R.G.

Bacteriorhodopsin (bR) transports one proton out of the cell per absorbed photon. For energetic and kinetic reasons it is expected that at a certain driving force the active transport stops. So far only a few measurements of its current-voltage relationship have been reported, the main difficulty being oriented insertion of bR into a membrane from which current measurements are possible.
Successful expression of bR in the fission yeast *S. pombe* was reported several years ago, but these cells are still very small. Therefore we expressed bR in *Xenopus* oocytes. The whole cell current of oocytes was measured 3 to 5 days after mRNA injection with a conventional two electrode voltage clamp setup. Whereas control oocytes (which were not injected), showed no current response upon illumunation with intense light (>550nm), mRNA injected oocytes developed a fast outward current response upon illumination. The action spectrum suggests a broad peak at 550 to 600 nm, consistent with the known properties of bR. Light induced currents up to 100 nA were recorded at different test potentials, showing a strong voltage dependence in the investigated range of -165mV to +60mV. The light induced current does not invert at any of these voltages, as expected for a highly oriented membrane insertion. A light induced current could also be demonstrated in giant patches from these oocytes which will allow current recordings with a much better time resolution.
(Supported by the Deutsche Forschungsgemeinschaft.)

Tu-AM-G6

CHLORIDE AND PROTON TRANSPORT IN BACTERIORHODOPSIN MUTANT D85T: DIFFERENT MODES OF ION TRANSLOCATION IN A RETINAL PROTEIN ((J. Tittor, D. Oesterhelt and E. Bamberg+)) Max-Planck-Institut für Biochemie, D82152 Martinsried, Germany, + Max-Planck-Institut für Biophysik, D60596 Frankfurt, Germany

Replacement of aspartate 85 (D85) in bacteriorhodopsin (BR) by threonine but not by asparagine creates, at pH < 7, an anion binding site in the molecule similar to that in the chloride pump halorhodopsin. Binding of various anions causes a blue shift of the absorption maximum by maximally 57 nm and a transition of the longest living photocycle intermediate with a positive difference maximum at 460 nm in the absence of chloride to one at 630 nm in its presence. Increasing anion concentrations cause decreasing decay times of this red-shifted intermediate. At physiological pH, BR-D85T but not BR-D85N transports chloride ions inward in green light, protons outward in blue light and protons inward in white light (directions refer to the intact cell). At pH 4, BR-D85T also mediates a chloride-dependent outward proton translocation in green light. Thus, creation of an anion binding site in BR is responsible for both chloride transport and restoration of wild type behaviour in proton transport at low pH.

Tu-AM-G7

TITRATION OF ASPARTATE-85 IN BACTERIORHODOPSIN: WHAT IT SAYS ABOUT THE MECHANISMS OF CHROMOPHORE ISOMERIZATION AND PROTON RELEASE ((S. P. Balashov[1,2], E. S. Imasheva[1,2], R. Govindjee[1] and T. G. Ebrey[1])) [1]Center for Biophysics and Dept. of Cell and Struct. Biology, UIUC, Urbana, IL 61801; [2]Dept. of Physico-Chemical Biology, Moscow State University, Moscow 119899, Russia

Titration of Asp-85, the proton acceptor and part of the counterion in bacteriorhodopsin, over a wide pH range (between 2 and 11), leads us to the following conclusions: **1)** Asp-85 has a complex titration curve with two pK_a's. In addition to a main transition with pK_a = 2.6 it shows a second inflection point at high pH (pK_a = 9.7 in 150 mM KCl). This complex titration behavior of Asp-85 is explained by interaction of Asp-85 with an ionizable residue X'. Deprotonation of X' increases the proton affinity of Asp-85 by shifting its pK_a from 2.6 to 7.5. Conversely protonation of Asp-85 decreases the pK_a of X' by 4.9 units, from 9.7 to 4.8. The interaction between Asp-85 and X' may have important implications for the mechanism of proton transfer. In the photocycle after the formation of the M intermediate (and protonation of Asp-85) the group X' should release a proton. This deprotonated state of X' would stabilize the protonated state of Asp-85 in M. **2)** The rate constant of dark adaptation is directly proportional to the fraction of blue membrane (in which Asp-85 is protonated) between pH 2 and 11. From this we conclude that thermal isomerization of the chromophore (dark adaptation) occurs upon transient protonation of Asp-85 and formation of the blue membrane. The rate constant of isomerization is at least 10^4 times faster in the blue membrane than in the purple membrane. The protonated state of Asp-85 may be important for the catalysis of not only all-*trans* <=> 13-*cis*,15-*syn* thermal isomerization during dark adaptation but also of the reisomerization of the chromophore during N -> O transition in the photocycle. Supported by NIH Grant GM52023 to T.G.E. and International Science Foundation Grant NAX000 to S.P.B.

Tu-AM-G8

STRUCTURAL MODEL AND MOLECULAR MECHANISM OF THE VISUAL PIGMENT RHODOPSIN ((May Han and Steven O. Smith)) Department of Molecular Biophysics and Biochemistry, Yale University, New Haven, CT 06511.

Rhodopsin is the photoreceptor in rod cells responsible for vision at low light intensities. The photoreactive chromophore is 11-*cis* retinal covalently bound to the protein as a protonated Schiff base with Glu113 as the counterion. The retinal ^{13}C NMR chemical shifts have been used to establish the major charge interactions in the retinal binding site of rhodopsin and bathorhodopsin, the primary photoproduct of rhodopsin. The NMR data constrain one of the carboxylate oxygens of Glu113 to be ~ 3 Å from the C_{12} position of the retinal with the second oxygen oriented away from the conjugated retinal chain. The NMR constraints are used to position 11-*cis* and distorted all-*trans* retinal chromophores in the interior of the apoprotein. The resulting structures of rhodopsin and bathorhodopsin can explain the anomalous NMR chemical shift data, the opsin shifts in these pigments, the spectral shifts in mutants E113D and G90D/E113Q, as well as crosslinking between the retinal ionone ring and helix VI. Based on the protein-retinal interactions predicted by the structural model, mutagenesis studies have been undertaken to define the key contact sites. The results of these studies will be presented and a model proposed for how light activates this G-protein coupled receptor.

Tu-AM-SymII-1

EXPERIMENTALLY DETERMINED HYDROPHOBICITY SCALES FOR MEMBRANE PROTEINS. ((William C. Wimley†,Trevor P. Creamer§ and Stephen H. White†)) †Department of Physiology and Biophysics, University of California, Irvine, CA, 92717. §Department of Biophysics and Biophysical Chemistry, Johns Hopkins University School of Medicine, Baltimore, MD 21205.

Membrane protein folding is a poorly understood process. However, it may proceed through consecutive stages of binding, insertion of secondary structure elements, and formation of tertiary structure. Although the general principles of these processes seem clear, a detailed quantitative understanding remains elusive. The first step towards understanding the physical basis for membrane protein folding is to understand the partitioning from water into the bilayer interface. We have approached this first step through the determination of an experimental interfacial hydrophobicity scale that is based on measurements of water-to-bilayer partitioning of two families of peptides: A complete set of host guest peptides of the form AcWL-X-LL and a set of peptides of the form $AcWL_n$ (n=1-6). These experimental measurements establish an interfacial hydrophobicity scale that gives the individual sidechain and backbone contributions to the free energy of interfacial partitioning. Comparison of bilayer partitioning with octanol partitioning of the same peptides reveals the complexity of the bilayer interface: the contributions of polar and aliphatic residues to bilayer partitioning are small and not well correlated with octanol partitioning. The aromatic residues make the largest contributions to bilayer partitioning. This observation suggests an important role for aromatic residues in membrane protein folding and may provide a physical basis for the preferential location of aromatic residues of membrane proteins in the *trans* interfacial region of membranes.

Tu-AM-SymII-2

ENGINEERED TRANSBILAYER HELICES AND THEIR EFFECTS ON LIPID ORGANIZATION. ((R.N.A.H. Lewis, Y.-P. Zhang and R.N. McElhaney*)) Department of Biochemistry, University of Alberta, Edmonton, Canada, T6G 2H7.

We have studied the interactions of the helical transmembrane peptides Ac-K_2-L_{24}-K_2-amide (L_{24}) and Ac-K_2-$(LA)_{12}$-K_2-amide $(LA)_{12}$ with a variety of phospho- and glycolipid bilayers of various thicknesses using a variety of physical techniques. The effect of these peptides on the thermotropic phase behavior of the host lipid bilayers varies markedly with the nature of the lipid polar headgroup. In lipids with strongly interacting polar headgroups, these peptides preferentially destabilize gel-state bilayers more or less independently of bilayer thickness and disorganize the hydrocarbon chains in both the gel and liquid-crystalline states. In lipids with weakly interacting headgroups, either the gel or liquid-crystalline states may be preferentially stabilized, depending on the sign and magnitude of the hydrophobic mismatch between the peptide and the host lipid bilayers. Perhaps surprisingly, peptide effects on lipid phase behavior are not dependent on lipid polar headgroup charge and in all systems the stoichiometry of lipid/peptide interactions is similar. The presence of these peptides also markedly effects the lamellar/reversed hexagonal phase behavior of lipids exhibiting reversed micellar phases. In general, the effects on $(LA)_{12}$ on the host lipid bilayer are greater than those of L_{24}, probably due to a greater surface roughness. We also have evidence that the conformation of the peptide is influenced by the thickness and phase state of the host lipid bilayer.
(Supported by the Medical Research Council of Canada and the Alberta Heritage Foundation for Medical Research).

Tu-AM-SymII-3

PROTEIN TRANSLOCATION ACROSS MEMBRANES ASSOCIATED WITH CHANNEL GATING. ((A. Finkelstein)) Albert Einstein College of Medicine, Bronx, NY 10461

Colicin Ia, a bacterial protein toxin of 626 residues, forms voltage-gated channels in planar lipid bilayer membranes. Exploiting the high-affinity binding of streptavidin to biotin, we have determined which parts of the channel-forming domain (roughly the 175 C-terminal residues) are exposed to the aqueous solutions on either side of the membrane and which are inserted into the bilayer in the channel's open and closed states. We did this by biotinylating cysteine residues introduced by site-directed mutagenesis, and monitoring by electrophysiological methods the effect of streptavidin addition on channel behavior. We have identified a region of at least 68 residues that flips back and forth across the membrane in association with channel opening and closing, based on our observations that for mutants biotinylated in this region, streptavidin added to the *cis* (colicin-containing) compartment interfered with channel opening and *trans* streptavidin interfered with channel closing. The upstream and downstream segments flanking the translocated region move into and out of the bilayer during channel opening and closing, forming two transmembrane segments. Surprisingly, if any of several residues near the upstream end of the translocated region is held on the *cis* side by streptavidin, the colicin still forms voltage-dependent channels, indicating that a part of the protein that normally is fully translocated across the membrane can become the upstream transmembrane segment. Evidently, the identity of the upstream transmembrane segment is not crucial to channel formation, and several open channel structures can exist.

Tu-AM-SymII-4

Helix Interactions in Membrane Protein Folding and Oligomerization

Engelman, D. M., Adams, P.D., Arkin, I.T., Brünger, A.T., Fleming, K.R., MacKenzie, K.R. and Smith, S.O.

Molecular Biophysics & Biochemistry, Yale University, New Haven, CT, USA

Glycophorin A, a protein from the erythrocyte membrane, dimerizes through an association of its transmembrane helix with that of another glycophorin molecule. We have previously studied this interaction using mutagenesis and modeling, resulting in a proposal for the structure of the dimer. We have now determined the structure of the transmembrane helix dimer in a detergent micelle using heteronuclear NMR, and it is found to be as predicted.

Phospholamban, a small regulatory protein from cardiac sarcoplasmic reticulum, also oligomerizes through interactions of its transmembrane helix, forming a pentamer. We have developed a model for the pentamer based on mutagenesis, optical spectroscopy, and modeling.

These two cases reveal that detailed packing of independently stable transmembrane helices can explain the stable association of helices to form higher order structure in membrane proteins.

MITOCHONDRIAL CHANNELS II

Tu-AM-H1

THE TRIGGERING OF MCC CHANNEL ACTIVITY ((M.L. Campo[1], H. Tedeschi[2], K.W. Kinnally[3])) [1]Dpto de Bioquímica, Univ. de Extremadura, 10071 Cáceres, Spain, [2]Dept. Biol. Sci., Univ. at Albany, Albany, NY[3] Wadsworth Center, NYS Dept. of Health, Albany, NY.

MCC is a mitochondrial channel activity studied by patch-clamping mitoplasts. While normally quiescent, several conditions and factors trigger this activity (*e.g.* high voltages or Ca^{2+}). We have found MCC is also induced by uncouplers. Preincubation of mitoplasts with μM FCCP or CCCP increased the detection of MCC from 28% (control) to >80% of the patches (±30 mV). The effects on MCC of peptides whose sequences target proteins to mitochondria, *e.g.* N-terminus of *N. crassa* cyt. aa_3 subunit IV (pCoxIV), is under investigation. We detected MCC more frequently after exposure to pCoxIV compared to control peptides (N-terminus of *N. crassa* VDAC, pVDAC). Activation of MCC by targeting peptide was achieved on attached patches under energized conditions at 15 mM KCl (but not at 150 mM KCl). Preincubation with pCoxIV induced swelling and reduced the probability of gigaseal formation when compared to those treated with pVDAC. The conditions of MCC activation are similar to those of Sokolove & Kinnally (Molec. Biol. Cell (1995) abstract) in which pCoxIV induced a permeability transition. While speculative, these results suggest that they may be an expression of the same entity. Supported by grants from Junta de Extremadura y Fondo Soc. Eur. EIA 94/11, DGICYT PB 92-0720, and NSF MCB 9117658.

Tu-AM-H2

EVIDENCE THAT THE ADENINE NUCLEOTIDE TRANSLOCATOR IS NOT RESPONSIBLE FOR THE MITOCHONDRIAL MULTIPLE CONDUCTANCE CHANNEL, MCC. ((T.A. Lohret[1,2], R.C. Murphy[3], T. Drgon[4], and K.W. Kinnally[1])) [1]Molecular Medicine, Wadsworth Center, NYS Dept. of Health, Albany, NY, Departments of [1]Biomed. Sci. and [2]Biol. Sci., University at Albany, SUNY, Albany, NY, [3]Biology Dept. Rennselaer Polytechnic Institute, Troy, NY, [4]NIDDK-LBM, NIH, Bethesda, MD., Dpt. of Biochemistry, Comenius University, Bratislava, Slovakia.

The functional relationship between the adenine nucleotide translocator (ANT) and the mitochondrial multiple conductance channel (MCC) was investigated using patch-clamp techniques. MCC activity with the same conductance, ion selectivity, voltage-dependence and peptide-sensitivity could be reconstituted from inner membrane fractions derived from mitochondria of ANT-deficient and wild-type *Saccharomyces cerevisiae*. In addition, the MCC activity of mouse kidney mitoplasts was unaffected by carboxyatractyloside, a known inhibitor of ANT. A 50 pS anion channel activity was also detected in the wild-type and ANTless proteoliposomes. These results suggest that ANT is not responsible for MCC activity, and similarly, it is unlikely that the 50 pS channel activity stems from ANT. This research was supported by NSF grant MCB9117658.

Tu-AM-H3

THE EFFECT OF TARGETING PEPTIDES ON A MITOCHONDRIAL CHANNEL, MCC, IS ALTERED IN THE PROTEIN IMPORT MUTANT *mas6-1*. ((T. A. Lohret[1], R. E. Jensen[2] and K. W. Kinnally[1,3])) [1]Mole. Med., Wadsworth Center, Empire St. Plaza, PO Box 509, Albany, NY, Depts. of [1]Biol. and [3]Biomedical Sci., Univ. at Albany, SUNY, Albany, NY. [2]Dept. Cell Biol., Johns Hopkins U. Sch. of Med., Baltimore, MD

The multiple conductance channel (MCC) has been linked to the import of precursor proteins into mitochondria by patch-clamp studies of reconstituted inner membranes from *S. cerevisiae* mitochondria [Lohret & Kinnally (1995) *J. Biol. Chem.* **270**, 15950]. The transient blockade of MCC by peptides whose sequences are based on mitochondrial targeting signals is altered by a point mutation in Mas6p, a 23 kDa inner membrane protein purported to be a part of the inner membrane protein import apparatus. The IC_{50} of the targeting peptides is 8-10 fold higher for the MCC from the *mas6-1* mutant than from wild-type. The *mas6-1* mutation is known to cause a 10-20 fold reduction in the import of several precursors (Emtage & Jensen (1993) *J. Cell Biol.* **122**, 1003). MCC from the wild-type and mutant yeast strains had the same conductance, selectivity and voltage dependence. These results suggest the G186D substitution in the *mas6-1* strain affects the recognition of the targeting peptides, and supports a role for Mas6p as a receptor in the import apparatus. Furthermore, the peptide sensitive channel (PSC) of the outer membrane is not affected by the mutation in Mas6p and hence can be distinguished from MCC. [Research supported by NSF grant MCB9117658.]

Tu-AM-H4

THE EFFECT OF THE CYTOCHROME c OXIDASE SUBUNIT IV LEADER PEPTIDE (P22) ON K^+ TRANSPORT BY MITOCHONDRIAL CHANNELS. ((Y. Lu and A.D. Beavis)) Med. Col. of Ohio, Toledo, OH 43699.

Flux studies in intact mitochondria reveal the existence of at least three pathways for K^+ transport. An electroneutral K^+/H^+ antiport, electrophoretic K^+ leakage and an electrophoretic pathway or channel which is modulated by adenine nucleotides and nucleotide analogs. These pathways are believed to be involved in volume homeostasis; however, it is also possible that one or more of the electrophoretic pathways may be involved in the import of newly synthesized proteins. Others have shown that protein import into mitochondria is blocked by a peptide (P22) with the same sequence as the leader peptide of subunit IV of Cytochrome c oxidase. We have now investigated the effect of this peptide on electrophoretic K^+ uptake in isolated rat liver mitochondria and on a K^+ channel we observe when proteins extracted from the inner membrane are reconstituted in a planar lipid bilayer. Assaying K^+ uptake in intact mitochondria driven by the respiratory chain, we find that the peptide stimulates K^+ flux almost 10-fold with an EC_{50} = 28 μM and a Hill coefficient of 1.5. This was a surprising result. We have previously shown that this transport process is stimulated 3.6-fold by treatment of the mitochondria with N-ethylmaleimide (30 nmol/mg). Using these mitochondria, we find the extent of stimulation by the peptide is diminished and the EC_{50} and V_{max} are almost the same. This result suggests that the peptide and N-ethylmaleimide act on the same K^+ transport pathway. In contrast, we find that the isolated K^+ channel examined by electrophysiological techniques is inhibited by the peptide as a result of a decrease in the open probability. (This work was supported by NIH grant HL36573).

Tu-AM-H5

INVOLVEMENT OF THE MITOCHONDRIAL PEPTIDE SENSITIVE CHANNEL IN THE PROTEIN IMPORT COMPLEX. ((M. Thieffry*, P. Juin*, J.P. Henry* and F.M. Vallette*)) C.N.R.S., *UPR 9040 (Gif sur Yvette) and *URA 1112 (Paris), France

The Peptide Sensitive Channel (PSC), a cationic channel of the mitochondrial outer membrane, is blocked by synthetic mitochondrial presequences and by non mitochondrial basic peptides such as the neuropeptide dynorphin B (1-13). The properties of the blockade suggest their translocation through the channel. We used dynorphin B (1-13) as a probe to determine the role of the PSC in mitochondrial physiology.

Dynorphin B (1-13), inactive on the import of mitochondrial presequences into intact organelles, becomes inhibitory on their import after proteolysis of outer membrane surface receptors. Moreover, it can direct the import of a cytosolic protein into mitochondria. These observations strongly suggest that the neuropeptide directly interacts with the General Insertion Pore of the import complex. Such an hypothesis is further supported by the fact that cross linking experiments using iodinated dynorphin B (1-13) leads to the labeling of ISP 42, a component of the outer membrane translocation machinery. Finally, anti ISP42 antibodies specifically immunoprecipitate the solubilized PSC activity.

Taken together, these results suggest that the PSC is associated with the outer membrane import machinery as a protein conducting pore.

Tu-AM-H6

CYCLOPHILIN INTERACTIONS WITH THE MITOCHONDRIAL INNER MEMBRANE: SELECTIVE DISRUPTION BY CYCLOSPORIN A AND PROTONS

((A. Nicolli, E. Basso, V. Petronilli and P. Bernardi)) CNR and Department of Biomedical Sciences, University of Padova, Via Trieste 75, I-35121 Padova, Italy (Spon. by M. Zoratti)

Mammalian mitochondria possess a unique matrix cyclophilin (CyP-M). We have studied the interactions of CyP-M with rat liver mitochondria by western blotting with a specific antibody against its unique N-terminus. A sizeable CyP-M fraction sediments with submitochondrial particles (SMP) after sonication in isotonic sucrose at pH 7.4. Interactions of this CyP-M pool with SMP are disrupted (i) by CSA but not CSH; and (ii) by acidic pH. Both conditions inhibit the permeability transition pore (MTP), a mitochondrial channel, suggesting that CyP-M binding is involved in opening of the MTP, and that pore inhibition by CSA and H^+ may be due to unbinding of CyP-M from its putative binding site on the MTP. A role for CyP-M in MTP regulation is also supported by a study with a series of CSA derivatives with graded affinity for CyP. With each derivative the potency at inhibition of the peptidyl-prolyl-*cis-trans*-isomerase activity of CyP-M purified to homogeneity is similar to that displayed at inhibition of MTP opening. Decreased binding to CyP-M (but not CyP-A) and decreased efficiency at MTP inhibition is obtained by substitutions in position 8 while a 4-substituted, non-immunosuppressive derivative is as effective as the native CSA molecule, indicating that calcineurin is not involved in MTP inhibition by CSA.

Tu-AM-H7

MODULATION OF THE MITOCHONDRIAL CYCLOSPORIN A-SENSITIVE PERMEABILITY TRANSITION PORE AT TWO REDOX-SENSITIVE SITES ((P. Costantini, B.V. Chernyak, V. Petronilli, and P. Bernardi)), CNR and Department of Biomedical Sciences, University of Padova, Via Trieste 75, I-35121 Padova, Italy (Spon. by C. Mannella)

Mitochondria from a variety of sources possess a voltage-dependent channel inhibited by cyclosporin A, the permeability transition pore (MTP). The channel's voltage threshold is profoundly affected under conditions of oxidative stress, with a shift to more negative values causing MTP opening at physiological membrane potentials. This is followed by collapse of the proton electrochemical gradient, which may be an early event in oxidant-induced cell death. Here we further clarify the mechanisms by which oxidative agents affect the apparent voltage dependence of the MTP. We show that two sites can be experimentally distinguished. (i) A first site is in apparent oxidation-reduction equilibrium with the pyridine nucleotide (PN) pool; PN oxidation is matched by increased MTP open probability under conditions where the glutathione pool is kept in the fully reduced state; this site can be blocked by N-ethylmaleimide (NEM) but not by monobromobimane (MBM), a thiol-selective reagent; (ii) a second site coincides with the oxidation-reduction sensitive dithiol we have recently identified. Dithiol cross-linking at this site by arsenite or phenylarsine oxide is matched by increased MTP open probability under conditions where the PN pool is kept in the fully reduced state; at variance from the first, this can be blocked by MBM, and is probably in equilibrium with the glutathione pool. Based on these findings, we reassess the mechanisms by which oxidative agents affect the MTP.

Tu-AM-H8

CHARACTERIZATION OF A PERMEABILITY TRANSITION PORE (PTP) IN ISOLATED YEAST MITOCHONDRIA. ((D.W. Jung & D.R. Pfeiffer)) Dept. of Medical Biochemistry, The Ohio State University, Columbus, OH 43210.

Mitochondria isolated from the yeast *S. cerevisiae* do not display the Ca^{2+} uniport or Na^+/Ca^{2+} antiport activities found in mammalian mitochondria. When incubated in a mannitol medium (0.3M, pH 7.3) containing 10 mM phosphate with ethanol as an oxidizable substrate, yeast mitochondria accumulate large amounts of Ca^{2+} (>400 nmol/mg prot.) on addition of the electrogenic Ca^{2+} ionophore ETH129. Ca^{2+} retention appears limited only by the availability of O_2. These mitochondria show no indication of a permeability transition as monitored by retention of Ca^{2+} and $\Delta\Psi$, or by swelling, although mammalian mitochondria undergo a rapid permeability transition under these conditions. A pore does open, as monitored by swelling, when ethanol or ATP (2 mM) is added to yeast mitochondria in the absence of phosphate. This response is blocked by ADP (2 mM) or phosphate (10mM), but cyclosporin (4 µg/ml), carboxyatractyloside (25 µM), and oligomycin (4µg/ml) have no effect. ATP-induced swelling is insensitive to uncoupler (2 µM FCCP). Contraction of swollen mitochondria induced by 0.4- to 4-kD PEG shows a 50% effect at 0.875-kD PEG, indicating that this pore is of a size comparable to the PTP in liver mitochondria. It is pH sensitive, opening more readily as pH is increased. The presence of an Ca^{2+}-insensitive PTP in yeast mitochondria implies an important role of the PTP in cell physiology and suggests that Ca^{2+}- and cyclosporin-sensitivities may have evolved at a later time along with mitochondrial Ca^{2+} cycling and dehydrogenase regulation. (Supported by USPHS Grant HL49182)

Tu-AM-I1

FUNDAMENTAL CALCIUM SIGNALING EVENTS IN CARDIAC MUSCLE

((P. Lipp, E. Niggli)) Department of Physiology, University of Bern, Bern, Switzerland.

In cardiac muscle Ca influx via L-type Ca channels triggers Ca release from the SR. Confocal microscopic studies have revealed subcellular spontaneous Ca release events occurring in a highly localized fashion as Ca "sparks", indicating that the SR may form a highly structured network of individual Ca release units. During EC-coupling this functional microarchitecture could account for graded Ca signals via a recruitment process whereby release units would be controlled locally by L-type Ca channels. Indeed, when the number of L-type Ca channels opening during EC-coupling was reduced pharmacologically, Ca sparks became resolvable, indicating that they might represent an elementary event in cardiac Ca signaling. We used a confocal microscopic detection of the Ca concentration and flash-photolysis of caged Ca compounds to investigate the elementary nature of the Ca sparks more directly, i.e. without opening L-type Ca channels. While activation of Ca channels clearly generated Ca sparks (as indicated by a surge of low-frequency components in a power spectral analysis), flash photolysis of DM-nitrophen triggered Ca release from the SR that was spatially homogeneous independent of the flash energy (i.e. the amplitude of the Ca jump). These results indicate that Ca sparks may arise from a group of SR Ca release channels under the control of a single L-type Ca channel. However, the real fundamental event of cardiac Ca signaling appears to be considerably smaller than Ca sparks and thus may reflect Ca release from individual SR Ca release channels. (Supported by SNF)

Tu-AM-I2

CAN CA^{2+} ENTRY THROUGH T-TYPE CA^{2+} CHANNELS TRIGGER CA^{2+} RELEASE FROM THE SARCOPLASMIC RETICULUM IN GUINEA-PIG VENTRICULAR MYOCYTES?

((Karin R. Sipido* and Edward Carmeliet)) Lab. of Physiology and *Lab.of Experimental Cardiology, University of Leuven, B3000 Leuven, Belgium.

Ca^{2+} entry through L-type Ca^{2+} channels is an important trigger for Ca^{2+}-induced Ca^{2+} release from the sarcoplasmic reticulum (SR) in cardiac cells. However, additional pathways for Ca^{2+} entry exist. We have investigated whether Ca^{2+} entry through T-type Ca^{2+} channels could trigger Ca^{2+} release from the SR. Experiments were performed on isolated guinea-pig ventricular myocytes under whole cell voltage clamp with fura-2 as a $[Ca^{2+}]_i$ indicator. The pipette solution contained: (in mM) N-methyl-D-glucamineCl 110, TEACl 20, $MgCl_2$ 0.8, MgATP 4, fura-2 0.05, TEA-HEPES 10, pH 7.20. The external solution contained TEACl 130, $MgCl_2$ 1, $CaCl_2$ 5.4, dextrose 10, HEPES 10, pH 7.40 (T = 23°C). By applying a number of depolarizing pulses in the Na^+ free solution, the amount of Ca^{2+} in the SR available for release could be varied; loading of the SR was evaluated during a test depolarization from -90 to 0 mV. T-type Ca^{2+} currents uncontaminated by L-type Ca^{2+} current, were elicited by voltage steps from -90 to -50 mV (peak current -0.63 +/- 0.15 pA/pF, mean +/- SD, n=7). Even with high loading of the SR no Ca^{2+} release was observed during these steps. Larger T-type currents were elicited during steps from -90 to -30 mV. For a comparable loading of the SR, a step from -90 to -30 mV with both T- and L-type current (peak current -2.31 +/- 0.59 pA/pF) versus a step from -50 to -30 mV with L-type only (-0.94 +/- 0.49 pA/pF) elicited more Ca^{2+} release ($\Delta[Ca^{2+}]_i$ at 40 ms 241 +/- 140 nM versus 156 +/- 103 nM, $p<0.05$, n=5). However during a step from -50 to -20 mV with L-type current only, but with a peak current (-2.57 +/- 1.50 pA/pF, n=5) comparable to the one during the step from -90 to -30 mV, even more Ca^{2+} was released ($\Delta[Ca^{2+}]_i$ at 40 ms 331 +/- 180 nM, $p<0.05$). These results indicate that T-type Ca^{2+} current can trigger Ca^{2+} release from the SR, but that Ca^{2+} entry through T-type channels is less efficient than the one through L-type Ca^{2+} channels.

Tu-AM-I3

DESCRIPTION OF CA-RELEASE INDUCED CALCIUM CURRENT INACTIVATION IN ISOLATED CARDIOMYOCYTES.

((*J. Zahradnik, J. Pavelková, A. Zahradníková*)) UMFG SAV, 833 34 Bratislava, Slovak Republic

Kinetics of whole-cell L-type Ca-channel currents were analyzed in rat cardiomyocytes contracting in response to voltage pulses. As opposed to non-contracting conditions, Ca-currents inactivated by two independent processes which could not be described by classical mechanisms. A new kinetic model implementing I_{Ca} inactivation by Ca^{2+} ions released from the sarcoplasmic reticulum was developed. The model assumes that: *1)* all channels have fourth-order exponential activation kinetics (τ_m); *2)* all channels undergo monoexponential inactivation (τ_X: compound current- and voltage-dependent mechanism); *3)* a portion of channels (R) localized at the tubulo-reticular junction inactivates by Ca^{2+} released from the terminal cisternae: and *4)* Ca-release driven I_{Ca} inactivation is a monoexponential process (τ_R) triggered with a variable delay (t_d) relative to the stimulus. The model was verified by approximating pure I_{Ca} through maximally phosphorylated Ca-channels employing an IBM RISC/6000 computer and the IMSL™ library. The release-dependent parameters of the model (τ_R, R, t_d) respond correctly to experimental manipulation of the E-C coupling process (see Figure). This approach allows use of I_{Ca} as an *in situ* probe of Ca-release, and quantitative assesment of the interaction between the channels of junctional membranes and its regulation.

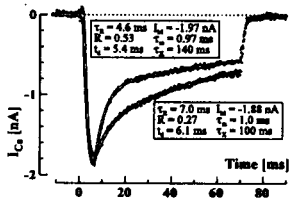

Two traces of I_{Ca} (•) differing in the degree of Ca-release induced inactivation. Superimposed are the corresponding fits using the new kinetic model (—).

Tu-AM-I4

ALTERATION OF THE ELEMENTARY CALCIUM RELEASE EVENTS BY FK506 BINDING PROTEIN IN CARDIAC MYOCYTES

((Rui-Ping Xiao, Edward G. Lakatta and Heping Cheng)) LCS, GRC, NIA, NIH, Baltimore, MD 21224

Ca^{2+} release channels in cardiac sarcoplasmic reticula (SR) consist of tetrameric ryanodine receptors (RR) and their stoichiometrically associated FK506 binding proteins(FKBP). In this study, we investigated the *in vivo* interaction between FKBP and the RR in rat and mouse cardiac myocytes. FK506 (50 µM), an inhibitor of FKBP isomerase activity, markedly enhanced and prolonged the electrically-elicited Ca^{2+} transient and induced Ca^{2+} and contractile oscillations whereas it has little effect on the amplitude and kinetics of the L-type Ca^{2+} current. Using the optical recording of the elementary Ca^{2+} release events ("Ca^{2+} sparks"), we further characterized the effect of FK506 on the modulation of single SR Ca^{2+} release channels in mouse cardiac myocytes. In the presence of FK506, release channels showed long openings with multiple stepwise amplitudes (Fig). Addition of ryanodine (5 µM) completely abolished these Ca^{2+} sparks. We conclude that the FKBP plays a critical role in terminating the positive feedback of the Ca^{2+}-induced Ca^{2+} release and thereby stabilize and regulate this ubiquitous Ca^{2+} signalling process.**Fig.** Top: Confocal line-scan image of a 5 µm-wide region scanned for 4485 msec. Bottom: Time course of local $[Ca^{2+}]$ in the central 1-µm region of the top image. Dash lines indicate $[Ca^{2+}]$ levels of 100 to 304 nM in 51 nM steps, corresponding to the resting $[Ca^{2+}]$, 1/4, 2/4, 3/4 and full opening of the FK506-modified channel.

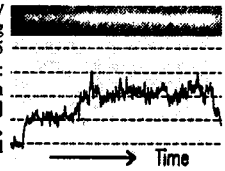

Tu-AM-I5

SIGNIFICANCE OF THE DISTANCE BETWEEN CALCIUM RELEASE UNITS IN CARDIAC AND SKELETAL MUSCLE.

((Feliciano Protasi and Clara Franzini-Armstrong)) Dept. Cell & Dev. Biol. Univ. of Penn., Philadelphia, PA 19104-6058.

Ca^{2+} release in cardiac and skeletal muscle occurs through ryanodine receptors, or feet, grouped in specialized domains of the sarcoplasmic reticulum (jSR). In adult avian cardiac muscle, there are two categories of jSR. One category is at the fiber periphery. Feet in this jSR face dihydropyridine receptor (DHPRs), grouped in plasmalemma domains (jPMs), and Ca^{2+} release is probably initiated by DHPR activity. The second category, the extended jSR (EjSR), is located in the fiber interior and its feet are far from DHPRs. Presumably, Ca^{2+} release from these feet is initiated by saltatory conduction from neighbouring EjSR (Sommer, J. Mol. Cell Card. 27:19-35, 1995). Using electron microscopy, we have measured the edge to edge distance between individual EjSRs and jPMs and their nearest neighbours. The average distance for EjSR is 135 ± 15 nm (mean ± 1 SEM, n=263), while the distance between jPMS is significantly larger, 472 ± 5 nm (n=3402). This is consistent with the need of interaction between neighbouring EjSRs, perhaps via Ca^{2+}, while probably jSRs at the fiber periphery are independently activated and therefore do not interact with each other. In skeletal muscle, the nearest distance between jSR domains in twitch fibers from frog (semitendinosus and ileofibularis) and from toadfish swimbladder is quite small (101 ± 2 nm, n= 225 and 107 ± 2 nm, n=358, respectively). Yet, all arrays of feet are associated with arrays of DHPRs and spread of Ca^{2+} release activity by jSR does not occur independently of surface membrane/T tubule depolarization. This would indicate that skeletal muscle feet *in situ* are more refractory to calcium activated calcium release than cardiac feet.

Tu-AM-I6

EFFECT OF BAYK8644 ON CROSS-SIGNALING BETWEEN DHP- AND RYANODINE-RECEPTORS IN RAT VENTRICULAR MYOCYTES.

((S. Adachi-Akahane, L. Cleemann, and M. Morad)) Inst. for Cardiovascular Sci., Georgetown Univ. Medical Center, Washington, DC 20007. (Spon. by R.E. Forster)

We have previously shown that cross-signaling between the DHP- and ryanodine-receptors persists even in highly Ca^{2+}-buffered ventricular myocytes (Biophys. J. 1995; Sham et al., PNAS, 1995). Under such conditions, we quantified the amount of Ca^{2+} released from the SR in response to influx of Ca^{2+} through the DHP-receptor and found an amplification factor of 20. Here we have attempted to further characterize the nature of cross-signaling and determine the voltage-, Ca^{2+}-, and drug-dependence of the amplification factor. Simultaneous recordings of I_{Ca} and Ca_i-transients were carried out using single rat ventricular myocytes dialyzed with 2 mM Fura-2 and 0.2mM cAMP through the whole cell clamp patch pipette. In cAMP dialyzed cells BayK continued to enhance I_{Ca} and slowed the kinetics of its inactivation, but surprisingly decreased the Ca_i-transients slightly, thus decreasing the amplification factor by 50%. The caffeine-induced Ca_i-transients, however, were not affected by BayK8644 (1-3µM), suggesting absence of direct BayK effect on ryanodine receptors. Rapid application of 10 mM Ca^{2+} enhanced both I_{Ca} and Ca_i-transient in control conditions and in the presence of BayK. Under control conditions we found that the rate of inactivation of I_{Ca} depended linearly on rate of Ca^{2+} release. The Ca^{2+}-dependence of inactivation of I_{Ca} was completely abolished by BayK. This finding coupled with the suppression of amplification factor by BayK suggests that Ca^{2+}-induced inactivation process may reflect a regulatory step in Ca^{2+} release and signaling of cardiac cells. Supported by NIH HL16152.

Tu-AM-I7

UNCOUPLING OF L-TYPE Ca^{2+} CHANNELS AND RYANODINE RECEPTORS ASSOCIATED WITH SLOW REGENERATIVE Ca^{2+} RELEASE IN CULTURED RAT VENTRICULAR MYOCYTES. **((James S.K. Sham and Li-Hua Deng)) Department of Medicine, The Johns Hopkins University, Baltimore, MD 21205.**

Morphological and physiological studies in ventricular myocytes showed that L-type Ca^{2+} channels and ryanodine receptors are co-localized and functionally coupled, which was suggested to be essential for the fast, graded Ca^{2+} releases activated by Ca^{2+} current (I_{Ca}). It had been also reported that structural changes, including loss of t-tubules, occurred in myocytes after short-term culture. We examined if the functional coupling of the two sets of channels, and the Ca^{2+} release induced by I_{Ca}, are altered in cultured (1-6 days) adult rat ventricular myocytes, using whole-cell voltage-clamp and Indo-1 fluorescence techniques. Membrane capacitance measurement showed that surface area of cultured ventricular myocytes was unchanged in day 1-2 (day 0: 96.5±3.9 pF, n=14; day 2: 94.6±4.1 pF, n=20), but reduced significantly in subsequent days of cell culture (day 5: 61.2±2.6 pF, n=29; day 6: 45.5±3.1 pF, n=6). In day 5, inactivation of I_{Ca} caused by SR Ca^{2+} release in myocytes dialysed with 10 mM EGTA and 5 mM Ca^{2+} (global free $[Ca^{2+}]$=150 nM), an indicator for functional coupling (Sham et al., 1995), was not observed in 30% of cells, despite the ability of SR to release Ca^{2+} was unaltered as tested by 5 mM caffeine. In addition, the kinetics of Ca^{2+} transients activated by I_{Ca} was changed dramatically, with significant reduction in the rate of rise. In some myocytes, two components of Ca^{2+} release (a small, fast, initial component, and a large, slow, 2nd component) could be identified. The slow component had a rate of rise similar to those activated by reverse Na^+-Ca^{2+} exchange. Interruption of I_{Ca} during the slow Ca^{2+} release did not abbreviate the Ca^{2+} transients, suggesting a regenerative mechanism. Our results, therefore, suggested that short-time cell culture caused gradual reduction of t-tubules and uncoupling of Ca^{2+} channels and ryanodine receptors, which appeared to be required for the fast, graded Ca^{2+} release in rat ventricular myocytes. (Supported by AHA and NIH grants).

Tu-AM-I8

NUMERICAL ANALYSIS OF CARDIAC EC COUPLING. ((C. Soeller and M.B. Cannell)), Dept. of Pharmacology, St. George's Hospital Medical School, London SW17 0RE.

We have modelled the spatial and temporal changes in [Ca] in the diadic junctional region that will occur when a sarcolemmal calcium channel opens. The model includes various classes of calcium bind sites and solves the reaction/diffusion equations with a finite difference scheme. Having derived the time course of [Ca] changes at all points within the junctional space we have examined the factors that determine the open probabilities for ryanodine receptors at various locations (and hence SR calcium release). The modelling shows that E-C coupling is extremely sensitive to the geometric organisation of the channels involved in E-C coupling, suggesting that other proteins may be involved in keeping the structural relationship between the sarcolemmal and SR calcium channels at an optimum for efficient E-C coupling. We compare the results with experimentally observed data and find good agreement for certain choices of parameters and geometrical arrangements indicating likely ultrastructural details of the junctional region that cannot be resolved with current experimental methods. Our analysis shows that the structure of the cardiac diad allows cardiac EC-coupling to have the necessary speed of response and sensitivity to the trigger calcium influx.

Supported by the Wellcome Trust.

NUCLEIC ACID-PROTEIN COMPLEXES II

Tu-AM-J1

SEQUENCE SPECIFIC DNA-BINDING DRIVEN BY THE HYDROPHOBIC EFFECT. ((T. Lundbäck and T. Härd)) Center for Structural Biochemistry, Karolinska Institutet, NOVUM, S-141 57 Huddinge, Sweden.

Several recent studies show that bound water molecules and dehydration effects play a significant role for the affinity and specificity of DNA-protein interactions. Still, thermodynamic studies of well-defined model systems for which three-dimensional structures are known have to be carried out in order to understand the physical basis for interactions involving water. We used fluorescence spectroscopy and, in particular, isothermal titration calorimetry to study the thermodynamics of binding of the glucocorticoid receptor DNA-binding domain (GR DBD) to four different, but similar, DNA-binding sites. The binding sites are two naturally occurring sites which differ in the composition of one base pair (an AT to GC mutation), and two sites containing chemical intermediates of these two base pairs. The calorimetrically derived $\Delta C_p°_{obs}$ for GR DBD binding agrees with that calculated for dehydration of accessible surface areas, without coupled folding reactions. The dominating effect of dehydration is also demonstrated by a linear relationship between $\Delta H°_{obs}$ and $\Delta S°_{obs}$ with a slope close to the experimental temperature. Thus, the binding reactions show the thermodynamic signature of the hydrophobic effect. Comparisons with structural data also allow us to rationalise individual differences in $\Delta H°_{obs}$ (and $\Delta S°_{obs}$) between the four complexes. For instance, we find that the removal of a methyl group at the DNA-protein interface is enthalpically favourable, but entropically unfavourable, which is consistent with a replacement by an ordered water molecule.

Tu-AM-J2

THE ROLE OF WATER IN CAP-DNA INTERACTIONS. ((M.G. Fried and K.M. Vossen)) Department of Biochemistry and Molecular Biology, Pennsylvania State University College of Medicine, Hershey, PA 17033

The formation of a protein-DNA complex in aqueous solution is accompanied by the displacement of water from the interacting surfaces. The water stoichiometry of such a reaction can be evaluated from the dependence of the observed equilibrium constant (K_{obs}) on water activity. Measurements with low molecular weight, non-ionic osmolytes indicate that the binding of the *E. coli* CAP protein to lactose promoter DNA is accompanied by the displacement of 80 ± 27 water molecules. Water is thus the dominant stoichiometric component of the reaction. If one water molecule occupies ~9Å^2 of macromolecular surface, this stoichiometric difference is consistent with a loss of 720 ± 250Å^2 of solvent-exposed surface. Isosteric surface area calculations predict a loss of 958Å^2 on complex formation. This suggests that conformation changes accompanying binding occur with little net change in the solvent exposed surface area. Binding to non-specific DNA results in the net displacement of ~20 water molecules. If these are displaced from interacting surfaces, the area of protein-DNA contact in the non-specific complex must be ≤ 180Å^2. A smaller contact area could explain, in part, the substantial difference in specific and non-specific binding affinities. Surface area estimates such as these provide a basis for evaluating the role of the hydrophobic effect in the stability of protein-DNA complexes. Supported by NSF grant DMB-91-96154.

Tu-AM-J3

DNA FOLDING IN COMPLEXES WITH PROTEINS: LOCAL ANISOTROPIC BENDING AND GLOBAL NON-PLANAR LOOPING. ((Andrey A. Gorin*, Wilma K. Olson* and Victor B. Zhurkin†)) *Department of Chemistry, Rutgers University, New Bruswick, NJ 08903, and †Laboratory of Mathematical Biology, NCI, NIH, Bethesda, MD 20892.

The DNA structures in ~40 available crystals of DNA-protein complexes were analyzed at two levels: in terms of the local sequence-specific bending, and in terms of formation of the overall tertiary structure.
(i) Local DNA anisotropy. DNA prefers bending in the ROLL direction over that in the TILT direction. This anisotropy reveals itself stronger in the protein-DNA complexes than in unbound B-DNA crystals. When DNA is bent by more than 30° per decamer, kinks, directed toward the major groove (Sobell *et al.*, 1976, *PNAS USA* 73, 3068-72), are formed. The sugar-phosphate backbone remains in the B-domain, however, so the DNA distortions are better described by a "mini-kink" model (Zhurkin *et al.*, 1979, *Nucl. Acids Res.* 6, 1081-96). These mini-kinks occur predominantly in the pyrimidine-purine YR dimers (CA:TG, TA, CG) and in AG:CT steps. Bending toward the major groove is accompanied by DNA unwinding, the tendency entirely consistent with the rules of DNA "conformational mechanics" recently found by us for "pure" unbound B-DNA (Gorin *et al.*, 1995, *J. Mol. Biol.* 247, 34-48).
(ii) Overall tertiary folds. In most of the complexes with transcription factors, DNA is bent into non-planar loops, closely resembling the path of the double helix in the nucleosome. This non-planarity correlates with, and appears to be predetermined by the non-random periodic distribution of the YR and AG dimers in the binding sites. This feature is expected to facilitate the binding of regulatory proteins to negatively supercoiled DNA *in vivo*.

Tu-AM-J4

MAJOR GROOVE RECOGNITION ELEMENTS IN THE MIDDLE OF THE T7 RNA POLYMERASE PROMOTER. ((Craig T. Martin, Hoi Hung Ho, Tong Li, Maribeth Maslak, Charlie Schick, Iaroslav Kuzmine & Andrea Ujvari)) Department of Chemistry and Program in Molecular & Cellular Biology, University of Massachusetts, Amherst 01003-4510.

T7 RNA polymerase recognizes a relatively small promoter extending only seventeen base pairs upstream from the start site for transcription. A model for this recognition suggests that the enzyme interacts with the major groove of duplex DNA in the region centered at position -9 and recent kinetic analyses of promoters containing base analogs at positions -10 and -11 have provided support for this model [Schick, C. & Martin, C. T. *Biochemistry 32*, 4275-4280 (1993), *Biochemistry 34*, 666-672 (1995)]. In the current work, we extend this analysis across the proposed major groove. Specifically, we identify as primary contacts the 6-carbonyl of G at positions -9 and -7, the 6-amino group of A at position -8, the 5-methyl group of T at position -6, and the 2-amino group of G at position -5. The results suggest that recognition continues along one face of the helix beyond the major groove and into the adjoining minor groove at position -5. Evidence indicates that helix melting begins at about position -4 and that the barrier to melting is low. More detailed studies are in progress to measure the kinetics of DNA binding, helix melting, and the initial stages of transcription, with the ultimate goal of relating previously identified structural contacts to individual steps in the initiation of transcription.

Tu-AM-J5

STRUCTURE OF THE *ESCHERICHIA COLI* LACTOSE OPERON REPRESSOR AND ITS COMPLEXES WITH DNA AND INDUCER. ((M. A. Kercher, G. Chang, N. C. Horton, H. C. Pace, M. Lewis and P. Lu)) Department of Biochemistry & Biophysics and Department of Chemistry, University of Pennsylvania, Philadelphia, PA 19104.

The *lac* operon of *E. coli* is the paradigm for gene regulation. The key component of the operon is the *lac* repressor, a product of the *lacI* gene. The 3-dimensional structures of the intact *lac* repressor, the *lac* repressor bound to the gratuitous inducer 1-isopropyl-β-D-thiogalactoside (IPTG) and the *lac* repressor complexed with a 21 base-pair symmetric operator DNA have been determined. These three structures show the conformation of the molecule in both the induced and repressed states and provide the framework for understanding a wealth of biochemical and genetic information. The DNA sequence of the *lac* operon has three *lac* repressor recognition sites in a stretch of 500 base pairs. The crystallographic structure of the complex with DNA suggests that the tetrameric repressor functions synergistically with catabolite gene activator protein (CAP) and is involved in the quaternary formation of repression loops in which one tetrameric repressor interacts simultaneously with two sites on the genomic DNA.

supported by NIH and US ARO

Tu-AM-J6

BINDING OF MODEL RNAS AND HIGH-AFFINITY LIGANDS TO YEAST RIBOSOMAL PROTEIN L32 ((Hu Li and Susan A. White)) Department of Chemistry, Bryn Mawr College, Bryn Mawr, PA 19010

In vivo, yeast ribosomal protein L32 binds to its own pre-mRNA and thus autoregulates its production. The structure of the 5' end has been postulated to contain two helices separated by a purine-rich internal loop (Eng & Warner, Cell, 65, 797-804, 1991). Studies of several RNAs bearing similar structural motif show that the protein binding site is in the internal loop region (Li et al., J. Mol. Biol., 250, 447-459, 1995). To evaluate the importance of a potential G:U base pair in the left-hand helix next to the internal loop the binding affinities of all possible pairs were measured. The results show that flexibility within the G:U base pair plays a pivotal role in protein binding. In order to identify the bases in the internal loop important for protein binding, SELEX was used. A small-scale experiment show that there are no variants in the upper bulge (positions 10 and 11), whereas some mutations in the lower bulge are tolerated. The dominant sequences after round 3 are similar to the wild-type one in that purines are preferred in positions 56, 58 and 59 in the lower bulge. However, cytosine is preferred in position 57 compared to adenine in the wild-type. A large-scale SELEX is currently in progress.

Tu-AM-J7

RNA HAIRPINS WITH (ETHYLENE GLYCOL)$_n$ LINKERS: THERMODYNAMIC CHARACTERIZATION, DYNAMIC SIMULATION, AND PROTEIN BINDING. ((D. Jeremy Williams and Kathleen B. Hall)) Washington University School of Medicine, St. Louis, MO 63110

The human U1A protein specifically recognizes a ten nucleotide RNA hairpin loop. In order to identify solution properties of the RNA that are critical to protein recognition, a model RNA hairpin was altered by replacement of three nucleotides with (ethylene glycol)$_n$ spacers, where n=3,6,12,18. RNA:protein binding was measured by nitrocellulose filter binding assays, to determine the affinity and energetics of the association. The substituted RNAs were characterized by UV melting and circular dichroism, to compare their stability and structure with the normal RNA hairpin. Monte Carlo/stochastic dynamic simulations on model ethylene glycol linkers, in conjunction with measurements of internucleotide distances from tRNA crystal structures, were used to determine the end-to-end span of the linkers and the nucleotide equivalence in the context of the stemloop. Binding results, thermodynamic parameters of the substituted RNAs, and the simulation data will be presented. The results will be interpreted in the context of the RNA:protein interaction and discussed in terms of how these non-nucleotide spacers affect RNA solution properties.

Tu-AM-J8

FURANOSE DYNAMICS IN A DNA-PROTEIN COMPLEX. ((M. Hatcher, J. Miller and G. Drobny)) Department of Chemistry, Box 351700 University of Washington, Seattle, WA 98195.

The furanose dynamics of a DNA dodecamer [d(CGCGAATTCGCG)]$_2$ have been studied via Solid-State Deuterium NMR. This dodecamer contains the binding site for the EcoRI Restriction Endonuclease GAATTC. We have found that the C9 nucleotide displays unusual, large amplitude motion in the furanose ring. The presence of unique dynamics at this nucleotide which is base-paired to the cleavage site (G4) may be very important. The crystal structure of the DNA-Protein Complex shows that the enzyme imposes a neokink and unwinds the DNA, making it accessible to cleavage. It may be that the large amplitude dynamics at the C9 nucleotide provide a soft spot in the recognition sequence allowing the enzyme to impose its kink. To better understand the furanose dynamics at the C9 nucleotide, we have bound the EcoRI endonuclease to the dodecamer and investigated the dynamics in the DNA-Protein complex.

Tu-AM-J9

A SYSTEMATIC APPROACH TO THE DEVELOPMENT AND VALIDATION OF MODELS FOR PROTEIN-LIGAND BINDING. ((J. A. Given and M. K. Gilson)) Center for Advanced Research in Biotechnology/NIST, Rockville, MD 20850.

One of the goals of theoretical structural biology is to develop predictive models for the noncovalent binding of small molecules by proteins. A successful model should be able to predict the bound conformation of a protein-ligand complex, and the binding affinity. In addition to their basic scientific interest, such models will have applications in protein engineering and drug design. Although a number of binding models have been described, characterized, and used, the connection between the models and the underlying statistical thermodynamics theory of binding is often obscure. Here, a formal expression for the free energy of binding is used to derive of a series of models, some of which are similar to approaches currently in use. The issue of validation is then addressed. One criterion for validity of an energy model is that it should assign greater stability to the true structure of a protein-ligand complex than to plausible but grossly incorrect alternatives. A novel method for generated plausible but mis-docked conformations is presented, and is used to test various treatments of long-ranged non-bonded interactions.

Tu-AM-K1

ELASTIC REGIONS OF I-BAND TITIN ISOFORMS IN SKELETAL AND CARDIAC MYOFIBRILS. ((M. Ivemeyer, S.Labeit, J.C. Rüegg and W.A. Linke)) Physiology II, Univ. Heidelberg, Im Neuenheimer Feld 326, D-69120 Heidelberg. (Spon. by G. Pfitzer)

Single myofibrils were prepared from rat skeletal and cardiac muscle and were suspended between two microneedles under an inverted microscope. Based on recently published data on the molecular structure of I-band titin (Labeit and Kolmerer, *Science*, 1995, in press), we aimed to study the extensibility of distinct regions of I-band titin by using immunofluorescence microscopy and image processing techniques. Relaxed myofibrils were labelled with fluorophore-marked antibodies against (a) N1-line titin; (b) N2-line titin and (c) titin at the A/I junction. Antibody-labelled myofibrils were then stretched to a series of sarcomere lengths (SLs), and the translational movement of the antibodies was measured, so that the contribution of different portions of the titin molecule to I-band elasticity could be estimated.

Near the lower end of the physiological SL range, titin extension was restricted mainly to the region between the N2-line and the A/I junction. In cardiac myofibrils, this extension amounted to ~100 nm per half-sarcomere (stretch, 2.0 to 2.2 μm SL), whereas in psoas myofibrils, it was 2 to 3 times larger (stretch, 2.2 to 2.7 μm SL). Since the N2-line-A/I junction region comprises both a repetitive IgC2 domain segment, which has similar length in cardiac and skeletal sarcomeres, and non-repetitive sequence insertions rich in proline and glutamate, which are longer in skeletal than in cardiac muscle, we argue that it is the non-repetitive sequence domain, which is likely to be responsible for the initial passive tension rise upon myofibril stretch. That domain's longer length in skeletal muscle relative to cardiac muscle determines its higher extension capacity. At moderate to high degrees of stretch, I-band titin appeared to lengthen predominantly between the N1-line and the N2-line (amount, 200-300 nm per half-sarcomere, depending on muscle type), a region consisting solely of IgC2 domains. Such lengthening occurred until titin filaments reached their strain limit at SLs of ~3 μm (cardiac), 3.5 μm (psoas), and ~4 μm (soleus), respectively, above which portions of previously bound A-band titin were released into the I-band.

We conclude that in both cardiac and skeletal myofibrils, passive tension rise is facilitated by extension of a two-spring-in-series element of I-band titin: one spring (non-repetitive sequence domains) has a relatively low elastic modulus and determines passive tension over most of the working SL range, whereas the other spring (repetitive IgC2 region) has a higher elastic modulus and may be recruited to prevent muscle from being overstretched.

Tu-AM-K2

RIGHT VENTRICULAR PRESSURE OVERLOAD ALTERS MYOCARDIAL CROSS-BRIDGE KINETICS WITH NO CHANGE IN MHC ISOFORM. ((JN Peterson and NR Alpert)) UVM College of Medicine, Burlington, VT 05405.

In small mammals, myosin heavy chain (MHC) type is a major determinant of intrinsic myocardial cross-bridge (XBr) kinetics. Across species, alterations in the predominant ventricular MHC isoform from V_1 to V_3 result in increased myothermal economy (isometric XBr force-time integral per ATP hydrolyzed) and decreased ATPase. This correlation also holds within species, where MHC isoform can be altered with chronic hormonal interventions. It does not hold, however, when animals are subject to hemodynamic stress. Hasenfuss *et al* (Circ Res 68: 836-846, 1991) showed that rabbit hearts subject to RV pressure overload exhibit a 100% increase in myothermal economy, with a small shift in MHC population (88% V_3 ctrl, versus 100% V_3 PO). To see whether this slight MHC shift is responsible, we compared animals with 100% V_3 induced hormonally (using propylthiouracil (PTU)) versus hemodynamically (PO).

	PTU (n=5)	PO (n=6)
econ (pNs)	0.44 ± 0.12	0.76 ± 0.24 *
F_{avg} (pN)	0.68 ± 0.06	0.64 ± 0.11
CR (s^{-1})	1.43 ± 0.24	0.88 ± 0.22 *
DC	0.27 ± 0.06	0.14 ± 0.05 *
F_{uni} (pN)	2.53 ± 0.64	5.01 ± 2.06 *

CR=Cycling Rate, DC=Duty Cycle, F_{uni}=Unitary Force

We measured myothermal economy, maximum Ca^{2+} activated force, and the time constant of final force decline. Using a simple 2-state model, we calculated the XBr parameters shown. These kinetic estimates, made in an intact, twitching preparation, demonstrate that MHC isoform is not responsible for altered cross-bridge kinetics in the PO rabbit heart.

Tu-AM-K3

STUDIES ON CALMODULIN[TROPONIN C] CHIMERAS SHOW THAT THE TROPONIN C CENTRAL HELIX IS ESSENTIAL FOR COOPERATIVE ACTIVATION OF THE THIN FILAMENT. ((F. Schachat†, S.E. George‡, and P.W. Brandt*)) Department of Cell Biology† and Departments of Medicine and Pharmacology‡, Duke University Medical Center, Durham, NC 27710, and Department of Anatomy and Cell Biology*, Columbia University School of Medicine, New York, New York, 10032.

Despite their evolutionary and structural homology, calmodulin (CaM) and troponin C (TnC) fulfill different cellular functions and are unable to substitute for one another. When CaM is substituted for TnC, it is deficient in all aspects of TnC function; in particular, based on the behavior of CaM[3,4TnC], it cannot restore either the cooperativity of activation or the maximal Ca^{2+}-activated tension (Brandt et al, FEBS Let. 353:99). By exchanging domains of CaM and cardiac TnC (cTnC) we investigated the TnC sequences that are critical for cooperative activation and restoration of full tension. We find that substitution with CaM containing the TnC central helix enables us to separate direct activation of a regulatory unit by Ca^{2+} from cooperative activation by adjacent regulatory units. Like TnC, the CaM[TnC-CH] chimera can be activated cooperatively, but like CaM it cannot fully restore maximum tension. These observations show that the TnC central helix is essential for the cooperative activation of the thin filament, even though it is unable in the context of the CaM[TnC-CH] chimera to fully restore tension. Studies with other chimeras are in progress to identify the additional elements required for full calcium activation.

Tu-AM-K4

REGULATION OF RATE OF FORCE DEVELOPMENT: A MONTE-CARLO SIMULATION STUDY. ((Jeroen H. Geerdink and Pieter P. de Tombe)). Bowman-Gray School of Medicine, Winston-Salem, NC 27157.

The molecular mechanism by which calcium regulates contractile protein force remains unresolved. Recently, it has been reported that the rate of force development following a quick release step in isolated myocardium (k_{tr}) varies with the level of activator calcium. This result has been interpreted to suggest that activator calcium regulates the kinetics of cross-bridge cycling, as opposed to acting as an "on-off switch". Interpretation of the k_{tr} parameter, however, may be limited due to dynamic interaction between calcium/troponin-C binding and crossbridge cycling. Accordingly, we developed a stochastic computer crossbridge model using a Monte-Carlo algorithm to evaluate whether variations of k_{tr} with activator calcium exclusively reflect alterations in actomyosin interaction rates of individual crossbridges. The model assumed that *i)* rates of actin-myosin binding and release were constant, and *ii)* calcium binding acts as an "on-off switch" by activating a segment of the actin filament. The response of the model to a quick release at two levels of calcium is shown in **A**. **B** shows the relation between k_{tr} and force over a wide range of calcium levels (0). Thus, our stochastic simulation predicted that k_{tr} varies with activator calcium even in the absence of changes in actin-myosin interaction rates. In fact, k_{tr} was constant only when the calcium binding kinetics were unphysiologically slow (●;**B**). We conclude that the rate of force development (k_{tr}) does not correlate uniquely with the kinetics of the molecular interaction between myosin and actin.

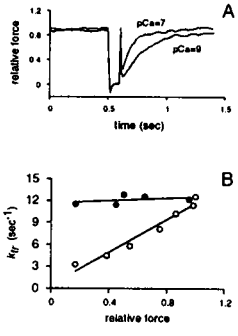

Tu-AM-K5

REMOVAL OF Ca^{2+} FROM CYTOSOL OF ARTERIAL SMOOTH MUSCLE CELLS: ROLES OF SR Ca^{2+} STORAGE AND Ca^{2+} EXTRUSION ACROSS THE PLASMALEMMA. ((H.Shimizu, M.L. Borin and M.P. Blaustein)) Dept. of Physiol., Univ. of Maryland Med. Sch., Baltimore, MD 21201.

We have examined the relative roles of four transport systems that remove Ca^{2+} from the cytosol of aortic smooth muscle (ASM) cells following the induction of increases in the cytosolic free Ca^{2+} concentration ($[Ca^{2+}]_{cyt}$). $[Ca^{2+}]_{cyt}$ was monitored with digital imaging methods in primary cultured rat ASM cells. First, the plasmalemma (PM) Ca^{2+} pump and Na/Ca exchanger (NCX) were inhibited with, respectively, 0.25 mM La^{3+} (does not inhibit NCX) and Na^+-free media in the absence of external Ca^{2+} (*FASEB J.* 9:A613, 1995). Then Ca^{2+} stored in the SR was released, and resequestration was blocked with 10 mM caffeine (CAF) + 10 μM cyclopiazonic acid (CPA). $[Ca^{2+}]_{cyt}$ promptly rose from a resting value of ≈ 100 nM to a peak of 692 ± 42 nM, and declined slowly at a rate of -34.7 ± 0.7 nM/min. When one or more of the Ca^{2+} removal systems was reactivated (see Fig. 1), the rate of $[Ca^{2+}]_{cyt}$ decline increased markedly (normalized rates in nM/min): -CAF, -156; -CPA, -217; -(CAF+CPA), -363; $-La^{3+}$, -239; +Na, -201; -(CAF+CPA+La^{3+}) +Na, -767. Recovery to baseline was virtually complete (84-94%) in all cases except the removal of CAF alone (31% recovery). The results indicate that: 1) There are two SR Ca^{2+} stores but only one is sensitive to CPA. 2) The capacity of the CPA-sensitive store is much larger than the CAF-sensitive store. And, 3) Together, the two Ca^{2+} extrusion systems in the plasmalemma can remove Ca^{2+} from the cytosol as fast as the two SR sequestration systems.

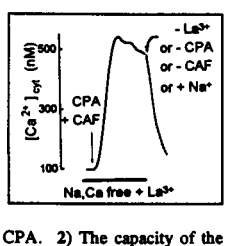

Tu-AM-K6

EFFECT OF INTRACELLULAR CALCIUM (Ca) CHELATORS ON Ca TRANSIENTS AND RELAXATION RATES IN FROG SKELETAL MUSCLE. ((J. David Johnson and Yandong Jiang)) Department of Medical Biochemistry, The Ohio State University College of Medicine, Columbus, OH 43210.

The effect of intracellular Ca chelators (EGTA-AM or EDTA-AM) on Ca transients (Fluo-3) and tension was examined to determine the rate limiting steps in relaxation of frog skeletal muscle at 10°C. Incubation with EGTA-AM (20 μM) produced a linear increase in the rate of fall in twitch [Ca] from 12/s to 21/s over 0-70 min. The rate of relaxation initially increased from 5/s to 9/s over 0-10 mins of incubation and then remained unchanged as force continued to decrease to 20% of control at 70 min. Thus, increasing the rate of fall in [Ca] increased the rate of relaxation until a rate-limiting step in the relaxation process was reached at ~9/s. Ca dissociates from the N-terminal regulatory sites of purified troponin (Tn) at ~8/s. Intracellular [EDTA] also increased the rate of fall in [Ca] and tension. It was less effective than EGTA and it produced less decrease in tension because its ability to bind Ca and promote relaxation was limited by its Mg off-rate (3/s). Both EDTA and EGTA were effective in promoting relaxation when the SR-Ca-ATPase was partially inhibited. Conclusions: The rate of fall in [Ca] is rate limiting for relaxation of intact skeletal muscle. When it is increased by intracellular EGTA a new rate limiting process, presumably Ca removal from Tn, is observed at ~9/s. Intracellular EDTA-Mg provides an effective "artificial" parvalbumin whose contribution to relaxation is limited by its Mg off-rate.

Tu-AM-K7

DRASTIC CHANGES IN VOLTAGE-DEPENDENCE AS A COMMON DISEASE-MECHANISM IN DOMINANT HUMAN MYOTONIA
((Michael Pusch, Klaus Steinmeyer and Thomas Jentsch)) ZMNH, Hamburg University, 20246 Hamburg, Germany.

Mutations in the muscle chloride channel gene, CLC-1, cause dominant myotonia (Thomsen's disease). We introduced several point mutations found in affected families (I290M, R317Q, P480L, and Q552R) into the CLC-1 cDNA and investigated their functional effects in Xenopus oocytes. All of these dominant mutations drastically shift steady-state probability of channel opening (P_{OPEN}) to more positive voltages in mutant/WT heterooligomeric channels, and, when measurable, even more so in mutant homooligomers. We predict that such "shifted" channels can no longer contribute efficiently to the repolarization of action potentials, fully explaining why they cause dominant myotonia. At position 290, most replacements of the native isoleucine shift P_{OPEN} to more positive voltages. Remarkably, a human mutation affecting an adjacent residue (E291K) is fully recessive. We conclude that large shifts in the voltage-dependence of gating may be a common mechanism in dominant myotonia congenita.

MEMBRANES - BILAYERS AND OTHER MODELS

Tu-AM-L1

THE EFFECT OF CHEMICAL STRUCTURE ON THE DEPTH OF MOLECULES IN MEMBRANES: DANSYL, FLUORESCEIN, RHODAMINE, AND OTHER FLUOROPHORES ATTACHED TO THE POLAR HEADGROUP OF PHOSPHOLIPIDS OR TO HYDROCARBONS.
((E. Asuncion-Punzalan, K. Kachel and E. London)) Dept. of Biochemistry and Cell Biology, State University of New York at Stony Brook, Stony Brook, NY 11794-5215

The location of molecules in membrane bilayers is a fundamental aspect of membrane structure. We measured the quenching of model membrane bound fluorescent molecules by nitroxide-labeled phospholipids in which the nitroxide is attached at a shallow, medium, or deep depth in the bilayer. The parallax analysis method was used to calculate the depth of the fluorescent groups in the bilayer from the quenching data. Dansyl, fluorescein and rhodamine groups attached to the amine of PE were found to locate in the polar headgroup region, about 20Å from the bilayer center. Pyrene and mansyl (methylanilinonapthalenesulfonic acid) derivatives located more deeply (6-12Å from the bilayer center). Comparison of these values to those measured for the probes unattached to PE, or attached to hydrocarbon chains, showed probe location is determined by a combination of probe structure, the polarity of the group attaching it to a lipid or to hydrocarbon, and the location of the site of attachment to a lipid or other molecule. Shallow depths were were also found for coumarin, styrylpyridinium, eosin, and acridine orange groups attached to hydrocarbon chains. Combining these results with earlier measurement of the depths of anthracene, anthroyloxy, carbazole, indole, NBD, and phenol derivatives in model membranes allows us to begin to predict depth of a molecules in membranes as a function of their chemical structure. Supported by NIH grant GM 48596.

Tu-AM-L2

ZERO-ORDER KINETICS OF HYDROLYSIS OF DIACETYLENIC LIPID TUBULES BY PHOSPHOLIPASE A_2; THE INFLUENCE OF MICROSTRUCTURE ON AN INTERFACIAL ENZYME
((P. Yager, P.A. Carlson and M.H. Gelb*)) Molecular Bioengineering Program, Center for Bioengineering, Box 352255, and *Department of Chemistry, Box 351700, University of Washington, Seattle, WA 98195.

Diacetylenic bilayer-forming lipids are known to form closed, hollow tubular microstructures of tightly packed crystalline lipids. The order in tubule bilayers is such that impurities such as fatty acids should be restricted to the edges of the bilayers, which should be primarily at tubule ends. Since some phospholipases are known to preferentially bind to negatively charged lipid surfaces, enzymatic hydrolysis might be initially restricted to microstructure ends, and the rate could remain constant as hydrolysis proceeded inward from the ends. We have studied the hydrolysis of diacetylenic phosphatidylcholine tubules by cobra venom phospholipase A_2 using a fluorimetric assay sensitive to changes in free fatty acid concentration. A cationic fluorescent dye was used to label anionic product domains generated within the degrading tubules. At early stages of hydrolysis, negatively charged patches were observed on the tubules, but, as the reaction progressed, tubules unraveled and the hydrolysis products converted to non-tubular microstructures. The hydrolysis of the tubules was much slower than that of fluid liposomes, presumably because of the rigidity of the lipid tubule wall. Although the hydrolysis often begins at sites other than the tubule ends, the kinetics are zero-order until all phospholipid is cleaved, as predicted. This suggests a novel approach to continuous drug delivery in which the drug and its lipid support matrix are created through molecular-level self-assembly of constituents into a tubular microstructure.

Tu-AM-L3

ON THE ORIGIN OF DETERGENT-RESISTANT MEMBRANES FROM CELLS: DETERGENT-RESISTANCE ARISES FROM LIPID/CHOLESTEROL MIXTURES THAT FORM LIQUID-ORDERED DOMAINS.
((R. Schroeder, E. London, and D. Brown)) Dept. of Biochemistry and Cell Biology, State University of New York at Stony Brook, Stony Brook, NY 11794-5215

Triton X-100-resistant membranes can be derived from cells. There is evidence that these membranes primarily originate in sphingolipid/cholesterol rich domains in cellular plasma membranes. To clarify the origin of these membranes, the detergent resistance of model membrane vesicles containing mixtures of lipids was measured, and correlated to the lipid phase behavior. Mixtures of dipalmitoyl PC and cholesterol (at 45°C) did not exhibit detergent insolubility at low cholesterol concentrations in which only the liquid-disordered phase (Ld) was present, but did at higher cholesterol concentrations when the liquid-ordered (Lo) phase was present. Insolubility of dioleoyl PC, palmitoyloleoyl PC and bovine PC mixtures with cholesterol could also be correlated with conditions in which Lo domains are predicted to be present. This was also true for dioleoyl PC/sphingolipid/cholesterol mixtures. Since insolubility is only seen in bilayers containing Lo domains prior to detergent treatment, we conclude detergent treatment does not create this phase. We also conclude that model membranes have both Lo and Ld domains at lipid compositions similar to those found in eukaryotic cell plasma membranes. Therefore, it is likely such domains co-exist in the plasma membrane *in vivo*. Supported by NIH grants GM 47897 and 48596.

Tu-AM-L4

REGULAR DISTRIBUTION OF CHOLESTEROL AND ERGOSTEROL IN SPHINGOMYELIN AND IN PHOSPHATIDYLCHOLINE LIPID BILAYERS.
((P. L.-G. Chong, F. Liu, M. M. Wang, I. P. Sugar# and R. E. Brown¶)) Dept. of Biochemistry, Temple Univ. School of Medicine, Philadelphia, PA 19140, #Dept. of Biomath. Sci., Mt. Sinai Med. Ctr., New York, NY 10029 & ¶the Hormel Institute, Univ. of Minnesota, Austin, MN 55912.

In 1994, we reported the first fluorescence evidence for sterol regular distribution into hexagonal superlattices in two-component liquid-crystalline phosphatidylcholine bilayers [1]. Using steady-state polarization of diphenylhexatriene (DPH) fluorescence, we showed that membrane free volume reaches a local minimum at a critical sterol mole fraction [2]. More recently, we obtained evidence for sterol regular distribution in three-component mixtures. In the present study, we will report evidence that sterol regular distribution occurs not only in sterol/phosphatidylcholine mixtures but also in sterol/sphingomyelin mixtures. The fractional sterol concentration dependence of dehydroergosterol fluorescence in 16:0-sphingomyelin/sterol multilamellar vesicles was examined at 48 °C. Abrupt changes in fluorescence properties near the critical sterol mole fractions for regular distribution into hexagonal superlattices were detected. These results support the idea that cholesterol regular distribution may occur in cell plasma membranes, where phosphatidylcholines, sterols, and sphingomyelins are abundant (supported by AHA). [1] Chong (1994) *Proc.Natl.Acad.Sci.USA* 91:10069-10073. [2] Chong (1994) the Proceedings of the 23rd Steenbock Symposium.

Tu-AM-L5

SIZE DEPENDENCE OF PERMEANT DIFFUSION THROUGH LIPID BILAYER MEMBRANES: A MOLECULAR DYNAMICS SIMULATION STUDY ((Terry R. Stouch and Donna A. Bassolino))
Bristol-Myers Squibb, P.O.Box 4000, Princeton, NJ 08543-4000.

A key role of lipid bilayer biomembranes is to mediate the passage of molecules between biological compartments. The heterogeneity of these lipid bilayer constructs makes membrane permeation a surprisingly complex phenomenon. Of particular discussion has been the role of molecular size in transmembrane transport; very small molecules (MW $\leq$ 50-100 amu) have anomalously high membrane permeation rates. We present atomic level molecular dynamics simulations of fully hydrated lipid bilayers containing a series of molecules of increasing size in order to probe the role of molecular volume in the permeation/diffusion process. We find that, due to the particulars of lipid bilayer structure and dynamics, these small molecules have a component of their diffusion unavailable to larger molecules that increases their diffusion rate. This component, rapid jumps between spontaneously arising voids, is unavailable to molecules too large to fit within the voids. The jumps are most noticeable in the bilayer center where the incidence of voids is greatest and their magnitude appears to be an exponentially decaying function of increasing molecular volume. In addition to diffusion, permeation is dependent on the free energy of partitioning into the bilayer. Free energy profiles will also be discussed.

Tu-AM-L6

3D-IMAGES OF MEMBRANES USING HIGH-RESOLUTION SOLID STATE NMR ((F. Volke, A. Pampel, R. Scott)) University of Leipzig, Physics, Biomembranes, Linnestr. 5, D-04103 and Biosym/MSI, Cambridge, U.K.

The combination of magic angle spinning (MAS) and multidimensional NMR techniques (1) of model and biomembranes is used to construct a 3D- image of a membrane (POPC) containing non-ionic surfactant molecules. Intermolecular crosspeaks (NOESY) between the matrix and the surfactant allow the determination of the position of the guest molecule within the membrane. On the other hand, NOE's between molecular segments of the lipid are used as constraints in molecular simulation techniques. In some case the MAS technique resolves J-couplings which are used as additional structural determination means.
Further constraints of the architecture are taken from SAXS and Deuterium NMR of labelled lipids.
This approach is useful to determine the position of structural important water in membranes as well as the structure of small polypeptides associated with the membrane. First results of two polypeptides are presented.

(1) F.Volke and A. Pampel.1995.*Biophys. J.* 68: 1960

Tu-AM-L7

CONTRIBUTION OF THE MEMBRANE TENSION TO THE OSMOTIC SWELLING OF UNILAMELLAR VESICLES INDUCED BY NON ELECTROLYTE PERMEATION. ((Disalvo, E.A, Giner, S. and Spiazzi E.)) Facultad de Farmacia y Bioquímica, U de Buenos Aires and CIDCA, University of la Plata, Argentina

The osmotic behavior of liposomes has been explained on the basis of theories that consider the fluxes occurring between two compartments separated by a membrane that are open to the atmosphere. This situation is physically incorrect since the increase in hydrostatic pressure on a liposome dispersion does not counterbalance the volume increase when the liposome swells. A formalism to fit the rate of volume increase of a liposome filled with an impermeant dispersed in an isotonic solution of a permeant has been derived. The swelling produces a membrane tension that exerts a pressure on the internal solution. Thus, the equilibrium is achieved when the chemical potential of the solute is equal inside and outside the particle. However, the chemical potential inside is a function of the concentration and the pressure exerted by the membrane tension. The volume increase developes the tension without leakage of the content. at the initial stages of swelling. Above a critical volume, the tension is null and leakage of the content entrapped inside the liposomes appears. The combination of changes in tension and increase of the diffusion of the trapped solute fit to the experimental observation that the increase of the volume with time reaches a constant value with a time lag in the leakge. Although volume equilibrium can also be achieved when either the tension or the leakage are maintained zero during the process, it is shown that they are not physically congruent. In addition, when tension and leakage are not zero during the whole time of the process the volume drops to the initial value after passing through a maximum, a situation that is not experimentally founded. It is concluded that membrane tension varies during swelling changing the diffusion coefficient of the species trapped inside the liposome.
With funds from Fundación Antorchas and UBACyT.

Tu-AM-L8

NEW FLUORESCENT PROBES FOR EVALUATING THE POLARITY PROPERTIES OF MEMBRANE INTERFACES. (([1]R.F. Epand, [1]R.M. Epand, [2]G.J. Sterk, [3]P.A. Thijsse, [3]H.W.W.F. Sang and [3]R. Kraayenhof))
[1]Dept. of Biochem., McMaster Univ., Hamilton, ON, L8N 3Z5, Canada, [2]Byk Nederland BV, 1160 AB Zwanenburg, The Netherlands, [3]BioCentrum Amsterdam, Vrije Universiteit, 1081 HV Amsterdam, The Netherlands.

Two polarity-sensitive probes were synthesized and their behaviour in a number of membranes evaluated. Both probes contained a 7-dimethylaminocoumarin moiety as fluorophore. In one probe, TAMAC, the fluorophore was attached so that the quaternary ammonium group would position the fluorophore approximately 6 Å from the membrane-water boundary. The other probe, DTMAC, contained an uncharged membrane-anchoring group, which should position the fluorophore at, or close to the membrane interface. The emission spectra of both probes were sensitive to solvent polarity. They generally exhibited rather similar emission spectra when embedded in L_α phase membranes composed of a number of different phospholipids. However, both probes are responsive to changes in the polarity of the interface as the hexagonal phase transition temperature (T_H) is approached. Several degrees below T_H the emission spectrum of both probes is shifted to shorter wavelengths in accord with the finding that phosphatidylethanolamines lose a substantial fraction of their bound water just prior to the conversion from lamellar to hexagonal phases. These probes provide novel tools for assessing the hydration properties at membrane interfaces.

Tu-AM-L9

THE SKIN BARRIER: DEUTERIUM NMR AND X-RAY DIFFRACTION STUDIES OF A MEMBRANE MODEL ((J. Thewalt, J. Bouwstra‡ and N. Kitson*)) Dept. of Physics/Inst. of Molec. Biol. and Biochem., S.F.U., Burnaby, B.C., Canada, V5A 1S6, ‡Div. of Pharmaceutical Technol., Gorlaeus Labs., 2300 RA Leiden, The Netherlands and *Div. of Dermatology, U.B.C., Vancouver, B.C., Canada, V6T 1Z1.

The skin barrier relies on specialized intercellular lipid membranes in the outer layer of the epidermis: the stratum corneum (SC). The composition of these membranes is approximately equal parts ceramide (Cer), cholesterol (Chol) and fatty acid. It has been previously shown using ^{2}H NMR [Kitson *et al.* (1994) Biochemistry 33: 6707-15] that a model SC membrane composed of bovine brain Cer, Chol and palmitic acid displays complex phase behaviour which parallels that found in human SC. At room temperature the model SC membrane is largely crystalline, beginning a transition to a fluid bilayer at ≈40°C and becoming fully melted at ≈80°C. Small and wide angle x-ray diffraction (SAXD, WAXD) measurements provide both corroboration and supplementation of the NMR results. Phase changes observed by NMR and WAXD primarily inform us about alterations to lipid chain motion and packing. SAXD results, sensitive to long-range membrane order, correlate well with these molecular-scale observations and improve our understanding of the impermeable crystalline phase.

Tu-AM-M1

SINGLE CHANNEL CONDUCTANCE OF A AMPA-TYPE GLUTAMATE CHANNEL IS DETERMINED BY AGONIST CONCENTRATION.

C. Rosenmund and C.F. Stevens Zelluläre Neurobiologie MPI Biophysical Chemistry Göttingen, Germany, and Howard Hughes Medical Institute, Salk Institute, La Jolla, CA.

Glutamate gated ion channels of the AMPA/Kainate family consist of multiple subunits, presumably five. All subunits seem to be able to bind agonist independently, and opening of the channel requires binding of more than one agonist molecules. These channels also produce openings to multiple conductance levels, of which the mechanism are not known. We investigated the possibility that the number of activated subunits governs the conductance state. As native receptor desensitize upon agonist binding, we have taken advantage of a GluR3/6 chimera (Stern-Bach, Y. et al. 1994, Neuron 13,1945-57), that does not exhibit any apparent desensitization. Macroscopic and single channel behavior were studied in outside-out patches from HEK293 cells transfected with cDNA. High and low agonist concentration were applied using a fast flow application system. Binding and unbinding rates were determined fron macroscopic currents using a simple kinetic model. Dose/response curves were constructed, and could be fitted with a hill slope of n=1.5.

Patches that had only one channel were used to determine single channel behavior. The main conductance states observed were 6,15,23 pS. In high concentrations of agonist (AMPA, 300 μM), open probability (Po) was 90 %, and 90% of Po were to the 23pS state, 10% to 15pS. For low concentrations (AMPA, 2μM), the majority of opening were of 6 pS state, and 23 pS openings were usually enframed by smaller levels. Upon removal of high agonist concentration, the channel usually went through lower conductance levels before closing. Channels examined from cells transfected with GluR3 receptors and from hippocampal cultures treated with cyclothiazide to block desensitization, showed similar properties as for the R3/R6 chimer. We suggest that each of the agonist-binding subunits contributes to determining conductance level for AMPA/kainate channels. We thank Drs. Y. Stern-Bach and S. Heinemann for the provision of the cDNAs. This work was supported by a Helmholtz fellowship (C.R.) and the HHMI (C. R.+C.F.S.).

Tu-AM-M2

OUTSIDE-OUT GIANT-PATCH AND LASER-PULSE PHOTOLYSIS TECHNIQUES FOR STUDYING NEUROTRANSMITTER RECEPTORS EXPRESSED IN *XENOPUS* OOCYTES. ((L. Niu*, G. Nagel†, K. Hartung†, E. Bamberg†, R. W. Vazquez‡, R. E. Oswald‡, G. P. Hess*)) *Section of Biochemistry, Molecular and Cell Biology; ‡Department of Pharmacology, Cornell University, Ithaca, NY 14853, USA; †Max Planck Institute of Biophysics, Frankfurt, Germany.

Xenopus oocytes have been used extensively in structural and functional characterizations of neurotransmitter-gated receptor proteins. Upon binding specific neurotransmitters, the receptors open ion channels in the μs-to-ms time region, and may desensitize (transiently inactivate) in the ms time domain. Using giant outside-out patches from *Xenopus* oocytes expressing the BC_3H1 muscle acetylcholine receptor, we have increased the time resolution of kinetic measurements to 2 ms using a rapid flow technique. This represents over a 50-fold improvement of the best time resolution reported previously. With the system used we obtain an average response of several nA (measured with 1-mM carbamoylcholine); the stable response frequently lasts for several hours. With the new technique, in contrast to previous methods, the peak current of the response, representing the concentration of the open-channel receptor form, can be determined virtually unaffected by desensitization. Recently we developed a laser-pulse photolysis technique with a 100-μs time resolution for investigation of neuronal receptors, but it requires the simultaneous use of a flow technique designed for use with cells, which are much smaller than oocytes. The technique to be described now makes it possible to use the laser-pulse photolysis technique with oocytes and increases the time resolution for such measurements into the submillisecond time scale. (Supported by grants from NIH, NSF, and DFG)

Tu-AM-M3

IDENTIFICATION OF AGONIST SELECTIVITY DETERMINANTS IN THE MUSCLE NICOTINIC ACETYLCHOLINE RECEPTOR (nAChR).

((R.J.Prince and S.M.Sine)) Receptor Biology Laboratory, Mayo Foundation, Rochester, MN 55905

The two agonist binding domains of the fetal nAChR, formed at the αγ and αδ interfaces, differ in their affinity for carbamylcholine (carbachol) by around 30-fold, with the αδ site exhibiting the higher affinity. This selectivity is hypothesized to arise from discrete sequence differences between the γ and δ subunits. To identify determinants of this affinity difference we constructed γ–δ chimeric subunits, expressed them as dimer binding complexes in HEK 293 cells, and measured carbachol affinity by competition against the initial rate of [^{125}I]α-bungarotoxin binding. By substituting progressively finer segments of γ into the δ template and visa-versa, we identified two residues in δ, S36 and I178 (corresponding to K34 and F172 in γ), as key determinants of high affinity carbachol binding. δS36 and δI178 have also recently been shown to be major determinants of conotoxin M1 selectivity (1). Mutation of a further conotoxin determinant, δY113->S, however, was without effect on carbachol binding. The figure shows the affinity shifts caused by double point mutations at δS36/γK34 and δI178/γF172. We conclude that these residues contribute, directly or allosterically, to the agonist binding site.

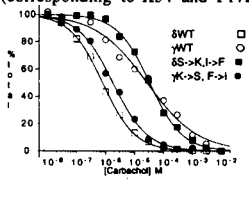

1) Sine et al. (1995) Neuron 15: 205-211
Supported by NIH NS31744

Tu-AM-M4

MECHANISM OF THE INHIBITION OF THE NICOTINIC ACETYLCHOLINE RECEPTOR (nAChR) IN BC3H1 CELLS BY MK-801. ((C. Grewer, L. Niu and G. P. Hess)) Section of Biochemistry, Molecular and Cell Biology, Cornell University, Ithaca, NY 15853-2703 (Spon. by N. Noy)

The recently developed laser-pulse photolysis technique with a 100 μs time resolution in combination with the cell-flow method provides a useful tool for investigation of the interaction of an inhibitor with a ligand-gated ion channel. We have used this method to investigate the inhibition of the nAChR receptor by MK-801, an anticonvulsant and potent inhibitor of the NMDA-receptor. We have determined the apparent dissociation constants of the inhibitor of the open- and, independently, the closed-channel forms and the effects of MK-801 on the observed first order rate constant of the current rise, reflecting the opening of the channel, as well as the falling phase of the current, reflecting receptor inhibition. Receptor inhibition occurs in at least two steps. In a rapid reaction the inhibitor actually increases the rate constant for both channel opening and closing. An interpretation of these results is that the receptor:inhibitor complex (RI) forms open channels, but with rates different from the receptor without inhibitor bound. RI is then converted in a slow step to an inactive receptor form. MK-801 was found to compete with cocaine for the inhibition of the receptor. It is of interest that MK-801 has been shown to alleviate cocaine toxicity in animals.

(Supported by grants from the National Institute of Health. CG is grateful for a Feodor Lynen Fellowship from the A. v. Humboldt Foundation)

Tu-AM-M5

INTERACTIONS OF LEUCINE RESIDUES AT THE 9' POSITION OF THE M2 DOMAIN OF THE ACHR PROBED USING UNNATURAL AMINO ACID MUTAGENESIS. ((P.C. Kearney[1], W. Zhong[2], M. W. Nowak[1], S. K. Silverman[2], H. Zhang[1], C. Labarca[1], M. E. Saks[1], J. R. Sampson[1], J. P. Gallivan[2], J. Abelson[1], N. Davidson[1], D. A. Dougherty[2], and H. A. Lester[1])), [1]Div. of Biology, [2]Div. of Chemistry, Caltech, Pasadena, CA 91125.

Leucine residues are highly conserved at the midpoints of the M2 transmembrane domains (position 9') in subunits of the AChR superfamily of ligand gated ion channels. It has long been speculated that these residues may form the gate of the receptor, an idea supported by the 9Å resolution structures of the AChR. We have probed the structural environment of these residues in the β, γ and δ, subunits of the AChR using unnatural amino acid mutagenesis.

In this method, mRNA containing a UAG stop codon at the position of interest is coinjected into *Xenopus* oocytes along with a suppressor tRNA. This tRNA possesses the corresponding CUA anticodon and has been chemically acylated with the amino acid of interest.

This method leads to expression of modified receptors at levels sufficient for measurements of macroscopic currents. Dose-response studies on receptors containing various amino acids at either the β, γ or δ 9' positions suggest that the leucine side chain on each subunit resides within a unique microenvironment. Of particular interest, experiments utilizing the diasteriomeric isoleucine and allo-isoleucine amino acids indicate a strong asymmetry at the δ 9' position. This asymmetry is also influenced by mutation of the β 9' leucine to serine, possibly indicating a direct interaction between side chains at the β and δ 9' sites. Support: NIH, TRDRP

Tu-AM-M6

HUMAN α7-NICOTINIC ACETYLCHOLINE RECEPTORS (nAChRs) STABLY EXPRESSED IN K28 CELLS REVEAL FAST DESENSITIZING CATIONIC CURRENT AND SUBSTANTIAL CONTRIBUTION TO INTRACELLULAR Ca^{2+} CONCENTRATION. (M.Renganathan+, M. Gopalakrishnan#, M.L. Messi+, J. Sullivan# and O. Delbono+*). Bowman Gray School of Medicine. Wake Forest University, Dept. of Physiology-Pharmacology* and Internal Medicine (Gerontology)+, Winston-Salem, NC 27157 and Neuroscience Research (D-47W), Abbott Laboratories#, 100, Abbott Park Road, Abbott Park, IL 60064.

The α7-nAChR is a Ca^{2+} permeable ligand gated ion channel that has been implicated in activating Ca^{2+}-dependent intracellular processes in the central nervous system. This subtype coexpresses with others nAChRs *in vivo* which limits the investigation of its functional properties. The human α7-subtype has been stably expressed in a mammalian cell line, K28 (Gopalakrishnan *et al.*, Eur. J. Pharmacol. 290:237,1995). In this study, currents carried by Na^+ (120 mM) and Ca^{2+} (2 mM) and $[Ca^{2+}]_i$ kinetics have been examined simultaneously in K28 using whole-cell patch clamp and frame-transfer CCD imaging techniques. For drug delivery a fast solution exchange system based on a piezoelectric device has been used. K28 cells exhibited fast activating (a) and desensitizing (d) inward currents ($\tau_a = 1.1 \pm 0.23$ ms; $\tau_d = 12.2 \pm 2.6$ ms; n = 5) with 50 ms pulses of 300 μM nicotine at -100 mV holding potential. Increase in $[Ca^{2+}]_i$ was detected (using fura-2 or rhod-2) within the first 10 ms of the drug-pulse. The signal reached a peak at the end of the desensitizing phase (356 ± 48 nM; n = 5). $[Ca^{2+}]_i$ declined slowly to 50% of the peak in 15 ± 3 s (n = 5) and completely in a range of 2-4 min (n = 5). nAchR antagonists (2 nM α-Bgt and 3 nM MLA) completely blocked current and intracellular Ca^{2+} responses. The EC_{50} values for (-)-nicotine, ACh, DMPP and [±]-epibatidine were similar for both current activation and Ca^{2+} transient responses. No responses were detected in untransfected cells (n = 8). This study provides direct evidence that the human α7-nAChR subtype promotes significant increase in $[Ca^{2+}]_i$ in mammalian cells.

Tu-AM-M7

GATING PROPERTIES OF THE HUMAN α7-NICOTINIC ACETYLCHOLINE RECEPTOR (nAChR) STABLY EXPRESSED IN K28 CELLS. (M.L. Messi*, J. Sullivan#, M. Renganathan+, M. Gopalakrishnan# and O. Delbono*+). Bowman Gray School of Medicine. Wake Forest University, Dept. of Physiology-Pharmacology* and Internal Medicine (Gerontology)+, Winston-Salem, NC 27157 and Neuroscience Research (D-47W), Abbott Laboratories#, 100,Abbott Park Road, Abbott Park, IL 60064.

Cation influx through the human α7-nAChR stably expressed in K28 cells promotes a fast activating and desensitizing inward current and a rapid intracellular Ca^{2+} transient with a long-lasting decaying phase in response to different agonists (Renganathan *et al.*, this Meeting). This process involves nAChR agonist-induced conformational changes in the α7-nAChR. These conformational changes can be studied by analyzing the channel gating properties in single channel recordings. Single channel activity has been recorded in K28 cells in outside-out configuration of the patch clamp and in membranes extracted from K28 cells and reconstituted into lipid bilayers. Similar solutions were used in patch-clamp and cell-free experiments, external or *cis* solution (mM): 120 Na, 2 Ca and internal or *trans* solution: 140 K, as the main ions. α7-nAChR was activated with different concentrations of [±]-epibatidine, (-)-nicotine or ACh. No single channel activity was recorded by preincubation of the preparation in 2 nM α-Bgt or 3 nM MLA. The magnitude of the channel activation and desensitization was related to agonist concentration and to membrane potential. The channel activity was recorded from -150 to +50 mV in low non-desensitizing agonist concentrations. Unitary current amplitude was 5 pA at V_h=-100 mV and the single channel conductance calculated as the slope of the I-V relationship was 65 pS. The open probability increased from -50 to -100 mV and the reversal potential was +10 mV. The gating properties of the α7-AChR will be modeled based on macroscopic currents and single channel recordings. The stable expression of the α7-subunit in mammalian cells provides a unique system to analyze ligand-induced gating of this nAChR subtype.

Tu-AM-M8

PURINOCEPTOR-OPERATED ION CHANNELS IN HUMAN B-LYMPHOCYTES. ((M. Löhn, M. Klapperstück and F. Markwardt)) J.B. Inst. for Physiology, M.L. University, D-06097 Halle, Germany

ATP-induced single channel currents were measured in normal tonsillar and Epstein-Barr-Virus-transformed human B-lymphocytes by means of the patch-clamp-technique in the outside-out-configuration. Single ionic channels are opened by the extracellularly applied free acid form of ATP (ATP^{4-}) but not by Mg^{2+}-bound ATP or ADP^{3-} and have a single-channel conductance of about 10 pS. From the current-voltage-relationships measured in different solutions at both sides of the patch, it is concluded that the channels are permeable for cations like Na^+ and Cs^+ but not for $choline^+$ or anions. The dose-response-curve for the mean single-channel-current is described by a model in which binding of ATP^{4-} to four equal and independent binding sites (K_D = 20 μM) is necessary for channel opening. Application of 1 mM ATP^{4-} opens and removal shuts the channels within less than 200 ms. For agonist concentrations up to 1 mM, the channels show no desensitization. Increasing the concentration of ATP^{4-} shortens the mean closed time of the channels but is without effect on the mean open times.

OXIDATIVE PHOSPHORYLATION

Tu-AM-N1

A HEMEPROTEIN MODEL FOR THE LIGAND SWITCH IN CYTOCHROME C OXIDASE

((Stefan Franzen[1], Sean M. Decatur[2], Steven G. Boxer[2], R. Brian Dyer[1], William H. Woodruff[1]))
1. Biosciences and Biotechnology Group, CST-4 MS C345, Los Alamos Natl. Laboratory Los Alamos, NM 87545 2. Dept. of Chemistry, Stanford University, Stanford, CA 94305

A change in the ligation state of the heme (ligand switch) has been observed using resonance Raman spectroscopy as a probe of the heme geometry in the myoglobin mutant H93G in which the proximal histidine has been replaced by glycine [1]. When expressed in *E. coli* grown on a medium containing 10 mM imidazole (Im), the heme iron has an Im ligand bound. If all exogenous ligands are dialyzed from the buffer (and presumably the cavity is filled with water) a ligand,L, with similar Raman frequency for the ferrous iron-L out-of-plane (OOP) mode (see Figure) appears to bind to the iron. The Raman spectrum of isotopically labeled ligands and H_2O/D_2O effects indicate that the ligand is the distal histidine. The reduced intensity, but identical frequency of the distally ligated H93G makes an interesting analogy to the ligand switch phenomenon observed in cytochrome c oxidase (CcO). In CcO, time-resolved data indicate that there is a much reduced intensity of the iron-L OOP mode after CO photolysis [3]. This has been interpreted be the results of a formation of five-coordinate complex that replaces the iron complex with the proximal histidine. The identity of the ligand is still not known, but the similarity with the H93G model system indicates that one of the histidines that is ligated to copper in the resting state may replace the proximal histidine transiently

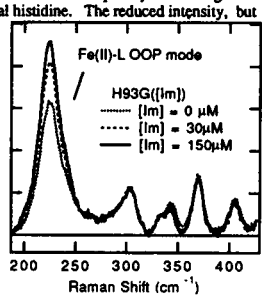

1. Barrick, D. Biochem. (1994) 33: 6546
2. DePillis et al. JACS (1994) 116: 6981
3. Woodruff et al. PNAS (1991) 88:2588

Tu-AM-N2

SUBUNIT IV OF *BACILLUS* PS3 CYTOCHROME *c* OXIDASE (*caa*$_3$-TYPE) IS NOT REQUIRED FOR MAXIMUM ELECTRON TRANSFER AND PROTON-PUMPING ACTIVITIES OF THE ENZYME. (L.J. Prochaska, R.A. Kirken, G. Hanrahan, and A.J. Lincoln) Department of Biochemistry & Molecular Biology, Wright State University, Dayton OH 45435.

Isolated cytochrome *c* oxidase (COX) from the thermophilic bacterium *Bacillus* PS3 exhibits four major bands on SDS-PAGE with MW of 50, 34, 20, and 12 kDa that correspond to subunits I-IV encoded in its operon. In attempt to understand the role of the subunit structure in PS3 COX functioning, the enzyme was first digested for 2 hrs in 20 mM TrisCl, pH 8.5 with α-chymotrypsin (0.05 mg/mg PS3 COX) and then for 2 hrs with thermolysin [0.1 mg/mg PS3 COX with 2 mM $CaCl_2$]. Analysis of the subunit labeling profiles of COX prelabeled with [^{3}H]-succinimidylpropionate by SDS-PAGE before and after digestion showed that greater than 75% of subunit IV (SIV) was removed by the proteases. Subunit III (SIII) was also cleaved by the proteases into truncated forms that exhibited MW of 18 and 16 kDa on SDS-PAGE. Both forms of digested SIII retained the dicyclohexylcarbodiimide (DCCD) binding site as shown by [^{14}C]-DCCD labeling. Protease-treated PS3 COX exhibited less than 20% inhibition of electron transfer activity. Both control and treated PS3 COX were incorporated into asolectin liposomes by cholate dialysis and these preparations had respiratory control ratios of 4 or greater. Proton-pumping activity measured electrometrically was not affected by the proteolysis; the liposomes containing protease-treated PS3 COX exhibited a vectorial proton translocated to electron transferred ratio of 0.6 compared to 0.7 for liposomes containing control PS3 COX. These results suggest that SIV of PS3 COX, which is not homologous to SIV of mitochondrial or *Paracoccus denitrificans* COX, has no role in the maximum proton translocating or electron transferring activities of the enzyme.

Tu-AM-N3

INTERACTION DOMAIN FOR THE REACTION OF CYTOCHROME c WITH THE RADICAL CATION AND OXYFERRYL HEME IN CYTOCHROME c PEROXIDASE. ((H. Mei[1], S. McKee[1], L. Geren[1], K. Wang[1], M. Miller[2], G. Pielak[3], B. Durham[1], and F. Millett[1])) [1]Dept. Chem. Biochem., Univ. of Arkansas, Fayetteville, AR, [2]Dept. Chem., Univ. California at San Diego, La Jolla, CA, and [3]Depts. Chem., Biochem., Biophys., Univ. N. Carolina, Chapel Hill, NC.

A ruthenium-labeled derivative of yeast iso-1-cytochrome c, Ru-39-Cc, was found to initially reduce the Trp-191 radical cation in cytochrome c peroxidase (CcP) compound I (CMPI) with an intracomplex rate constant of 1.2 x 10^6 s^{-1} at low ionic strength. A new technique was developed to measure the dissociation rate constant, k_d, for the high affinity complex between Ru-39-Cc and CMPI. The value of k_d increases from 50 s^{-1} at 5 mM ionic strength to 4000 s^{-1} at 120 mM ionic strength. The value of k_d was increased 10-fold by the mutations E34N, E290N and A193F on the surface of CcP, but was not affected by the mutations E32Q or E291Q. These results indicate that Ru-39-Cc uses the Pelletier-Kraut binding domain for the reaction with both the Trp-191 radical cation and the oxyferryl heme. Cc binding to the low affinity site on the Cc:CMPI complex at low ionic strength increases k_d to 350 s^{-1}, but does not participate directly in electron transfer to either the radical cation or the oxyferryl heme. The steady-state reaction is rate-limited by k_d at ionic strengths up to 100 mM. Supported by NIH grants GM20488 and GM42501 and NSF Grant MCB9119292.

Tu-AM-N4

DESIGN OF A RUTHENIUM-CYTOCHROME c DERIVATIVE TO MEASURE ELECTRON TRANSFER TO THE RADICAL CATION AND OXYFERRYL HEME IN CYTOCHROME c PEROXIDASE. ((K. Wang[1], L. Geren[1], H. Mei[1], M. Miller[2], G. Pielak[3], B. Durham[1], and F. Millett[1])) [1]Dept. Chem. Biochem., Univ. of Arkansas, Fayetteville, AR, [2]Dept. Chem., Univ. California at San Diego, La Jolla, CA, and [3]Depts. Chem., Biochem., Biophys., Univ. N. Carolina, Chapel Hill, NC.

A ruthenium-labeled cytochrome c derivative was prepared which will rapidly transfer an electron to the cytochrome c heme group without altering the interaction with cytochrome c peroxidase. Site-directed mutagenesis was used to replace His-39 on the backside of yeast C102T iso-1-cytochrome with a cysteine residue which was then labeled with a ruthenium trisbipyridyl reagent to form Ru-39-Cc. Laser excitation of a complex between Ru-39-Cc and cytochrome c peroxidase compound I (CMPI) in low ionic strength buffer (2 mM phosphate, pH 7) resulted in electron transfer from the excited state Ru(II*) to heme c Fe(III) with a rate constant of 5 x 10^5 s^{-1}, followed by electron transfer from heme c Fe(II) to the Trp-191 radical cation in CMPI with a rate constant of 1.2 x 10^6 s^{-1}. A second laser flash resulted in electron transfer from heme c Fe(II) to the oxyferryl heme in CMPII with a rate constant of 5 x 10^3 s^{-1}. Stopped-flow experiments indicated that the kinetics of the reaction of Ru-39-Cc with CMPI were the same as those of wild-type iso-1-Cc under all ionic strength conditions. *Supported* by NIH grants GM20488 and GM42501 and NSF Grant MCB9119292.

Tu-AM-N5

THREE DIMENSIONAL STRUCTURE OF BEEF HEART MITOCHONDRIAL CYTOCHROME bc_1 COMPLEX.((D. Xia, C. A. Yu, J. Deisenhofer, J-Z. Xia and L. Yu)), Howard Hughes Medical Institute and University of Texas, Southwestern Medical Center at Dallas, TX 75235 and Oklahoma State University, Stillwater, OK 74078.

The cytochrome bc_1 complex from bovine mitochondria is the largest membrane protein complex crystallized so far. It contains ten protein subunits and five redox centers with a molecular weight of 240,000 Da. It plays a central role in cell respiration. The successful crystallization has been reported from several laboratories. Our crystals, grown in the presence of glycerol, diffract X-rays to better than 3 Å under cryogenic conditions. They have the symmetry of the space group $I4_122$ with unit cell dimensions of a=b=153.5 Å and c=597.7 Å. There are eight bc_1 dimers in a unit cell. Phases have been determined to 3.3 Å resolution by the MIR method with two heavy atom derivatives. The electron density clearly shows the transmembrane region with thirteen transmembrane helices. Four high peaks in the electron density and in maps calculated using anomalous scattering data are interpreted as the redox-centers of the bc_1 complex. Two of these sites are 20 Å apart in the transmembrane region and most likely represent the heme irons of cytochromes b_{562} and b_{565}. Another site near the membrane surface and 26 Å away from the nearest b-heme could be the iron-sulfur center; the fourth site, presumably the cytochrome c_1 heme is 31 Å apart from this center. The majority of the molecular mass outside the membrane is located on the side of the membrane opposite from the redox centers, presumably the matrix side of the mitochondrial membrane. Supported by a grant from the NIH (GM 30721 to CAY).

Tu-AM-N6

THE F_oF_1 ATP SYNTHASE UNCOUPLING MUTATION, γMET-23→LYS, FORMS AN ADDITIONAL CHARGE INTERACTION TO A β SUBUNIT AND DISRUPTS THE STABILITY OF THE $\alpha_3\beta_3\gamma$ COMPLEX.
((M. K. Al-Shawi and R. K. Nakamoto)) Department of Molecular Physiology and Biological Physics, University of Virginia, Charlottesville, VA 22908.

The γ subunit γMet-23→Lys energy coupling mutation does not strongly affect transport or catalytic functions and primarily perturbs the linkage between catalysis and transport. We sought to understand the perturbations caused by the mutation in order to understand the mechanism of coupling. When mutant F_1 was diluted to dissociate δ and ε subunits, ATPase activity was lost. Affinity for δ and ε subunits was unchanged which suggested that the mutation affected the stability of the catalytically active $\alpha_3\beta_3\gamma$ complex. Arrhenius analysis revealed that the mutant enzyme had a transition state with the $\Delta H^{\ddagger}$ parameter more positive, the $\Delta S^{\ddagger}$ less negative and the $\Delta G^{\ddagger}$ unchanged, when compared to wild type. These results suggested that an additional bond was formed that had to be broken to achieve the transition state. Isokinetic analysis indicated that the general reaction scheme had not changed and that the rate limiting step of the mutant enzyme cycle was the same as wild type. The recently solved structure of the F_1 ATPase suggested that a lysine in place of γMet-23 was likely to form an extra charge interaction with βGlu-381 on one of the three β subunits. Moreover, the second-site mutation γArg-242→Cys which eliminated another charge interaction with the same β subunit residue, resulted in stabilization of the enzyme complex and the restoration of efficient coupling. These results suggested that formation of the additional β–γ interaction was the principle cause for the observed changes in F_oF_1 properties, including uncoupling. Supported by PHS grant GM50957.

Tu-AM-N7

FORMATE IS NOT BOUND AS A BRIDGE IN THE SLOW FORM OF CYTOCHROME C OXIDASE FROM BOVINE HEART.
((S. Yergul and G.M. Baker)) Northern Illinois University, Department of Chemistry, DeKalb, IL 60115. (Spon. by AHA, IL Aff.)

The binding of formate to rapid enzyme induces an apparent blue shift in the Soret band and a conversion to the slow form. The blue shift (measured as an absorbance increase at 414 nm) is biphasic at $[HCOO^-]$ / [heme A] ≥ 2×10^3, and can modeled by a two stage reaction of the form $E_0 \rightleftharpoons E_1 \rightleftharpoons E_2$. The fast phase is first order in formate and the slow phase is zero order, indicating that only 1 formate is bound in the overall conversion of E_0 to E_2. The observed equilibrium dissociation constant, $K_{D,f}^{app}$ is 0.1 ± 0.03 mM. From this, we can calculate $k_{d,f}$, the dissociation rate constant for the slow step, as $1.1 \times 10^{-5} \pm 4.2 \times 10^{-6}$ s^{-1}. The binding site of formate has been probed with cyanide. It is now accepted, based on FTIR analysis, that CN^- forms a bridge between Fe_{a3} and Cu_B. If formate is present as a bridge, then subsequent binding rates with CN^- should be limited by $k_{d,f}$ when $k_{a,c}[CN^-] = k_{d,f}$. A kinetic analysis shows that k_{obs} should saturate at ≈ 3 mM CN^-, yet it depends linearly on $[CN^-]$ over the 1 - 150 mM range. We conclude that formate is not bound as a bridge in the slow form.

Tu-AM-N8

BIOCHEMICAL AND BIOPHYSICAL CHARACTERIZATION OF NADH:UBIQUINONE OXIDOREDUCTASE FROM PURPLE BACTERIA; IN SEARCH OF A MODEL SYSTEM TO STUDY ENERGY COUPLING. ((C.Hägerhäll, V.D.Sled, F.Daldal and T.Ohnishi)) Univ. of Penn., Philadelphia, PA 19104, USA,

Purple bacteria have been extensively studied with regards to their primary photochemistry and bioenergetics but rather little is known about coupling site I (NDH-1, Complex I). When grown aerobically their respiratory chain is very similar to that of the mitochondria. EPR features of the iron-sulfur clusters seems to be very similar to their mammalian equivalents. The chromatophores can be made tightly coupled, and in addition the carotenoid band shift can be used as an internal probe to monitor the energetic state of the membrane under various conditions. Furthermore, genetic manipulations can be utilized. Thus purple bacteria provide an excellent experimental system to address how electron transfer is coupled to proton translocation in NDH-1 and to improve understanding of the membrane part of the enzyme. We have compared NDH-1 in chromatophores from *Rhodobacter sphaeroides, Rhodobacter capsulatus* and *Rhodospirillum rubrum* with respect to enzymatic properties, inhibitor sensitivity and enzyme stability. EPR characteristics and redox properties of the iron-sulfur clusters were investigated *in situ* and in partially purified preparations. Methods and preliminary data are presented. (Supported by NIH grants GM 30376 to T.O. and GM38237 to F.D.).

BIOPHYSICAL APPROACHES TO PRESYNAPTIC TERMINALS

Tu-PM-Sym-1

MICRODOMAINS OF ELEVATED Ca^{2+} CONCENTRATION DUE TO CLUSTERED ION CHANNELS AT PRESYNAPTIC ACTIVE ZONES OF HAIR CELLS FROM THE BULLFROG'S INTERNAL EAR. ((A. J. Hudspeth and N. P. Issa)) Howard Hughes Medical Institute and Laboratory of Sensory Neuroscience, The Rockefeller University, New York, NY 10021-6399.

Ca^{2+} channels mediate two critical processes in hair cells, the mechanoreceptors of the auditory and vestibular systems. First, synaptic signaling from such a cell to afferent nerve fibers depends upon the influx of Ca^{2+} at presynaptic active zones. Second, a hair cell's responsiveness is tuned to a specific frequency of stimulation by electrical resonance, which involves an interplay between currents borne by Ca^{2+} channels and Ca^{2+}-activated K^+ channels.

By simultaneously monitoring the whole-cell Ca^{2+} current and the rise and fall of fluo-3 fluorescence intensity, we measured the time course of Ca^{2+} entry, accumulation, and diffusion in hair cells isolated from the bullfrog's sacculus. Upon membrane depolarization, the Ca^{2+} concentration approximately 200 nm from the presynaptic membrane approached a steady state with a time constant of less than 10 ms. Because the sectioning depth of the confocal imaging system exceeded the space constant of fluo-3 fluorescence in the steady state, we developed a numerical procedure to compensate for the effects of out-of-focus fluorescence. Application of this algorithm to fluorescence profiles obtained by rapidly scanning across maximally stimulated active zones indicated that the presynaptic Ca^{2+} concentration reached at least 100 mM. Inclusion in the recording pipette of a Ca^{2+} buffer, such as BAPTA or EGTA, slowed the approach to steady-state fluorescence and restricted the spread of fluorescence from the presynaptic membrane. Both the concentration and the binding rate of the exogenous Ca^{2+} buffer affected the steady-state fluorescence and Ca^{2+} concentration. The observed dynamics of the presynaptic Ca^{2+} concentration is consistent with models of Ca^{2+} entry at and diffusion from a point source.

This research was supported by National Institutes of Health grant DC00241.

Tu-PM-Sym-2

CAPACITANCE MEASUREMENTS OF EXOCYTOSIS AND ENDOCYTOSIS AT A RIBBON SYNAPSE. ((G. Matthews)) Department of Neurobiology & Behavior, SUNY, Stony Brook, NY 11794-5230.

Bipolar neurons are interneurons in the retina that release glutamate from ribbon-type synapses. Ribbons are sheet-like structures found at synaptic active zones in photoreceptors and bipolar neurons and are thought to be a mechanism to increase the population of docked vesicles at the output site. The retina of the goldfish contains a class of bipolar neuron with giant synaptic terminals (10-12 μm in diameter) that are well-suited for patch-clamp analysis of presynaptic mechanisms. In single isolated giant terminals, regulation of membrane fusion and membrane retrieval has been investigated by monitoring the associated changes in membrane capacitance. Activation of presynaptic calcium current induces a rapid increase in capacitance, which reaches a maximum amplitude of about 150 fF within 200 msec. This capacitance response has properties consistent with the rapid exocytosis of a limited pool of synaptic vesicles. Electron microscopy shows that the average vesicle diameter is about 29 nm, so this readily releasable pool corresponds to about 6000 synaptic vesicles. This likely represents the total population of vesicles tethered to the ~55 synaptic ribbons in the terminal. The initial rate of fusion of this pool exceeds 40,000 vesicles per sec. After a bout of exocytosis has been stimulated by a brief depolarization, the added membrane is retrieved with an exponential time constant of 1-2 sec under normal conditions. When resting [Ca] is elevated, retrieval slows dramatically (half-inhibition at 500 nM) and stops altogether when internal calcium exceeds about 1000 nM.